MEMBRANES FOR THE RECOVERY OF A HOMOGENEOUS CATALYST

A Thesis
Presented to
The Academic Faculty

by

David J. Desrocher

In Partial Fulfillment
of the Requirements for the Degree
Doctor of Philosophy in
Chemical Engineering

Georgia Institute of Technology
July 2004

MEMBRANES FOR THE RECOVERY OF A HOMOGENEOUS CATALYST

Approved by:

Dr. Mary E. Rezac, Advisor

Dr. Haskell Beckham

Dr. Christopher W. Jones

Dr. William J. Koros

Dr. John D. Muzzy

June 11, 2004

ACKNOWLEDGEMENTS

Primary financial support for this work was provided by the National Science Foundation, grant number CTS-9985552. Additional support was provided from the National Science Foundation Chemical Sensors Traineeship.

I would like to thank to express my deepest gratitude to my advisor, Dr. Mary Rezac. She has always been a steadying influence, providing me with the confidence and insight that have allowed me to grow not only in technical breadth, but also personally. She has always maintained the delicate balance between allowing my own self-discovery and providing guidance when I was most at need, which has made my graduate experience a rewarding one.

I am particularly indebted to Dr. William Koros and the members of his research group. They provided me with a place to call home when I was in the difficult position of having an off-campus advisor. I can only hope that I have given them a fraction of the help and friendship that they have given me.

Several people have contributed to this work. For their assistance with the NMR, I would like to thank Johannes Leisen and Leslie Gelbaum. Those who have helped with my experiments at Georgia Tech deserve many thanks: Mike Buchanan, Tab Shah, Young-Bin Park, Mike McKittrick, and Swati Singla.

Also, special thanks are necessary to those who entered my life during my experience at Tech, but will hopefully remain in it long afterwards. Roy Furbank is a true friend and he was a tremendous source of support during our experience as graduate students. Matt Spuller's friendship and endless optimism have always made any situation

tolerable. "Old" Rezac group members Kip Sturgill and Broderick Wilks are great friends who filled life in Bunger-Henry with laughter. I would also like to thank Roy's wife Mary and her parents John and Carole Seffrin for giving me an extended family during my stay in Atlanta.

Finally, I would like to thank my parents Ron and Carol Desrocher for their love and support.

TABLE OF CONTENTS

Acknowledgements iii

Table of Contents v

List of Figures ix

List of Tables xiv

Summary xvi

CHAPTER 1: INTRODUCTION 1

1.1 Membrane Technology 1

1.2 Membrane Recovery of a Homogeneous Catalyst 3

1.3 Membrane Stabilization 4

1.4 Research Objectives 5

1.4.1 Stabilization with Crosslinked Polyimide Blends 6

1.4.2 Proof of Concept for Homogeneous Catalyst Recovery 6

1.5 Organization of the Dissertation 7

1.6 References 8

CHAPTER 2: BACKGROUND 10

2.1 Membrane Fundamentals 10

2.1.1 The Solution-Diffusion Model 10

2.1.2 Sorption and Diffusion in Polymers 15

2.1.3 Membrane Stabilization Techniques 17

2.2 Catalyst Recovery Background 20

2.2.1 Model Reaction: Hydroformylation of 1-Dodecene 24

2.3 References 29

CHAPTER 3: DIACETYLENE CROSSLINKING AND POLYIMIDE BLENDS 34

3.1 Introduction 34

3.2 Background 40

3.2.1 Polymer Blends 41
3.2.2 Diacetylene Crosslinking 43
3.2.3 Membranes with Crosslinkable Diacetylene Functionalities 44
3.3 Experimental 44
3.3.1 Materials 44
3.3.2 Film Casting 46
3.3.3 Thermal Activation 46
3.3.4 Differential Scanning Calorimetry (DSC) 47
3.3.5 Dynamic Mechanical Analysis (DMA) 47
3.3.6 Atomic Force Microscopy (AFM) 48
3.3.7 Solid-State ^{13}C-NMR 48
3.4 Results and Discussion 48
3.4.1 Oligomer Solubility 49
3.4.2 Activation of Oligomer Crosslinking 50
3.4.3 Macroscopic Phase Behavior of Matrimid Blends 57
3.4.4 Microscopic Phase Behavior of Matrimid Blends 60
3.4.5 Thermo-mechanical Properties of Matrimid and Blends 65
3.5 Conclusions 70
3.6 References 72

CHAPTER 4: SORPTION AND SWELLING BEHAVIOR OF MATRIMID AND BLENDS IN TOLUENE 76
4.1 Introduction 76
4.1.1 Blend Morphology 77
4.2 Background 78
4.3 Experimental 80
4.3.1 Materials 80
4.3.2 Film Casting 81
4.3.3 Vapor Sorption 81
4.4 Results and Discussion 85
4.4.1 Sorption Kinetics 85
4.4.2 Sorption in Matrimid 90
4.4.3 Model Interpretation of Sorption 93
4.4.4 Influence of Annealing and Blending on Sorption 95

4.5 Conclusions 99
4.6 References 101

CHAPTER 5: TRANSPORT OF HOMOGENEOUS REACTION COMPONENTS 104
5.1 Introduction 104
5.2 Background 109
5.3 Experimental 110
5.3.1 Materials 110
5.3.2 Film Casting 111
5.3.3 Toluene Diffusion and Hydraulic Permeability 112
5.3.4 Dialysis Permeability Measurements 113
5.3.5 Solute Rejection 114
5.3.6 Catalyst Rejection 116
5.3.7 Solute Solubility in Polymers 117
5.4 Results and Discussion 118
5.4.1 Toluene Transport 119
5.4.2 1-Dodecene and Triphenylphosphine Transport 123
5.4.3 Rejection Studies 127
5.4.4 Catalyst Rejection 130
5.4.5 Homogeneous Catalyst Recovery Application 132
5.5 Conclusions 133
5.6 References 135

CHAPTER 6: ANALYSIS OF TRANSPORT AND COUPLING VIA MAXWELL-STEFAN EQUATIONS 138
6.1 Introduction 138
6.2 Original Maxwell Stefan Formulation 141
6.3 Maxwell-Stefan Relationship for Membrane Separations 145
6.3.1 Flux Equation for Single Component Transport 147
6.3.2 Flux Equations for Binary Mixture Transport 150
6.4 Application of the Transport Model 152
6.4.1 Model Description of Experimental Triphenyl-phosphine Rejection 153
6.4.2 Modeling of a Membrane with Inert Filler 157

6.4.3 Generalized Model of Homogeneous Catalyst Recovery 159
6.5 Conclusions 164
6.6 References 165

CHAPTER 7: CONCLUSIONS AND RECOMMENDATIONS 167
7.1 Conclusions 167
7.2 Recommendations for Future Work 171
7.3 References 173

APPENDIX A: PERMEATION MEASUREMENT AND CALCULATIONS 175
A.1 Experimental Apparatus 175
A.2 Hydraulic Permeation of Toluene 178
A.2.1 Equilibrium Thermodynamic Model 178
A.2.2 Determination of Diffusion Coefficient 181
A.2.3 Hydraulic Permeability 183
A.2.4 Experimental 184
A.2.5 Sample Calculation 186
A.3 Dialysis Measurements 189
A.3.1 Theory 189
A.3.2 Experimental 191
A.3.3 Sample Calculation 192
A.4 References 193

Vita 195

LIST OF FIGURES

Figure 2.1: Schematic of transport of a binary mixture through a membrane following the solution-diffusion mechanism. 11

Figure 2.2: Structure of the diacetylene crosslinking agent (1,1-BTDA-DIA) used in this work. 19

Figure 2.3: General representation of homogeneous catalyst recovery 20

Figure 2.4: Membrane performance in desalination of water for different membrane types.[32,33] 23

Figure 2.5: Hydroformylation of a terminal alkene..... 25

Figure 2.6: Hydroformylation of 1-dodecene..... 26

Figure 2.7: Mechanism for hydroformylation of terminal olefins catalyzed by carbonylhydridotris(triphenylphsophine) rhodium(I).[51,52] 27

Figure 2.8: Structure of hydroformylation catalyst 28

Figure 3.1: Structure of 1,1-BTDA-DIA crosslinking agent..... 36

Figure 3.2: Chemical structure and select properties of Matrimid and P84. 37

Figure 3.3: Two-dimensional representation of a semi-interpenetrating network. The dark lines represent the crosslinked network surrounding the host polymer, shown with lighter lines. 39

Figure 3.4: General representation of the 1,4-addition solid-state polymerization of diacetylenes. R is a substituent group. 43

Figure 3.5: DSC of Oligomer 1 and monomer before and after crosslinking. "Annealed Oligomer" denotes a sample that has been heated at 250 °C for 24 hours under vacuum. DSC traces have been shifted along the y-axis for clarity. 51

Figure 3.6: ^{13}C-NMR CP/MAS solid-state spectra of annealed and original oligomer. The annealing process is thermal treatment of the oligomer at 250 °C for 24 hours under vacuum. 53

Figure 3.7: Proposed mechanism for the thermally initiated reaction of ethynyl-terminated imide oligomers in the solid-state.[35] 55

Figure 3.8: DSC of annealing process for Oligomer 2. "Annealed Oligomer" denotes a sample that has been heated at 250 °C for 24 hours under vacuum. 56

Figure 3.9: Photographs of polymer film appearance before and after annealing at 250 °C for 24 hours. All films were cast in HFIP and dried at 180 °C for 3 days prior to annealing. Text underneath the films is present to illustrate transparency of the films. 59

Figure 3.10: Height (a) and phase (b) AFM micrographs of solution cast film of Matrimid. 62

Figure 3.11: Height (a) and phase (b) AFM micrographs of solution cast film of Matrimid blended with 5 wt% Oligomer 1 62

Figure 3.12: Height (a) and phase (b) AFM micrographs of solution cast film of Matrimid blended with 10 wt% Oligomer 1 63

Figure 3.13: Elastic (E') and viscous (E'') modulus for films of Matrimid and blends yielded from dynamic mechanical analysis. All films annealed prior to testing 67

Figure 3.14: tan(δ) plots for Matrimid and Blends from dynamic mechanical analysis. All films annealed prior to testing 68

Figure 4.1: Schematic pictures of blend morphologies. The crosslinking agent is shown as the dark lines with the host Matrimid is shown as the lighter, continuous lines. 78

Figure 4.2: Diagram of gravimetric vapor sorption apparatus. Key components are: (B) electronic microbalance, (S) sample, (VO) ballast volume, (VA) vacuum pump, (P) pressure transducer, and (F) flask.[16] 82

Figure 4.3: Confirmation of p_{Tol}/p^0_{Tol} = 0.76 as a suitable preswelling condition. After initially exposing the 10% Oligomer 2 sample to 35 mmHg toluene (♦), isotherm data points were sequentially collected (□) and then points at p/p_0 = 0.43, 0.65 and 0.86 (○) were confirmed within +/- 1% of the originally recorded sorption values. 85

Figure 4.4: Sorption kinetics of toluene in thin films of Matrimid and blends with Oligomer 1 recorded for a $p = 0 \rightarrow 35$ mm Hg sorption step. M_t is mass of penetrant sorbed at time t; M_∞ is the mass of penetrant sorbed at equilibrium. The time scale has been normalized by polymer thickness. All materials display non-Fickian kinetics. 86

Figure 4.5: Toluene sorption isotherm in untreated Matrimid at 35 °C. The weight fraction of toluene corresponding to a glass transition for the sorbed polymer equal to the isotherm temperature as calculated by the Fox equation[31] shown by the dashed line. 91

Figure 4.6: Sorption of toluene in Matrimid modeled by the Dual Mode Sorption for low activities and Flory-Rehner at high activities. 94

Figure 4.7: Toluene sorption isotherm at 35 °C for annealed Matrimid compared to untreated Matrimid. 95

Figure 4.8: Sorption of toluene in Oligomer 1 blends at 35 °C. Untreated and annealed Matrimid included for comparison. Lines have been drawn for clarity. 97

Figure 4.9: Toluene sorption at 35 °C in raw Oligomer 1 crosslinking agent before and after activation of crosslinking. No sorption of toluene was observed after crosslinking above the error limits of the balance. 97

Figure 4.10: Plot of 10% Oligomer 1 blend toluene sorption with a fit based on interpreting the phase morphology as annealed Matrimid containing 8.4% inert, non-sorbing material. 98

Figure 4.11: Sorption of toluene in Oligomer 1 blends at 35 °C. Untreated and annealed Matrimid included for comparison. Lines have been drawn for clarity. 99

Figure 5.1: The hydroformylation of 1-dodecene to form tridecanal with a rhodium tristriphenylphosphine organometallic catalyst. 105

Figure 5.2: Diagram of experimental apparatus employed in rejection studies. 115

Figure 5.3: Hydraulic permeability and diffusivity of toluene in Matrimid and blends with Oligomer 1 measured at 35 °C. Transport data was obtained in hydraulic permeation. 120

Figure 5.4: Permeability and diffusivity of dodecene in Matrimid and blends with Oligomer 1 measured at 35 °C. Transport data was obtained in dialysis through toluene-swollen polymer. 125

Figure 5.5: Permeability and diffusivity of triphenylphosphine in Matrimid and blends with Oligomer 1 measured at 35 °C. Transport data was obtained in dialysis through toluene-swollen polymer. 125

Figure 5.6: Plot of single component permeability as a function of molar volume for hydroformylation components in annealed Matrimid (▲), 5% Oligomer 1 blend (○), and 10% Oligomer 1 blend (□). 126

Figure 5.7: Process flow diagram for two-stage membrane recovery of a homogeneous catalyst. Based on the catalyst rejection of the 10% Blend this results in catalyst rejections exceeding 99%. 132

Figure 6.1: Maxwell-Stefan view of diffusion as relative motion of components 1 and 2 caused by the exertion of a force on the two molecules. This force is balanced by frictional drag between the two components. 143

Figure 6.2: Flux-driving force relationship for toluene permeation in an annealed Matrimid film. The linear increase of flux with driving force indicates a constant $\widetilde{D}_{1M}$ over this concentration range according to Eq. 6.4. The volume fraction difference data points correspond to pressure driving forces = 25, 50, 75, 100 psi from left to right..... 149

Figure 6.3: Rejection of triphenylphosphine in solution with toluene in annealed Matrimid (▲), 5% Blend (●) and 10% Blend (■) as a function of pressure. Lines are the best fit for the modified Maxwell-Stefan transport equations with $\overline{D}_{12}$ as the adjustable parameter. Error bars are deviation from average values. 155

Figure 6.4: Predicted triphenylphosphine rejection for a composite membrane of annealed Matrimid blended with 8.4% filler (—) relative to annealed Matrimid and 10% Oligomer 1 Blend (--)..... 159

Figure 6.5: Model results showing the effect of diffusivity selectivity (α_D) and solvent content on solute rejection and solvent flux for a solubility selectivity of $\alpha_S = 1$..... 161

Figure 6.6: Model prediction of the relative change in rejection (R/R^0) as a function of the relative changes in membrane diffusivity selectivity (α_D/α_D^0) and solubility selectivity (α_S/α_S^0)..... 163

Figure A.1: Membrane permeation apparatus. Diagram of component parts and interconnecting tubing provided in Figure A.2. 176

Figure A.2: Diagram of membrane test permeation system for dialysis, hydraulic permeation, and rejection experiments. 177

Figure A.3: Schematic representation of transport of component *i* in a membrane. Gradients and concentration differences are exaggerated for effect. 178

Figure A.4: Sample calculation of toluene diffusivity in annealed Matrimid film in a hydraulic permeation experiment. The volume fraction driving force arises from the application of a pressure drop across the film. An average toluene diffusivity for the experiments is calculated from the slope of this line. Determination of volume fraction differences is shown in Table A.1. 187

Figure A.5: Sample calculation for the hydraulic permeability, A_0', for an annealed Matrimid film. Fluxes have been measured at various pressure drops, Δp, across the film. The linear relationship between driving force (abscissa) and flux allows determination of an average hydraulic permeability for the experimental pressure range..... 188

Figure A.6: Dodecene permeate concentration vs. time in dialysis experiment for a 10% Oligomer 1 Blend polymer film. The line shown is a fit of Eq. A.24 with dodecene permeability as the adjustable parameter..... 193

LIST OF TABLES

Table 2.1: Comparison of enzymes and transition metal catalysts for membrane recovery process..... 22

Table 2.2: Molecular weights and volumes for the 1-dodecene hydroformylation reaction. 29

Table 3.1: Oligomer batches fabricated for study and their corresponding degrees of polymerization (DP). 45

Table 3.2: Solvents used in film casting and solubility tests. 46

Table 3.3: Survey of oligomer solubility in various solvents. All tests conducted at ambient temperatures. Highly polar solvents (DMAc, DMF, DMSO, NMP, HFIP) were tested in a nitrogen atmosphere to eliminate exposure to atmospheric water. 50

Table 3.4: Summary of thermal properties of Oligomers 1 and 2 obtained in DSC. The content of terminal acetylenes relative to internal diacetylenes is provided to support the difference in reaction energy..... 57

Table 3.5: Analysis of AFM micrographs of Oligomer 1 blended with Matrimid. 63

Table 3.6: Glass transition temperatures, T_g, and crosslink densities, v, for Matrimid and blends. T_g's determined from maximum in E''.[41] v calculated using Eq. 3.2 for modulus data averaged over 380 – 400 °C. 70

Table 4.1: Blend formulations and Matrimid states studied in sorption experiments. 80

Table 4.2: Experimental parameters for sorption experiments. These are all values that can influence results due to history effects..... 84

Table 4.3: Flory-Rehner parameters (Eqs. 4.5 and 4.6) for toluene sorption in Matrimid and blends at 35°C. All values reported within +/- 5%. 94

Table 5.1: Physical properties of membrane feed components.[2] 106

Table 5.2: Hydroformylation reaction components studied in transport experiments. 108

Table 5.3: Reagents for transport studies and their function in the model reaction..... 110

Table 5.4: Thickness normalized fluxes of toluene in Matrimid and Oligomer 1 blends for a feed pressure of 10 atm at 35 °C..... 119

Table 5.5: Partition coefficients for dodecene (DOD) and triphenylphosphine (TPP) in Matrimid and blends with Oligomer 1 relative to solutions in toluene. 124

Table 5.6: Experimentally measured rejections for dodecene and triphenylphosphine in solution with toluene for Matrimid and Oligomer 1 Blends for a feed pressure of 7 atm at 35 °C. Rejection values reported as mean values with deviation as error. 128

Table 5.7: Predicted values for the rejections for dodecene and triphenylphosphine using the solution-diffusion model equations neglecting interactions between the solvent and solute in the membrane..... 128

Table 5.8: Rejection of $HRh(CO)(PPh_3)_3$ catalyst for various materials for a feed pressure of 7 atm at 35 °C. Feed for rejection experiments was a 2 mmol/L catalyst solution in toluene..... 130

Table 6.1: Indices for transport calculations. 147

Table 6.2: Experimentally measured values for toluene (1) and triphenylphosphine (2) used in Eqs. 6.17 and 6.18 to model transport in triphenylphosphine rejection. 155

Table 6.3: $\overline{D}_{12}$ values determined from least-squares fit of Eqs. 6.17 and 6.18 for rejection of triphenylphosphine (2) in solution with toluene (1). 156

Table A.1: Example of calculated volume fraction differences for the hydraulic permeation of toluene in annealed Matrimid at various pressures..... 187

SUMMARY

Homogeneous catalysts demonstrate the ability to perform extremely selective organic syntheses with high yields. These catalysts are usually quite expensive and the commercial viability of processes that use homogeneous catalysts depends on the efficiency of catalyst recovery, which is normally quite complex. This obstacle often excludes the use of homogeneous catalysts from commercial processes. This work investigates the implementation of membranes as the unit operation for catalyst recovery as a means to expand the use of homogeneous catalysis.

The oxo hydroformylation of 1-dodecene catalyzed by a rhodium-triphenylphosphine [$RhH(CO)(PPh_3)_3$] catalyst, a soluble transition metal complex, has been investigated as a model reaction to determine the membrane property requirements and transport phenomena present in membrane-mediated homogeneous catalyst recovery. The large size of the rhodium catalyst – and many other transition metal catalysts employed in organic synthesis (>400 Da) – relative to other components of the reaction provides the opportunity for a membrane separation based on retention of the catalyst species while permeating the other components. This liquid-phase organic synthesis presents the challenge of developing a membrane that is resistant but highly permeable to the organic chemicals of the reaction – which are typically quite aggressive to polymers – while at the same time maintaining the membrane's ability to reject the catalyst.

The membrane materials considered for this separation are blends of a high-performance commercial polyimide, Matrimid®, with a diacetylene-functionalized crosslinking agent. Characterization of the crosslinking agent has shown that it contains

two reactive functionalities, diacetylenes and terminal acetylenes. Each of these groups can be activated by thermal treatment at 250 °C for 24 hours to form a distributed network. Blending of these crosslinking agents with Matrimid has been performed for the purpose of enhancing material stability in the aggressive environment of the homogeneous catalysis solution.

Mixtures of crosslinking agent with Matrimid form compatible blends up to 10 wt% crosslinking agent content. Blends of 5 wt% (5% Blend) and 10 wt% (10% Blend) crosslinking agent in Matrimid exhibit two different morphologies. The 5% Blend appears to form a semi-interpenetrating network (s-IPN) with the crosslinking agent forming a network surrounding the host Matrimid. Blends containing 10% crosslinking agent exhibit a phase-separated morphology with domains of crosslinking agent dispersed in a continuous phase that is likely an s-IPN.

The blends enhanced the material stability and reduced polymer swelling in toluene, the model reaction solvent, as demonstrated in toluene sorption experiments. Heat treatment (250 °C for 24 hours) of Matrimid alone can also impart increased solvent resistance. The average reduction in Matrimid's sorption of toluene through heat treatment is 22% with the crosslinking agents adding another 7% reduction beyond that. Solvent sorption is sufficiently high to cause a transition in the polymers from a glassy to rubbery state as indicated from the sorption studies and toluene fluxes through the materials.

These materials have proved to be capable of permeating solvent and product at high fluxes while restricting the permeation of the rhodium-triphenylphosphine catalyst ligand complex. The 10% Blend gives the highest catalyst rejection at 91.5%. Rejection

efficiencies were: 10% Blend > 5% Blend > Matrimid. An estimate of the membrane area requirements using the properties of the 10% Blend indicate the feasibility of this material and membranes in general as a means to recover homogeneous catalysts.

In the investigation of separation characteristics of homogeneous catalyst recovery, it was found that flux coupling significantly affects the solute rejections that can be achieved by the membrane. Therefore, an analysis of the membrane transport observed in this work has been performed using modified Maxwell-Stefan equations, which describe multicomponent and coupled transport well. In this treatment, it was found that sorption of both the solute and solvent are key factors that influence coupling (with increasing levels of both increasing coupling) and consequently the level of solute rejection that can be achieved by the membrane. Lower sorption and diffusivity of the solute relative to the solvent both result in improved rejection, with sorption as the dominant factor of the two. Further analysis relating membrane material properties to the observed transport is contained in the following chapters with the aim of aiding future material selection for homogeneous catalyst recovery.

CHAPTER 1

INTRODUCTION

Homogeneous catalysis is an area rich with opportunities for the implementation of membranes as a means to recover and reuse catalysts. This work endeavors to expand the understanding of the factors governing transport in this type of membrane process. In its execution, novel membrane materials have been evaluated. Therefore, the overarching themes of this work are the characterization of these materials and assessment of their feasibility as homogeneous catalyst recovery membranes. The following chapter is an introduction to the concepts of membrane technology and the concerns relevant to the catalyst recovery application.

1.1 Membrane Technology

Membranes can offer a simple means of achieving a chemical separation. A membrane material's ability to preferentially transport one component over another, even at equal driving forces,[1] allows the separation to occur. There are two main routes, or membrane separation mechanisms, that can be exploited in a membrane material. One is the use of materials with fine pores, on the order of 0.1 to 10 μm,[2] to sieve particles larger than the pore diameters and allow smaller species to pass through the membrane. These microporous membrane materials perform well in applications with heterogeneous or macromolecular species that are to be rejected by the membrane. For separations involving species with size differences on the molecular scale or species of similar size, nonporous, dense membranes are used. In these membranes, the separation is based on the

relative transport rates of components through the material. These transport rates are determined by the component solubility and diffusivity in the membrane material.[3] As will be discussed in Section 1.2, the nonporous, dense membrane type is the focus of this research due to the small scale of the species to be retained by the membrane in most homogeneously catalyzed organic syntheses. These membranes can achieve remarkably high separation selectivities based on very subtle differences in component size. For example, oxygen and nitrogen have kinetic diameters of 3.46 and 3.64 Å, respectively,[4] and many glassy polymers (polymers below their glass transition temperature, T_g) have oxygen diffusivities in excess of *six* times greater than nitrogen.[5]

A majority of membranes in research and commercial use are organic polymers, owing to their facile processing into viable membrane forms and the variety of polymers available, as well as the ability to synthesize novel polymer structures. It is evident from the body of membrane research that the nature of the polymer material has a strong influence on species' permeation rates in nonporous membranes. Although, in general, membrane material selection is an empirical procedure, trends in the variance of membrane transport as a function of properties such as polymer free volume, composition of the polymer backbone, and polymer chain rigidity are fairly well understood. These structure-property relationships allow membrane researchers to better exploit the array of synthetically attainable polymers.

Membrane research can take a variety of approaches. Application specific studies conducted to optimize membrane material selection, evaluation of new membrane materials, and demonstration of new membrane applications are among some of the routes pursued by membrane researchers. In the research presented here, novel polymer

materials have been investigated for their applicability in a homogeneous catalyst recovery in an organic synthesis, focusing on the latter two research areas cited. Homogeneous catalyst recovery has not received much attention as a membrane application, due in part to some of the difficulties it presents.[6] The opportunities and challenges for membranes as a unit operation in homogeneous catalyst recovery will be presented in the following sections.

1.2 Membrane Recovery of a Homogeneous Catalyst

Homogeneous catalysts demonstrate the ability to perform extremely selective organic syntheses with high yields. However, heterogeneous catalysts are used in roughly 85% of all catalytic processes[7] owing to their greater range of thermal stability and general ease of separation, but inclusion of homogeneous catalysts into industrial processes is increasing as a result of their routinely higher selectivity and activity than their heterogeneous counterparts.

Soluble transition metal complexes are homogeneous catalysts that are capable of catalyzing a wide range of organic syntheses. Transition metal catalysts can provide extremely selective reactions that are faster and require fewer steps than stoichiometric or heterogeneously catalyzed reactions. However, these catalysts are usually expensive and the commercial viability of processes that use them depends on the efficiency of catalyst recovery, which is normally quite complex. Typically, conventional separation steps such as distillation or extraction result in degradation of the thermally and chemically sensitive catalysts. The factors of unacceptable catalyst losses in the product stream, through degradation, or both, coupled with poor process economics are the primary

reasons for the limited use of homogeneous catalysis in commercial processes. Membranes, due to their lack of thermal input, general chemical inertness, and energy efficiency are a potential means to circumvent these deleterious effects and effectively recover and recycle transition metal catalysts.

Dense, nonporous membranes can be used to selectively restrict permeation of the catalyst, which is typically large (>400 Da) relative to reaction product(s), while allowing the smaller, more permeable product(s) to pass through the membrane. A generic process approach to membrane recovery of a homogeneous catalyst is a system that has effluent from a reactor fed to a membrane separator that, under an imposed driving force (generally pressure), selectively retains the dissolved catalyst and permeates the product. The portion of the feed to the membrane that does not permeate through (defined as the "retentate") is catalyst-rich and recycled back to the reactor for further reaction.

1.3 Membrane Stabilization

The use of polymers as membrane materials for organic liquid separations is limited.[8] Many chemicals involved in organic synthesis are aggressive towards polymers. Because many commercially available polymers have an organic based repeat unit, the "like dissolves like" rule of thumb of solution chemistry is applicable and membranes made of these polymers tend to swell or even dissolve in an organic fluid environment. A major criterion for a membrane material to be utilized in a catalyst recovery operation is stability in the reaction environment. Catalytic reactions are typically run in solvent-rich environments that not only affect the long-term structure of a membrane polymer, but also the transport properties of the membrane due to polymer swelling and plasticiza-

tion that are likely to occur. Under these conditions, membrane separation performance often degrades and stabilization of the membrane material is necessary.

Stabilization can be achieved through a variety of routes. Material selection, blending, and crosslinking are methods that have been employed in similar environments to that of an organic synthesis and will be covered in more detail in subsequent sections of this thesis. In most cases, stabilization of a membrane material results in a compromise of membrane productivity, in terms of flux, in order to gain separation selectivity. This can often lead to fluxes that are too low for a membrane to be a viable unit operation. This work uses the stabilization method of polymer blending combined with covalent crosslinking. A commercial polyimide, Matrimid®, has been blended with crosslinkable oligomers functionalized with diacetylene groups that can be thermally crosslinked. In this manner, a polymer with high productivity has been combined with a crosslinkable component, with the objective of increasing the selectivity of the blend, while retaining some the productivity of the original material.

1.4 Research Objectives

The objectives of thesis research fall into two basic areas: membrane stabilization through blending with diacetylene-functionalized crosslinking agent and assessment of the feasibility of these materials for use as membranes for homogeneous catalyst recovery. In each case, the analysis draws from existing theories of polymer physics and transport so that the conclusions can be extended beyond the specific applications examined. Further detail on each objective is provided below.

1.4.1 Stabilization with Crosslinked Polyimide Blends

Development of polymer materials that are stable in aggressive environments is requisite for membrane recovery of a homogeneous catalyst, as outlined in Section 1.3. Polyimides have demonstrated their utility as membrane materials in a variety of applications including gas, vapor and liquid separations.[9-13] Their chemical resistance allows polyimides to be used in a variety of applications. Prior work of Rezac and Beckham[14-17] pertaining to gas separations has shown that further thermal and chemical stabilization of polyimides can be gained through the addition of crosslinkable diacetylene-functionalized oligomers in polymer blends. The same crosslinking method and blending has been extended to the aggressive solvent application of this research.

The specific approach taken in this research is to blend a commercially available polyimide, Matrimid®, with the crosslinkable oligomers for the optimization of membrane properties and economics. In order to fully understand the impact of the blends on membrane properties, characterization of the diacetylene reaction and blend morphologies have been conducted. In this manner, the practical and theoretical considerations for future work with these materials can be addressed in the conclusions.

1.4.2 Proof of Concept for Homogeneous Catalyst Recovery

Homogeneous catalyst recovery is a relatively new niche of membrane technology.[18] This work seeks to address the lack of information relating separation characteristics to material properties, particularly in nonporous membrane media. Additionally, it is of practical interest to examine the feasibility of using the materials outlined above for homogeneous catalyst recovery.

For these purposes, the hydroformylation of 1-dodecene has been analyzed as a model reaction for catalyst recovery. This reaction is catalyzed by a large rhodium-triphenylphosphine transition metal catalyst and is well suited for the membrane application following the rationale of Section 1.2. (Further details of the reaction are provided in Section 2.2). Transport of the individual reaction components will be investigated to determine the mechanisms of separation in membrane permeation studies. Further information on the effect of material properties on separation characteristics will be investigated by varying the concentration of crosslinking agent in blends with Matrimid.

1.5 Organization of the Dissertation

The thesis contains six subsequent chapters to address the above research objectives. Chapter 2 provides background information on transport in membranes as well as the model hydroformylation reaction used as a template for analysis. Chapter 3 characterizes the reaction of the diacetylene crosslinking agent and the morphology of blends with the commercial polyimide Matrimid® to provide some understanding of the material influence on transport properties observed in the subsequent chapters. In Chapter 4, the stability of the materials in the model reaction solvent, toluene, is studied through analysis of sorption in the polymers. Chapter 5 provides a detailed investigation of the transport of the various reaction components and ultimate catalyst recovery characteristics of the materials. Chapter 6 provides an analysis of the observed transport (coupled flux in particular) in terms of Maxwell-Stefan equations for multicomponent mixtures. Generalizations for membrane recovery of homogeneous catalysts based on the transport models are also provided in Chapter 6. Lastly, Chapter 7 provides a summary and

conclusions regarding the findings of this work as well as future directions for the homogeneous catalyst recovery process and the materials studied.

1.6 References

1. Michaels, A. S. and H. J. Bixler. In *Progress in Separation and Purification*, E. S. Perry, Ed.; Wiley-Interscience: New York, p 143 (1968).

2. Baker, R. W., *Membrane Technology and Applications*, McGraw-Hill: New York (2000).

3. Wijmans, J. G. and R. W. Baker, "The solution-diffusion model: a review," *J. Memb. Sci.*, **1**, 107 (1995).

4. Breck, D. W., *Zeolite Molecular Sieves*, John Wiley: New York (1974).

5. Robeson, L. M., "Correlation of Separation Factor versus Permeability for Polymeric Membranes," *J. Memb. Sci.*, **62**, 165 (1991).

6. Sirkar, K. K., P. V. Shanbhag and A. S. Kovvali, "Membrane in a reactor: A functional perspective," *Ind. Eng. Chem. Res.*, **38**, 3715 (1999).

7. Bhaduri, S. and D. Mukesh, *Homogeneous Catalysis*, John Wiley: New York (2000).

8. Bhanushali, D., S. Kloos, C. Kurth and D. Bhattacharyya, "Performance of solvent-resistant membranes for non-aqueous systems: solvent permeation results and modeling," *J. Memb. Sci.*, **189**, 1 (2001).

9. Ohya, H., V. V. Kudryavtsev and S. I. Semenova, *Polyimide membranes: applications, fabrications, and properties*, Gordon and Breach: Tokyo (1996).

10. White, L. S. and A. R. Nitsch, "Solvent recovery from lube oil filtrates with a polyimide membrane," *J. Memb. Sci.*, **179**, 267 (2000).

11. White, L. S., "Transport properties of a polyimide solvent resistant nanofiltration membrane," *J. Memb. Sci.*, **205**, 191 (2002).

12. Ren, J., C. Staudt-Bickel and R. N. Lichtenthaler, "Separation of aromatics/aliphatics with crosslinked 6FDA-based polyimides," *Sep. Purif. Tech.*, **22-23**, 31 (2001).

13. Okamoto, K., H. Wang, T. Ijyuin, S. Fujiwara, K. Tanaka and H. Kita, "Pervaporation of aromatic/non-aromatic hydrocarbon mixtures through crosslinked mem-

branes of polyimide with pendant phophonate ester groups," *J. Memb. Sci.*, **157**, 97 (1999).

14. Rezac, M. E., E. T. Sorensen and H. W. Beckham, "Transport properties of crosslinkable polyimide blends," *J. Memb. Sci.*, **136**, 249 (1997).

15. Bayer, B., B. Schoberl, K. Nagapudi, M. E. Rezac and H. W. Beckham, "Crosslinked diacetylene-functionalized polyimides for gas separation membranes: polymer reactivity and resultant properties," *ACS Symp. Ser.*, **733**, 244 (1999).

16. Rezac, M. E. and B. Schoberl, "Transport and thermal properties of poly(ether imide) acetylene-terminated monomer blends," *J. Memb. Sci.*, **156**, 211 (1999).

17. Sturgill, G. K., "Stabilization of polyimide blends through solid-state crosslinking," *Ph.D. Thesis*, Georgia Institute of Technology (1999).

18. Scarpello, J. T., D. Nair, L. M. F. dos Santos, L. S. White and A. G. Livingston, "The separation of homogeneous organometallic catalysts using solvent resistant nanofiltration," *J. Memb. Sci.*, **203**, 71 (2002).

CHAPTER 2

BACKGROUND

A review of material germane to the membrane recovery of homogeneous catalysts is presented in this chapter. An overview of membrane fundamentals and penetrant transport in polymers illustrates the factors that influence material selection. Following that, a review of catalyst recovery and the model reaction highlights the considerations necessary for the membrane process. The material presented here is intended as a general reference for the subsequent chapters. More details specific to the chapter topics are addressed therein.

2.1 Membrane Fundamentals

2.1.1 The Solution-Diffusion Model

The accepted model for permeation through a dense polymer film is the solution-diffusion model. This model describes the transport of a species through a membrane in three steps: (1) sorption of the solute onto the feed side of the membrane, (2) transport of the solute through the thickness of the membrane down a gradient in concentration, and (3) desorption of the solute into the fluid phase on the permeate side of the membrane. Steps 1 & 3 are referred to as "sorption" and Step 2 is "diffusion". This process is illustrated in Figure 2.1.

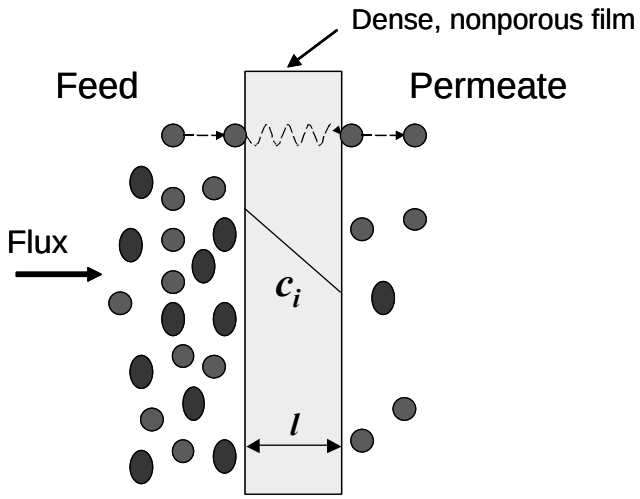

Figure 2.1: Schematic of transport of a binary mixture through a membrane following the solution-diffusion mechanism.

Transport across the membrane is motivated through the driving forces of pressure, concentration, temperature, and electromotive force (though not in consideration in this work). These forces can all be described through the thermodynamic property of chemical potential.[1] The flux of component *i* is related to the driving force of the gradient in chemical potential by a proportionality factor, L_i (which is usually not constant) and the relationship:

$$J_i = -L_i \nabla \mu_i \tag{2.1}$$

can be used to describe the component's transport through the film. Since in most cases the membrane is viewed as an infinite plane sheet, the flux occurs only one dimension and the equation is simplified to:

$$J_i = -L_i \frac{\partial \mu_i}{\partial x} \tag{2.2}$$

If a concentration gradient is the only driving force, the chemical potential is described by the equation:

$$\mathrm{d}\,\mu_i = RT\mathrm{dln}(\gamma_i c_i) \tag{2.3}$$

where γ_i is the activity coefficient relating concentration to activity. Combining Eq. 2.3 and Eq. 2.2 yields:

$$J_i = -\frac{RTL_i}{c_i}\frac{\partial c_i}{\partial x} \tag{2.4}$$

which is of the same form as Fick's Law for diffusion through an isotropic medium. This describes the diffusion of a component down a concentration gradient through random molecular motion, which is a governing equation for diffusion in polymer films.[2] If D_i, a concentration dependent diffusion coefficient averaged over the range of concentrations, replaces the RTL_i/c_i term, the familiar form of Fick's Law is obtained. Integrating Fick's Law for the thickness of the membrane yields:

$$J_i = D_i\frac{c_{io}^m - c_{il}^m}{l} \tag{2.5}$$

with the superscript *m* indicating that concentration is that of the membrane phase and *l* as the membrane thickness. Subscript *o* denotes the feed position of the membrane and subscript *l* denotes the permeate position in the membrane. Thus, the term c_{io}^m is the concentration in the membrane of component *i* at the feed side.

The solution-diffusion model can be used to describe all methods of membrane separations[3] provided an equilibrium relationship between the penetrant in the membrane phase (c_i^m) and the feed and permeate phases is established. Equilibrium between the continuous phases and the membrane at the feed and permeate sides is a valid assumption

for most membrane processes,[3] save those that involve a chemisorption mechanism, which are not in the scope of this research. The use of a simple partitioning relationship for the concentration of a component in the continuous phase and the membrane at its surface, $c_i^m = K_i c_i$, illustrates the origins of membrane permeability. Substituting this relationship into Eq. 2.5 gives:

$$J_i = D_i \frac{(K_{io} c_{io} - K_{il} c_{il})}{l} \tag{2.6}$$

The product of the partition coefficient and diffusivity is the membrane permeability (Eq. 2.7). Permeability is a property that is extensively used to characterize membrane transport and has the advantage of predicting component fluxes for varying driving forces. Granted, many membrane separations do not follow the simple Henry's Law equilibrium from which Eq. 2.6 was derived, but this simplified approach is provided to illustrate the manifestation of the solution-diffusion model as a permeability that is a function of solute diffusivity and solubility in the membrane material. Application of solubility relationships for specific membrane processes still results in the fundamental characteristic of having penetrant solubility and diffusivity as the material properties that influence flux.

$$P_i = D_i K_i \tag{2.7}$$

Separation of mixtures in membranes is achieved through selective permeation of components. Therefore, membrane material selection aims to maximize the difference in permeability among feed components. Eq. 2.7 illustrates that this can achieved through the two processes of diffusion and sorption in the membrane material. The challenge for

the membrane researcher is to find a membrane material that exploits differences in one or both of these properties for a given feed mixture.

A value commonly used to characterize a membrane's preferential transport of one component versus another is the ideal selectivity α^*. The ideal selectivity of a membrane for component A over B is shown in Eq. 2.8 and is simply the ratio of the permeability of component A to that of component B. If this value is positive, then the membrane selectively transports component A. Selectivity can be further broken down into its fundamental components of diffusivity selectivity, α_D, and solubility selectivity, α_S (Eqs. 2.9 and 2.10, respectively). In many cases one of these properties dominates and the membrane is said to be either "solubility selective" or "diffusivity selective."

$$\alpha_{AB}^{*} = \frac{P_A}{P_B} = \alpha_D \alpha_S \tag{2.8}$$

$$\alpha_D = \frac{D_A}{D_B} \tag{2.9}$$

$$\alpha_S = \frac{K_A}{K_B} \tag{2.10}$$

Another quantity describing the separation characteristics of the membrane materials in this work is the rejection, $\Re$ (Eq. 2.11). The rejection is a measure of the membrane's ability to separate a dissolved solute from a feed solution and is expressed as a percentage of the feed concentration of solute retained by the membrane. For a perfectly permselective membrane, $c_{jl} = 0$, and $\Re$=100%. Unlike the ideal selectivity, which can be obtained from single component experiments, the rejection is a quantity that is observed from the permeation of mixtures.

$$\Re = \left(\frac{c_{jo} - c_{jl}}{c_{jo}} \right) \times 100 \tag{2.11}$$

As previously stated, these are simplified models presented to illustrate the fundamental properties that can be manipulated by the membrane researcher to affect a separation through material selection. Methods to determine permeabilities and their constituent properties for applications specific to this research will be given in Chapter 5 and Appendix A. Also, it should be noted that this development of membrane transport does not account for bulk flux effects and diffusion coupling, which influence the separations involved in this research and will be covered in detail in Chapter 6.

2.1.2 Sorption and Diffusion in Polymers

As conclusions in this research will be drawn on the basis of solubility and diffusivity interactions between the mobile species and polymers being studied, a review of some of the fundamental factors controlling these properties is provided below.

The thermodynamic interactions between the penetrant and the polymer dictate the level of sorption. Physicochemical forces such as dispersion forces, hydrogen bonding, and polarity influence the level of attraction of the polymer and penetrant molecules.[4] As these physicochemical forces increase between the polymer and the penetrant, so does the amount of penetrant sorbed. When the forces of attraction are sufficiently strong, swelling of the polymer or dissolution results. In the opposite extreme of forces of repulsion between the polymer and penetrant, the penetrant is absent from the membrane phase. Often in liquid separations, the solubility parameters of the permeating species can be used to predict their relative solubility in a membrane material.[4]

The rate of diffusion of a permeating species is dictated by its surrounding environment. In a dense polymer film, the permeant molecule is in contact with segments of the polymer chain. An amorphous polymer, or amorphous portion of a semi-crystalline polymer, contains unoccupied regions between the polymer molecules resulting from packing defects called free volume. The amount of free volume in membrane polymers is characterized by its fractional free volume (FFV). A sorbed molecule occupies these gaps between the polymer segments. The frequency and size of the motions of the polymer chains (and permeant molecule) are the determining factors for the rate of diffusion.

Diffusion of a component through a polymer requires gaps in the polymer's free volume equal to or greater in size than its own. Mobility selectivity discriminates between solutes based on their size and frequency of their motion. If the movement of a solute through a dense, isotropic polymer matrix occurs through a characteristic jump length, λ, and frequency, f, the diffusion coefficient can be described as:

$$D = \frac{f\lambda^2}{6} \tag{2.12}$$

The diffusion coefficient can be expressed as an Arrhenius relationship as a function of a preexponential factor, activation energy for diffusion, and temperature.[5] The activation energy of diffusion has an inverse dependence on the size of the gap required for solute diffusion, indicating that diffusivity decreases for solutes of increasing size.[6] For catalyst recovery in nonporous membranes, this relationship allows for the faster diffusion of smaller species relative to the catalyst. For polymers above their glass transition temperature, called rubbery polymers, segments of the polymer chain can freely rotate around their axis. These segmental motions are normally large in scale

relative to the penetrant molecule, and result in high diffusion coefficients relative to glassy polymers but usually at the expense of mobility selectivity.

Increased segmental mobility of polymers can also occur as a result of plasticization. If a permeating component sorbs to a sufficient extent, interactions between the penetrant and polymer cause the polymer mobility to increase. This results in increased diffusion coefficients for all components in the polymer. Often the change in diffusion is greater for the larger species, resulting in a drop in mobility selectivity. Plasticization is relevant to membranes for homogeneous catalyst recovery as a result of the typically high affinity polymers have for common solvents. Techniques for the stabilization and plasticization reduction of polymers exposed to aggressive feeds are addressed in the following section.

2.1.3 Membrane Stabilization Techniques

Polymer modification for aggressive feed applications follows two general paths for gaining stability: restriction of polymer mobility or selection of materials with limited affinity for the penetrants. Each of these methods involves a compromise in flux due to reduced diffusivity (mobility restriction) and / or sorption (limited affinity). Typically a balance between flux loss and stability is achieved in the final material used for the membrane separations.

The bulk of work with hydrocarbons in membranes is in pervaporation, a membrane separation of a liquid feed mixture with a vapor phase permeate. Examples of each of the two stabilization methods have been employed with success in pervaporation. For the reduction of penetrant sorption in the membrane, blends or copolymers containing

functional groups that have alternating strong and weak interactions with the selectively permeating component can be employed for stability. Using a solubility parameter approach to predict strength of interaction, Cabasso[7] formed blends of cellulose acetate and a polyphosphonate that gave selective separations of benzene for a benzene / cyclohexane feed mixture. Tanihara et al.[8] achieved a benzene selective material for the same separation with a copolymer containing alternating hard polyimide segments and soft polyether segments for this separation. These are but two of a host of examples[9-13] highlighting the success of the solubility restriction approach to membrane stabilization. This type of approach for polymer selection is best suited for membrane separations that require a high degree of solubility selectivity. Although the catalyst recovery application is predominantly based on mobility selectivity, the blends and copolymers are a valuable illustration of membrane stability that can be imparted through their use.

Polymer stabilization via crosslinking achieves mobility restriction and this process is more suited to size selective membrane processes. In crosslinking, covalent or ionic bonds are formed between the polymer chains. A requisite for membrane materials is the ability to process them into thin films. Consequently, crosslinking of these materials is performed in the solid-state after they are processed. Several groups have developed stable materials for the selective pervaporation of hydrocarbons through post-processed crosslinking of films. The work of Okamoto et al.,[14,15] Ren et al.,[16] and Xu et al.[17] with polyimides have shown increased polymer stability and membrane selectivity upon the introduction of crosslinks.

Polyimides in general are good materials for organic liquid separations due to their chemical resistance. Application of polyimides in nanofiltration studies (which

more closely resemble catalyst recovery) by White[18,19] and Ohya et al.[20] showed long-term stability and selectivity for the rejection of higher hydrocarbons from low molecular weight solvents.

The stabilization approach of this work is a combination of blending and crosslinking. In an effort to achieve the balance between flux and selectivity, a high performance commercial polyimide, Matrimid® (manufactured by Ciba-Geigy), has been blended with a diacetylene-functionalized crosslinking agent (Figure 2.2). The utility of blending a crosslinking agent with a high permeability host polymer has been demonstrated by Bos et al.[21] through reduction of plasticization of the blends in CO_2/CH_4 separations. Prior work with polyimides blended with a diacetylene-functionalized crosslinking agent[22-24] has shown increased chemical and thermal resistance for blends compared to the host polymer, indicating the promise of these materials for the catalyst recovery application of this work.

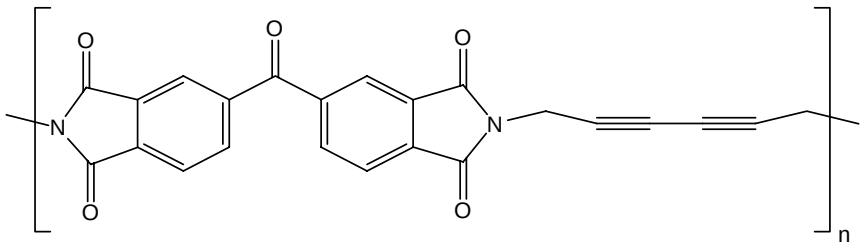

Figure 2.2: Structure of the diacetylene crosslinking agent (1,1-BTDA-DIA) used in this work.

2.2 Catalyst Recovery Background

Because of their large size (>400 Da) relative to reaction products, transition metal catalyst recovery can be envisioned as a membrane process that restricts permeation of the catalyst, while allowing the smaller, more permeable product(s) to pass through the membrane. A generic process approach to membrane recovery of a homogeneous catalyst is a system to have effluent from a reactor fed to a membrane separator that, under an imposed driving force (generally pressure), selectively retains the dissolved catalyst and permeates the product (Figure 2.3). The portion of the feed to the membrane that does not permeate through the membrane (defined as the "retentate") is catalyst-rich and recycled back to the reactor for further reaction.

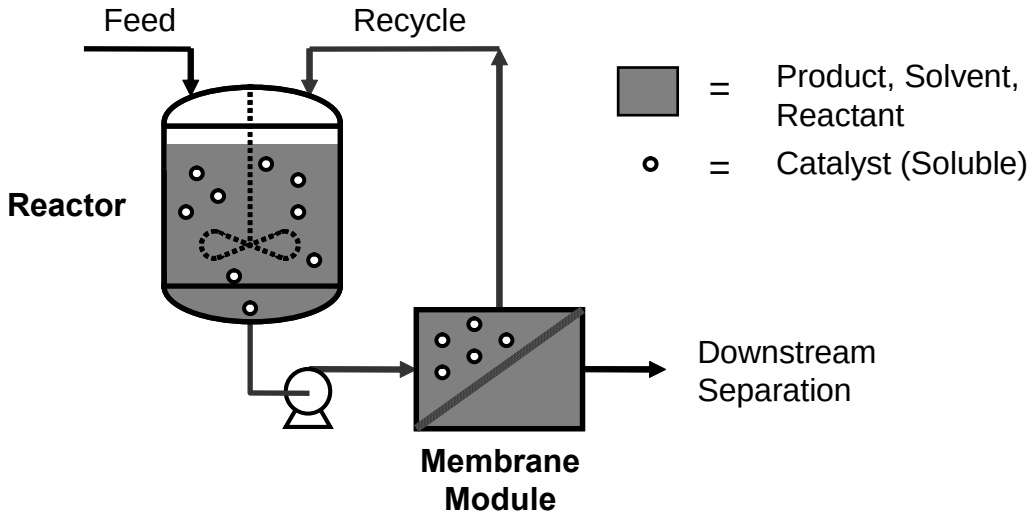

Figure 2.3: General representation of homogeneous catalyst recovery

Strictly speaking, Figure 2.3 is not necessarily a membrane reactor per se, but a reactor using a membrane as the unit operation to recover and recycle the catalyst. Due

to the dependence of the catalyst and reactant concentrations on the membrane permeability, many people consider the two operations coupled and include them in their discussions on membrane reactors.[25,26] The separation of the reactor and membrane unit has advantages such as: separating reaction and membrane engineering, scalability (with membrane modules), independent operating conditions (flow, mixing, temp.) in each unit, and capital cost (assuming that a true membrane reactor would have high engineering costs)

An example of this type of process is the recovery of enzymes in enzyme-catalyzed syntheses using ultrafiltration (UF) membranes (membranes with pore diameters between 1 and 100 nm). It is a well-established process originated in the late 1960's and early 70's[27-29] and used commercially for the manufacture of amino acids.[30,31] The macromolecular nature of the enzymes (Mol. Wt.; 10,000 – 100,000 Da) enables the continuous pores of the UF membranes to retain and segregate them from the aqueous products that permeate through. The demonstrated success of this membrane process is a function of the high enzyme recoveries achieved with UF membranes (>99%), high product fluxes, and membrane stability.

When considering membranes for the recovery of the transition metal catalysts of interest in this research, the process of material selection becomes significantly more complex than the case of enzyme recovery. Due to the smaller size of transition metal catalysts (Table 2.1), particularly relative to the other feed components to the membrane, ultrafiltration membranes are generally unable to recover the catalyst at appreciable levels, if at all. Dense, non-porous membranes, such as those used for the reverse osmosis desalination of water, are capable of selectively rejecting solutes that are on the same

size scale as the solvent to be permeated. Since there are no pores, transport occurs via the solution-diffusion mechanism (Section 2.1.1), in which selective separations occur as a result of differences in component solubilities and diffusivities in the membrane material. The nature of the material strongly influences these properties and subsequently the selectivity of separation that can be achieved. A caveat that accompanies the higher selectivity that can be achieved with the solution-diffusion membranes is a typically lower flux due to the reliance on diffusion versus flow through pores.

Table 2.1: Comparison of enzymes and transition metal catalysts for membrane recovery process

Catalyst	Mol. Wt. (Da)	Membrane Type
Enzyme	10,000 – 100,000	Ultrafiltration
Transition Metal	400-1000	Dense, non-porous

This relationship is illustrated for desalination of water using membranes of different separation regimes in Figure 2.4. (As labeled on the graph, the "reverse osmosis region" denotes nonporous membranes; nanofiltration is defined as the transition region between porous and nonporous membranes.) Ultrafiltration membranes provide fluxes exceeding two orders of magnitude higher than the nonporous films tested in this study. However, their salt rejection – defined as the percentage of the feed concentration of solute retained by the membrane – is far lower than the nonporous membranes. Most catalyst recovery applications will require catalyst rejections greater than 99%, falling into the area of operation where flux is sacrificed for higher membrane selectivity. Lower fluxes translate to larger membrane areas.

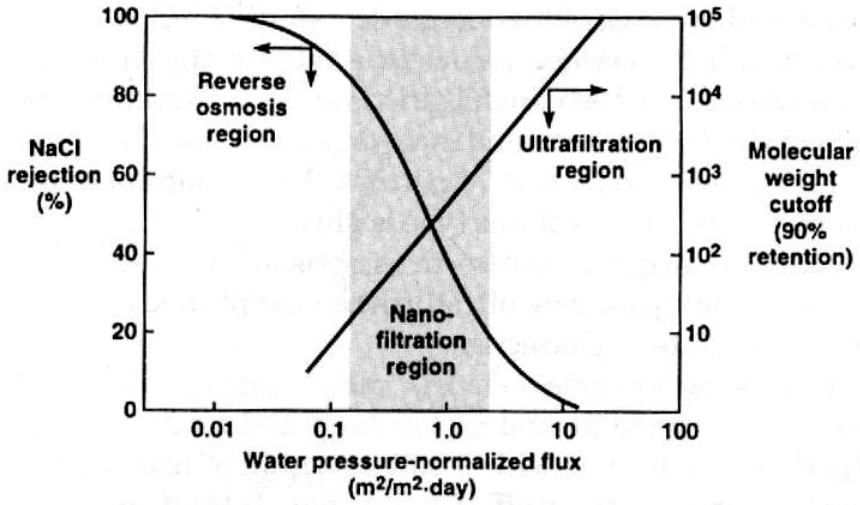

Figure 2.4: Membrane performance in desalination of water for different membrane types.[32,33]

The sacrifice of membrane productivity, in terms of flux, as well as the complexity of material selection has led some researchers to pursue alternatives to using homogeneous catalysts in their "native" state. One method is to enlarge the catalyst, which is accomplished by attaching large (usually polymeric), soluble ligands to the catalyst center[34,35] or through the formation of catalytic dendrimers,[36,37] star-shaped macromolecules with catalytic sites at the chain-ends. In each of these cases, retention of the enlarged catalytic species has been demonstrated using commercial nanofiltration, and ultrafiltration membranes. Some drawbacks of this catalyst modification are that the synthesis of the enlarged catalysts is typically complex and the catalyst has limited solubility. Another approach is to impregnate polymers with the catalyst and use the resulting polymer-catalyst matrix as a reactive membrane or heterogeneous pellet.[26] However, implementation of these so-called "heteroginized" homogeneous catalysts has

been hampered due to catalyst leaching, mass transfer limitations in the polymer, and dispersion of the catalyst in the polymer phase during formulation.

Both of the methods cited for catalyst modification require the reaction engineering and kinetics to be readdressed after the alterations to the catalyst are made. Reaction mechanisms involving transition metal catalysts often include many steps (Figure 2.7) of complexation and de-complexation of ligands and reactant. When the composition of the ligand or the phase of the reaction is changed, it is likely that the reaction kinetics and selectivity will also be altered. In some cases, the effect of catalyst modification can be beneficial,[38] but there are an equal or greater number for which this is not true and in either case, further investigation of the reaction behavior after catalyst modification is required.

A membrane capable of containing the "off the shelf" catalyst would provide a more ubiquitous solution to this problem of catalyst recovery. Membrane-mediated catalyst recycle for transition metal catalysts has been demonstrated with some success in the past,[39-41] but these studies were performed as proof of concept exercises and provide little insight into membrane engineering required to achieve catalyst recovery. A fundamental understanding of the behavior of membrane materials in the type of systems under consideration for catalyst recovery will provide a basis for future development of membranes and material selection for this application.

2.2.1 Model Reaction: Hydroformylation of 1-Dodecene

For some industrial processes, the economic problem of catalyst separation has been eclipsed by the benefits of these homogeneous catalysts offer. One such process is

the rhodium-catalyzed oxo hydroformylation of terminal alkenes to form aldehydes (Figure 2.5), which provides the benefits of mild reaction conditions, high efficiencies, and high yields. A majority of commercial hydroformylation processes use distillation as the primary means for catalyst recovery. This requires the use of a reaction solvent that has a higher boiling point than the aldehyde product so the dissolved, nonvolatile catalyst and solvent can be recovered in the column bottoms. Although distillation is feasible for lower molecular weight aldehydes, the separation of aldehydes with carbon numbers greater than C_6-C_7 poses great difficulties.[42] The higher boiling point of these products requires higher temperatures for their volatilization, which causes separation problems due to the narrowing differences in product and catalyst solution volatilities. More importantly, the catalyst thermal stability range is encroached at these higher distillation temperatures and degradation significantly increases.

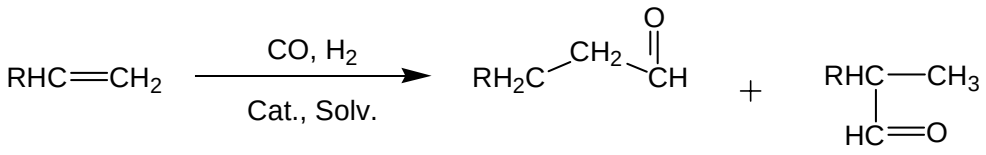

Figure 2.5: Hydroformylation of a terminal alkene.

Alternatives to distillation as the catalyst recovery step have been proposed. Water-soluble rhodium complexes have been developed[43,44] and implemented[45] utilizing a liquid-liquid separation of the aqueous phase from the organic product to recover the catalyst. In the hydroformylation of propylene and butyraldehyde, catalyst recovery is extremely efficient, with catalyst losses in the parts per billion range.[42] However, hydroformylation of the higher molecular weight aldehydes is limited with this system as well.

The solubility of the higher olefin reactants in the aqueous phase is not sufficient to give an acceptable reaction rate.[42] Another proposed means of performing hydroformylation with limited catalyst loss is the use of immobilized catalysts[46,47] such as those cited in at the beginning of this section. These have not achieved technical realization due mainly to insufficient long-term stability.

Another attractive feature of the hydroformylation reaction is that it is particularly well suited for a membrane separation because of the use of hydrogen and carbon monoxide (syngas) at high pressures (12-50 bar), present as a reactant. The pressure of the syngas can act as the driving force for membrane permeation. For this and the above reasons hydroformylation is a reaction that membrane catalyst recovery can expand and at the same time, fit well into the existing framework of the commercial reaction.

The specific hydroformylation that has been examined in this research is the reaction of 1-dodecene (C_{12}) to form tridecanal (C_{13}), shown in Figure 2.6. It is a reaction that presents difficulties in catalyst separation due to the higher molecular weight constituents, making it an interesting subject for membrane research. The rhodium tris(triphenylphosphine) [$HRh(CO)(PPh_3)_3$] catalyst is the predominant catalyst used commercially[48] and in the presence of excess triphenylphosphine (PPh_3) ligand gives high yields of the linear versus branched aldehyde products**.**

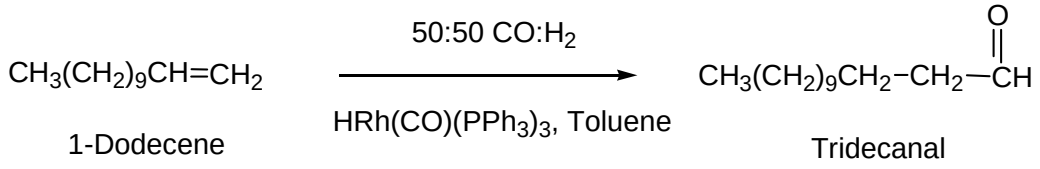

Figure 2.6: Hydroformylation of 1-dodecene

The commercial value of tridecanal is as a fragrance compound as well as an intermediate for the formation of an alcohol, which can be used as a surfactant or plasticizer.[49] Bhanage et al.[50] have conducted a thorough examination of the kinetics of this reaction.

The mechanism for the catalysis of this reaction using the rhodium triphenylphosphine catalyst-ligand complex is shown in Figure 2.7. This is provided as an illustration of the presence of free triphenylphosphine ligand and the general complexity of the reaction. It would be advantageous to retain the free ligand with the catalyst recovery membrane in addition to the whole catalyst since it is a necessary part component in the catalytic cycle.

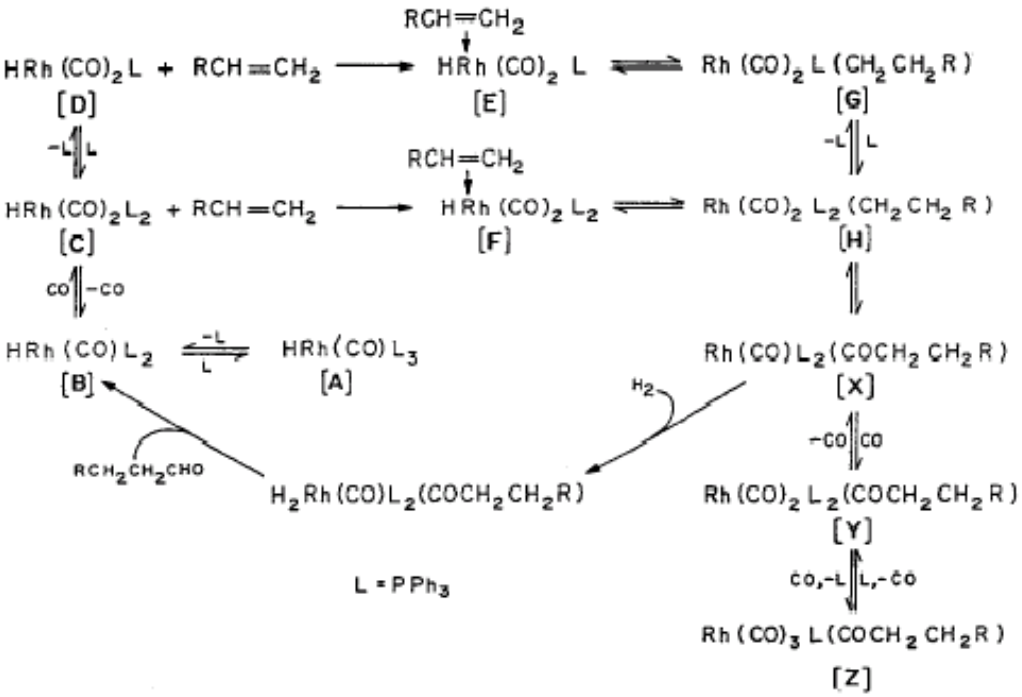

Figure 2.7: Mechanism for hydroformylation of terminal olefins catalyzed by carbonylhydridotris(triphenylphsophine) rhodium(I).[51,52]

As shown in Figure 2.8 and Table 2.2, the catalyst is the largest molecule that will be fed to the membrane, similar to the enzyme recovery reviewed in Section 2.2. This should aid in providing membrane selectivity for rejecting the catalyst based on its lower relative diffusion rate (called diffusivity selectivity which will be defined in Section 2.1). As species size increases, polymeric solution-diffusion membranes generally have decreasing solute diffusivities, due to the increased polymer chain motion required to move through the polymer matrix.

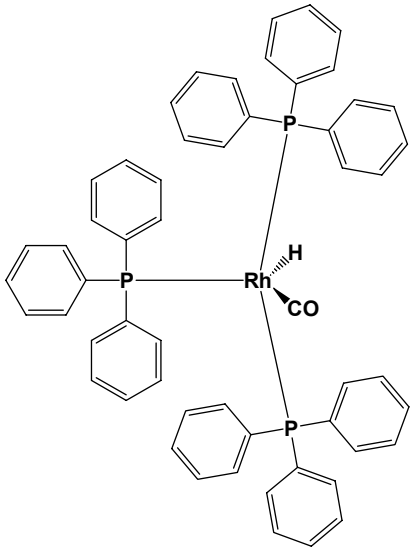

Figure 2.8: Structure of hydroformylation catalyst

Table 2.2: Molecular weights and volumes for the 1-dodecene hydroformylation reaction.[53]

Component	Mol. Weight (g/mol)	van der Waals Volume (cm^3/mol)
$HRh(CO)(PPh_3)_3$	919	517[a]
Triphenylphosphine	262	161
Tridecanal	198	149
1-Dodecene	168	126
Toluene	92	60

[a]Additive contribution of tristriphenylphosphine, rhodium, carbon monoxide and hydrogen

2.3 References

1. Mulder, M., *Basic Principles of Membrane Technology*, Kluwer Academic: Dordrecht, Netherlands (1991).

2. Crank, J. and G. S. Park, *Diffusion in Polymers*, Academic Press: New York (1968).

3. Wijmans, J. G. and R. W. Baker, "The solution-diffusion model: a review," *J. Memb. Sci.*, **107**, 1 (1995).

4. Lloyd, D. R. and T. B. Meluch, "Selection and evaluation of membrane materials," *Mat. Sci. of Synth. Membr.: ACS Symp. Ser.*, **269**, 47 (1985).

5. Barrer, R. M., "Nature of the diffusion processes in rubber," *Nature*, **140**, 106 (1937).

6. Koros, W. J., M. R. Coleman and D. R. B. Walker, "Controlled permeability polymer membranes," *Annu. Rev. Mater. Sci.*, **22**, 47 (1992).

7. Cabasso, I., "Organic liquid mixtures separation by permselective polymer membranes. 1. Selection and characteristics of dense isotropic membranes employed in the pervaporation process," *Ind. Eng. Chem. Prod. Res. Dev.*, **22**, 313 (1983).

8. Tanihara, N., N. Umeo, T. Kawabata, K. Tanaka, H. Kita and K. Okamoto, "Pervaporation of organic liquid mixtures through poly (ether imide) segemented copolymer membranes," *J. Memb. Sci.*, **104**, 181 (1995).

9. Villaluenga, J. P. G. and A. Tabe-Mohammadi, "A review on the separation of benzene/cyclohexane mixtures by pervaporation processes," *J. Memb. Sci.*, **169**, 159 (2000).

10. Acharya, H. R., S. A. Stern, Z. Z. Liu and I. Cabasso, "Separation of liquid benzene cyclohexane mixtures by perstraction and pervaporation," *J. Memb. Sci.*, **37**, 205 (1988).

11. Ho, W. S. W., G. Sartori and D. A. Thaler, "Polyimide copolymers containing polycarbonate soft segment," In *U.S. Patent No. 5,756,643* (1998).

12. Tanihara, N., K. Tanaka, H. Kita and K. Okamoto, "Pervaporation of organic liquid mixtures through membranes of polyimides containing methyl-substituted phenylenediamine moieties," *J. Memb. Sci.*, **95**, 161 (1994).

13. Yamaguchi, T., S. Nakao and S. Kimura, "Plasma-graft filling polymerization - preparation of a new type of pervaporation membrane for organic liquid mixtures," *Macromolecules*, **24**, 5522 (1991).

14. Fang, J., K. Tanaka, H. Kita and K. Okamoto, "Pervaporation properties of ethynyl-containing copolyimide membranes to aromatic/non-aromoatic hydrocarbon mixtures," *Polymer*, **40**, 3051 (1999).

15. Okamoto, K., H. Wang, T. Ijyuin, S. Fujiwara, K. Tanaka and H. Kita, "Pervaporation of aromatic/non-aromatic hydrocarbon mixtures through crosslinked membranes of polyimide with pendant phophonate ester groups," *J. Memb. Sci.*, **157**, 97 (1999).

16. Staudt-Bickel, C. and W. J. Koros, "Improvement of CO2/CH4 seoparation characteristics of polyimides by chemical crosslinking," *J. Memb. Sci.*, **155**, 145 (1999).

17. Xu, W. Y., D. R. Paul and W. J. Koros, "Carboxylic acid containing polyimides for pervaporation separations of toluene/iso-octane mixtures," *J. Memb. Sci.*, **219**, 89 (2003).

18. White, L. S. and A. R. Nitsch, "Solvent recovery from lube oil filtrates with a polyimide membrane," *J. Memb. Sci.*, **179**, 267 (2000).

19. White, L. S., "Transport properties of a polyimide solvent resistant nanofiltration membrane," *J. Memb. Sci.*, **205**, 191 (2002).

20. Ohya, H., I. Okazaki, M. Aihara and S. Tanisho, "Study on molecular weight cut-off performance of asymmetric aromatic polyimide membrane," *J. Memb. Sci.*, **123**, 143 (1997).

21. Bos, A., I. G. M. Punt, M. Wessling and H. Strathmann, "Suppression of CO_2-plasticization by semiinterpenetrating polymer network formation," *J. Polym. Sci. B: Pol. Phys.*, **36**, 1547 (1998).

22. Rezac, M. E., T. John and P. H. Pfromm, "Effect of copolymer composition on the solubility and diffusivity of water and methanol in a series of polyether amides," *J. Appl. Polym. Sci.*, **65**, 1983 (1997).

23. Bayer, B., B. Schoberl, K. Nagapudi, M. E. Rezac and H. W. Beckham, "Crosslinked diacetylene-functionalized polyimides for gas separation membranes: polymer reactivity and resultant properties," *ACS Symp. Ser.*, **733**, 244 (1999).

24. Sturgill, G. K., "Stabilization of polyimide blends through solid-state crosslinking," *Ph.D. Thesis*, Georgia Institute of Technology (1999).

25. Sirkar, K. K., P. V. Shanbhag and A. S. Kovvali, "Membrane in a reactor: A functional perspective," *Ind. Eng. Chem. Res.*, **38**, 3715 (1999).

26. Vankelecom, I. F. J., "Polymeric membranes in catalytic reactors," *Chem. Rev.*, **102**, 3779 (2002).

27. Michaels, A. S. In *Progress in Separation and Purification*, E. S. Perry, Ed.; Wiley-Interscience: New York, p 297 (1968).

28. Ghose, T. K. and J. T. Kostic, "A model for continuous enzymatic saccharification of cellulose with simultaneous removal of glucose syrup," *Biotechnol. Bioeng.*, **12**, 921 (1970).

29. Closset, G. P., Y. T. Shah and J. T. Cobb, "Analysis of membrane reactor performance for hydrolysis of starch by glucoamylase," *Biotechnol. Bioeng.*, **15**, 441 (1973).

30. Wandrey, C., R. Wichmann, W. Leuchtenberger and M. R. Kula, "Process for the continuous enzymatic change of water soluble α-ketocarboxylic acids into the corresponding amino acids," In *U.S. Patent No. 4,304,858* (1981).

31. Woltinger, J., K. Drauz and A. S. Bommarius, "The membrane reactor in the fine chemicals industry," *Appl. Catal. A-Gen.*, **221**, 171 (2001).

32. Baker, R. W., *Membrane Technology and Applications*, McGraw-Hill: New York (2000).

33. Egli, S., A. Ruf and F. Widmer, "Entwicklung und Charakterisierung von Kompositmembranen," *Swiss Chem.*, **11**, 53 (1989).

34. Felder, M., G. Giffels and C. Wandrey, "A polymer-enlarged homogeneously soluble oxazaborolidine catalyst for the asymmetric reduction of ketones by borane," *Tetrahedron-Asymm.*, **8**, 1975 (1997).

35. Giffels, G., J. Beliczey, M. Felder and U. Kragl, "Polymer enlarged oxazaborolidines in a membrane reactor: enhancing effectivity by retention of the homogeneous catalyst," *Tetrahedron-Asymm.*, **9**, 691 (1998).

36. Astruc, D. and F. Chardac, "Dendritic catalysts and dendrimers in catalysis," *Chem. Rev.*, **101**, 2991 (2001).

37. Oosterom, G. E., J. N. H. Reek, P. C. J. Kamer and P. W. N. M. van Leeuwen, "Transition metal catalysis using functionalized dendrimers," *Angew. Chem. Int. Edit.*, **40**, 1828 (2001).

38. Neys, P. E. F., A. Severeyns, I. F. J. Vankelecom, E. Ceulemans, W. Dehaen and P. A. Jacobs, "Manganese porphyrins incorporated in polydimethylsiloxane membranes: selective catalysts for the epoxidation of deactivated alkenes," *J. Mol. Catal. A: Chem.*, **144**, 373 (1999).

39. Miller, J. F., D. R. Bryant, K. H. Hoy, N. E. Kinkade and R. H. Zanapalidou, "Membrane separation process," In *US Patent No. 5,681,473* (1997).

40. De Smet, K., S. Aerts, E. Ceulemans, I. F. J. Vankelecom and P. A. Jacobs, "Nanofiltration-coupled catalysis to combine the advantages of homogeneous and heterogeneous catalysis," *Chem. Commun.*, 597 (2001).

41. Nair, D., S. S. Luthra, J. T. Scarpello, L. S. White, L. M. F. dos Santos and A. G. Livingston, "Homogeneous catalyst separation and re-use through nanofiltration of organic solvents," *Desalination*, **147**, 301 (2002).

42. Beller, M., B. Cornils, C. D. Frohning and C. W. Kohlpaintner, "Progress in hydroformylation and carbonylation," *J. Mol. Catal. A: Chem.*, **104**, 17 (1995).

43. Kuntz, E. G., "Homogeneous Catalysis ... In Water," *Chemtech*, **17**, 570 (1987).

44. Herrmann, W. A., C. W. Kohlpaintner, H. Bahrmann and W. Konkol, "Water-Soluble Metal-Complexes and Catalysts .6. A New, Efficient Water-Soluble Catalyst for 2-Phase Hydroformylation of Olefins," *Journal of Molecular Catalysis*, **73**, 191 (1992).

45. Chauvel, A., B. Delmon and W. F. Holderich, "New Catalytic Processes Developed in Europe During the 1980s," *Appl. Catal. A-Gen.*, **115**, 173 (1994).

46. Ro, K. S. and S. I. Woo, "Catalytic Properties of $RhCl_3$-H_2O Immobilized on the Modified Poly(Styrene-Divinylbenzene) Copolymer in Aqueous-Phase Hydroformylation of Propylene," *J. Catal.*, **145**, 327 (1994).

47. Guo, I., B. E. Hanson, I. Toth and M. E. Davis, "Bis[Tris(Meta-(Sodium Sulfonato)Phenyl)Phosphine] Hexacarbonyl Dicobalt, $Co_2(CO)_6(P(meta\text{-}C_6H_4SO_3Na)_3)_2$, in a Supported Aqueous Phase for the Hydroformylation of 1-Hexene," *J. Organomet. Chem.*, **403**, 221 (1991).

48. Arnoldy, P. In *Rhodium Catalyzed Hydroformylation*, P. W. N. M. van Leeuwen and C. Claver, Eds.; Kluwer Academic: Dordrecht (2000).

49. Ullmann, F., *Industrial organic chemicals : starting materials and intermediates*, Wiley-VCH: New York (1999).

50. Bhanage, B. M., S. S. Divekar, R. M. Deshpande and R. V. Chaudhari, "Kinetics of hydroformylation of 1-dodecene using homogeneous $HRh(CO)(PPh_3)_3$ catalyst," *J. Mol. Catal. A: Chem.*, **115**, 247 (1997).

51. Evans, D., J. A. Osborn and G. Wilkinson, "Hydroformylation of alkenes by use of rhodium complex catalysts," *J. Chem. Soc. A*, **12**, 3133 (1968).

52. Bianchini, C., H. M. Lee, A. Meli and F. Vizza, "In situ high-pressure $^{31}P\{^1H\}$ NMR studies of the hydroformylation of 1-hexene by $RhH(CO)(PPh_3)_3$," *Organometallics*, **19**, 849 (2000).

53. Poling, B. E., J. M. Prausnitz and J. P. O'Connell, *The properties of gases and liquids*, McGraw-Hill: New York ; London (2001).

CHAPTER 3

DIACETYLENE CROSSLINKING AND POLYIMIDE BLENDS

The fundamentals of the diacetylene crosslinking reaction and the crosslinking agents used in this work are introduced in this chapter. Material characterization of the crosslinking reaction as well as the properties of the blends and blend components are investigated. Of primary interest in this chapter are the "non-transport" properties of the blends, which give some indication as to whether a crosslinked network is formed and if so, the nature of the network. For the transport properties of the blends and components, the reader is referred to the subsequent chapters.

3.1 Introduction

The objective of the membrane materials developed here is to recover a dissolved solute from an organic liquid feed, specifically a homogeneous catalyst from reactor effluent. As established in Section 1.3, a material requirement for this application is to resist swelling and dissolution. It is also desirable for these materials to possess high transport rates. The product from the reaction is contained in the permeate stream (see Section 2.2 for process description) and high permeate fluxes will translate to higher productivity and lower membrane area requirements. These two objectives of membrane stability and productivity are generally in conflict with one another when considering means to tailor polymer structure and composition in order to affect membrane transport. Polymer stabilization methods such as crosslinking and incorporation of chemically

resistant units in the polymer backbone typically result in flux reduction due to limitation of polymer chain motions and subsequently slower diffusion. It is therefore a major challenge to simultaneously impart stability and productivity in a membrane material.

In an effort to combine the benefits of effective transport and material stability in the face of aggressive feed streams, this research has focused on the use of polymer blends. Blends have the potential to offer the combined benefits of their constituent components. Furthermore, it is possible to optimize the blend concentrations for peak membrane performance and economics. Therefore, this work has investigated the combination of a high transport performance polymer with a crosslinkable component. The goal of the polymer blend approach is to obtain membranes that have good productivity and stability imparted by the host polymer and crosslinking agent, respectively.

Diacetylene cross-polymerization is the crosslinking method that has been pursued in this work based on prior promise exhibited in membrane polymers,[1-3] reviewed in the background section of this chapter (Section 3.2.3). This functionality has been incorporated into oligomers (low molecular weight polymers), which will act as the crosslinking agent in the blends. The structure of the 1,1-BTDA-DIA oligomer – so called because of the benzophenone tetracarboxylic dianhydride (BTDA) and diacetylene (DIA) groups in the backbone linked by single methylenes – is shown in Figure 3.1. The diacetylene crosslinking group offers the benefit of ease of activation in the solid-state;[4] thermal, UV radiation, and ionic radiation will activate the cross-polymerization reaction under mild conditions. This allows the materials to be processed into membranes or other forms prior to crosslinking while still soluble. Following the processing step the

materials can be crosslinked in the solid-state in a manner that does not risk degradation of the surrounding polymer matrix.

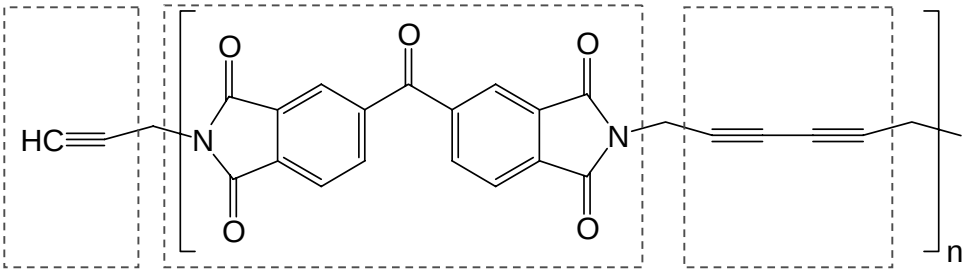

Figure 3.1: Structure of 1,1-BTDA-DIA crosslinking agent.

The BTDA group is present in the crosslinking agent to aid in phase mixing with the chosen host polymer for transport evaluation: polyimides. Polyimides are known to exhibit good chemical resistance, an aid in the aggressive homogeneous catalyst recovery under investigation. Polyimides have been extensively studied for gas transport[5-8] and to a lesser extent, used as membrane materials for organic liquid applications.[9-17] These materials have proven to be quite attractive as selective membranes for separations of gas, vapor and liquid mixtures.

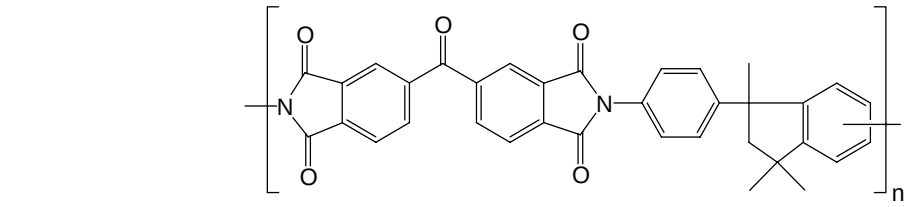

Matrimid

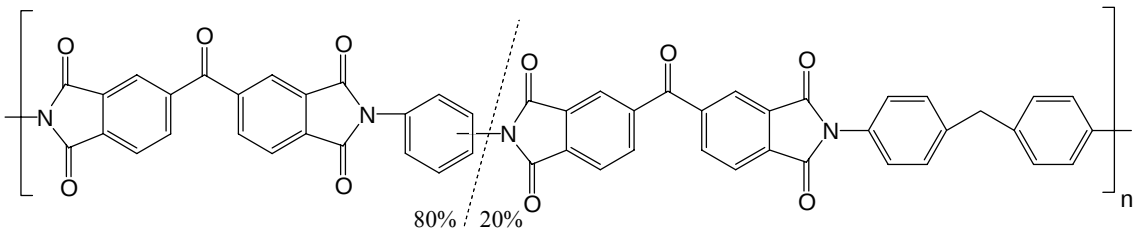

P84

Material	T_g (°C)	ρ (g/cm^3)	FFV
Matrimid	313	1.249	0.133
P84	300	1.359	0.105

Figure 3.2: Chemical structure and select properties of Matrimid and P84.

This work has taken the approach of using commercial polymers as the host component of the blend. Matrimid® (Ciba-Geigy) and P84 (Lenzing, AG) are both high performance BTDA-based polyimides that were studied for this purpose. Polymer blending in this manner can be viewed as a "value added" type of modification. In this case, commodity polymers are combined with low concentrations of a specialty material (the crosslinking agent). The chemical structures and properties of the host polymers are shown in Figure 3.2. During the course of research it was found that Matrimid had much greater potential as a membrane material for homogeneous catalyst recovery and consequently the bulk of this work focuses on Matrimid specifically. Fluxes for the reaction solvent and other components were immeasurable in dense films of P84, possibly due to its lower free volume and sorption.

Another advantage of using polyimides is their high glass transition temperature and thermal stability. The membrane materials analyzed in this work are in the form of dense films, but for large-scale and industrial applications, they would have to be asymmetric membranes containing a thin active layer supported by a porous substructure. Asymmetric membranes are typically quite delicate and could be damaged during the crosslinking procedure. It is not certain that these materials will withstand the crosslinking treatment in the asymmetric form, but their thermal robustness will increase the likelihood. More encouraging than speculation is the preservation of asymmetric membrane morphology observed in a polyimide material (6FDA-based) by Wallace[18] at a temperature of 230 °C, which is near the activation temperature for diacetylene functionalized polyimides.[19]

It is generally agreed that the combination of a crosslinkable oligomer and an inert host polymer form a semi-interpenetrating network (s-IPN) upon activation of crosslinking[20] (Figure 3.3). s-IPNs are polymer systems consisting of crosslinked network and a linear or branched polymer with no covalent bonds between the linear and crosslinked components. The formation of the crosslinked network around the host polymer should stabilize the polymer by reducing the chain mobility and degree of plasticization that occurs when exposed to a swelling agent.

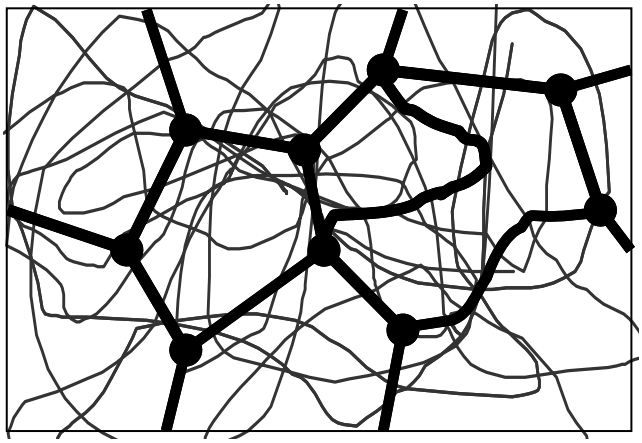

Figure 3.3: Two-dimensional representation of a semi-interpenetrating network. The dark lines represent the crosslinked network surrounding the host polymer, shown with lighter lines.

The reactivity of these diacetylene-functionalized oligomers has been investigated in this chapter for the purpose of establishing the crosslinking protocol for the blends to be evaluated in membrane transport studies. Additionally, characterization of the crosslinking reaction itself is presented. Knowledge of the nature and extent of the reaction can be valuable when interpreting the transport behavior of these materials due

to the sensitivity of penetrant transport in polymers to subtle changes in their chemical and physical morphology.

Also presented in this chapter are the "non-transport" physical properties evaluated for the blends formed with Matrimid and the crosslinking agents. Properties such as glass transition temperature, phase morphology, and crosslink density will aid in understanding the limits and possibilities for the blended materials.

3.2 Background

As previously stated, the selection of polymers for membrane applications is primarily an empirical task. Though models based on polymer physical properties such as solubility parameters[21] and fractional free volume[22,23] can give the membrane researcher some understanding of the general transport trends to be expected for a given system, material selection is based primarily on an assay of available experimental data combined with an understanding of how polymer architecture affects transport. Information in all of these categories: models, data, and structure-property relationships for polymeric membranes for solute recovery from organic solvents is particularly scarce, which is a source of motivation for this thesis. However, with the empirical nature of membrane science in mind, this background section's purpose is to provide some information supporting the material choices that have been made, as well as context for the evaluation of results found in this work.

3.2.1 Polymer Blends

Polymer blending can be a good and inexpensive way to modify material properties. In some cases, blends can be formed based on identifying properties to be exploited. Kapantaidakis and coworkers[24] formed miscible blends of Matrimid and polysulfone to analyze for CO_2 plasticization, a common occurrence in polymer membranes. The plasticization pressure (partial pressure at the onset of plasticization) of polysulfone in CO_2 is higher than that for Matrimid. They found that the film plasticization pressures increased with increasing polysulfone content, i.e. the films were more stable. This is an example of combining two polymers with a knowledge of the desired pure component properties to be exploited – Matrimid to provide superior transport and polysulfone for stability – to obtain a blend with a combination of their properties. However, it is also evident from their work that some unanticipated results based on simple phase mixing rules can also occur, which was observed as CO_2 permeabilities in the blends that were lower than either of the neat materials.

In an interesting study pertinent to this work due to membrane exposure to hydrocarbon liquids, Cabasso[25] was able to form miscible blends of cellulose acetate and crosslinkable polyphosphonates in a 1:1 ratio that were stable in benzene/cyclohexane mixtures after thermal treatment. A solubility parameter approach was taken where the composition and ratio of blend components was predicted from the component polymer Hildebrand solubility parameters and mapped to benzene's to form a solubility-selective membrane material. The separation performance of these polymer blends in benzene/cyclohexane pervaporation relative to other polymeric materials[26] was excellent.

Cabasso's work is notable because the use of a modeling approach to select the blend components was demonstrated.

The challenge in forming polymer blends is forming miscible blends. Miscible films are desirable because phase separated films are typically mechanically weak and can have a random morphology that is difficult to reproduce.[27] Because of their high molecular weights, polymers are inherently prone to phase separation. This can explained through the basic thermodynamics of mixing. A requirement for two materials to form a single phase is a negative Gibb's free energy of mixing (Eq. 3.1). That is, the system is in a lower free energy state as a mixture compared to the single components in separate phases.

$$\Delta G_{Mix} = \Delta H_{Mix} - T\Delta S_{Mix} \qquad (3.1)$$

The entropy of mixing (ΔS_{Mix}) is small for high molecular weight polymers[28] limiting significant entropic contribution to the overall free energy. Low molecular weight materials like oligomers are often used as one or both of the blend components to overcome this and increase miscibility. Chemical compatibility of the blend components determines the enthalpy of mixing (ΔH_{Mix}).[29] Compatible components have negative enthalpies ($\Delta H_{Mix}<0$) and contribute to phase mixing. Thermodynamically speaking, this is why blends are more readily formed from polymers with similar chemical constitution. Although this thermodynamic argument seems elegant and straightforward, the prediction of ΔG_{Mix} for polymers is complicated and empirical data is heavily relied upon. This has lead some to call researchers of polymer blends "part scientist, part artist, and part statistician."[30]

3.2.2 Diacetylene Crosslinking

The diacetylene crosspolymerization reaction can be activated in the solid-state though a variety of different methods including heat, UV radiation, and pressure, all under mild condtions.[4] The reaction is proposed to proceed via a 1,4-addition[31] (Figure 3.4) without the evolution of volatile byproducts. Reactivity of the diacetylenes is strongly dependent on their physical state; reactions either do not occur in the solution state or the products differ from the solid-state reaction.[32] Even in the solid-state, diacetylenes require proper orientation for the reaction to occur.[33] These characteristics of the diacetylene reaction have lead to its characterization as a "topochemical" reaction – where crosslinking only occurs in diacetylene groups of a specific orientation, preserving the structure of the polymer while forming covalent crosslinks. Some membrane researchers[1,2] believe the topochemically controlled crosslinking of polymers can stabilize the materials through network formation with minimal disruption of the surrounding structure. This gives the possibility of gaining polymer stability without a large compromise of polymer chain mobility and product flux through the membrane.

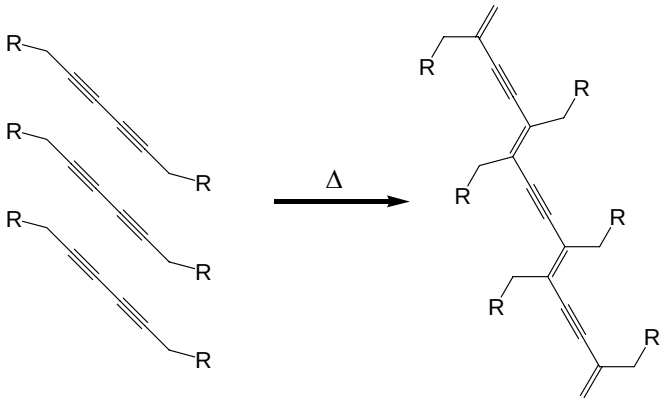

Figure 3.4: General representation of the 1,4-addition solid-state polymerization of diacetylenes. R is a substituent group.

3.2.3 Membranes with Crosslinkable Diacetylene Functionalities

Rezac et al.[1,2] first formed crosslinkable blends for gas separation using blends of a 6FDA-IPDA [4,4'-(hexafluoroisopropylidene)diphthalic dianhydride and 4,4'-isopropylidene diamine] polyimide and a 6FDA-based diacetylene oligomer. The blends exhibited minimal reduction in permeability relative to the host material when compared to other crosslinking methods for polyimides. Selectivities of the crosslinked materials for gases were maintained relative to the uncrosslinked membranes. Sturgill[3] followed their work by examining the effectiveness of diacetylenes blended with the BTDA-based polyimides Matrimid and P84. Similar post-crosslinked permeability behavior as the 6FDA polyimides was observed in gas separation studies. In each case, polymer stabilization through crosslinking was concluded on the basis of observation of increased chemical resistance and thermal stability (through thermogravimetric analysis). However, investigation in a plasticizing environment has not been conducted on these materials until now.

3.3 Experimental

3.3.1 Materials

Matrimid® 5218 was obtained from Ciba-Geigy (Hawthorne, NY). P84 (Lenzing AG) was donated for research purposes by HP Polymer, Inc. (Lewisville, TX). Both polymers are in the fully imidized state. Each of these polymers was received as a powder.

Polysciences, Inc. (Warrington, PA) was contracted to synthesize the oligomeric (low molecular weight polymer) diacetylene-functionalized crosslinking agents contain-

ing 3,3',4,4'-benzophenone tetracarboxylic dianhydryde (BTDA) imide groups, following the synthesis developed by Karangu.[19] The oligomer chemical structure is given in Figure 3.1. Infrared (IR) spectroscopy, solution-state proton nuclear magnetic resonance (^{1}H-NMR) spectroscopy, elemental analysis, and inherent viscosity measurements were performed on-site to confirm the formation of the desired product. Two batches of the crosslinking agent were made with differing degrees of polymerization (or number of repeat units). The batches were designated "Oligomer 1" and "Oligomer 2". The oligomer degrees of polymerization (DP) were determined using solution ^{1}H-NMR in deuterated dimethyl sulfoxide (DMSO-d_6, Aldrich). The DP was calculated from the ratio of integrated peak areas of methylene protons neighboring the diacetylenes (δ=4.58 ppm) to the methylene protons neighboring the terminal acetylenes of the oligomers (δ=4.42 ppm; d, J=2.0 Hz). The degrees of polymerization calculated are shown in Table 3.1 along with concentration of reactive groups per gram of crosslinking agent.

Table 3.1: Oligomer batches fabricated for study and their corresponding degrees of polymerization (DP).

Oligomer Designation	DP	Mol Reactant Groups /g*
Oligomer 1	2.2	3.7×10^{-3}
Oligomer 2	6.1	3.0×10^{-3}

*Defined as internal diacetylenes plus terminal acetylene groups

All solvents were used as received and are listed in Table 3.2.

Table 3.2: Solvents used in film casting and solubility tests.

Solvent	CAS No.	Purity	Provider
Hexafluroisopropanol (HFIP)	920-66-1	> 99%	Fluka
n-Methyl pyrolidinone (NMP)	872-50-4	99.5%	Aldrich
Dimethyl sulfoxide (DMSO)	67-68-5	99.9%	Aldrich
Dimethyl acetamide (DMAc)	127-19-5	99.8%	Aldrich
Dimethyl formamide(DMF)	68-12-2	99.8%	Aldrich

3.3.2 Film Casting

Although the studies in this chapter do not involve membrane transport measurements, testing of Matrimid and blends with oligomer was conducted on polymer films of the same form used in transport studies for consistency. The procedure for film casting is given in Section 5.3.2.

Experiments performed on the pure oligomers were conducted on the raw powder form of the materials since films could not be formed from these low molecular weight materials. There were no further treatments of the powder prior to testing.

3.3.3 Thermal Activation

Thermal activation of the oligomers and blends was conducted under vacuum at 250 °C for 24 hours, which is defined in this document as "annealing." The determination of the temperature and time profile for the thermal activation was based on the differential scanning calorimetry results of 3.4.2. Unless otherwise noted, films prepared

from the host polyimides alone (0% crosslinking agent content) were treated under the same conditions for comparative purposes.

3.3.4 Differential Scanning Calorimetry (DSC)

DSC was conducted with a Seiko DSC 220 to monitor crosslinking and terminal acetylene reactions as well as transitions, such as the glass transition temperature. The average sample mass was ~5 mg. In order to represent the inert conditions of thermal treatment in vacuum, DSC tests were conducted with a nitrogen (Air Products, ultra high purity, 99.998%) purge rate of ~150 cm^3/min. Samples were held at 100 ºC for 30 minutes for moisture removal and then heated at rate of 10 °C/min to 400 ºC. Peak integration for exotherms was performed using the Seiko software.

3.3.5 Dynamic Mechanical Analysis (DMA)

A Rheometric Scientific RSA-III model dynamic mechanical analyzer was used to conduct DMA tests on the blends and host polymers. Mechanical properties, polymer transition temperatures, and degrees of crosslinking were obtained from these studies. Samples were heated at a rate of 10 °C/min from 30 ºC to 400 °C. A constant strain amplitude of 0.1% was applied sinusoidally at a frequency 10 Hz. Specimen dimensions were approximately 20 x 5 mm with a thickness of 25 μm. The initial gap width of the instrument (length of specimen between clamp arms) was ~10 mm. All tests were run under a nitrogen purge (Air Products, liquid nitrogen supply) for inert conditions and to prevent oxidative reactions at the higher temperature ranges (>300°C).[34]

3.3.6 Atomic Force Microscopy (AFM)

Films were imaged with a Nanoscope IIIA multimode SPM microscope (Digital Instruments, Inc., Santa Barbara, CA) operating in tapping mode. A microfabricated Nanopore silicon nitride tip was used at a scan rate of 0.5-2.0 Hz. Height and phase images were obtained simultaneously. Phase images represent the variations of the phase angle of the interacting cantilever relative to the phase angle of the freely oscillating cantilever at the resonance frequency. There were no further modifications to the film surfaces from as-cast state.

Image analysis was performed using the MATLAB (The MathWorks, Inc.) Image Analysis Toolbox software. Image files generated by the AFM were used as input.

3.3.7 Solid-State ^{13}C-NMR

Solid-state ^{13}C-NMR spectra were acquired using a Bruker DSX 400 operating at 100 MHz. Cross-polarized, magic angle spinning (CP/MAS) was employed using a contact pulse of 1 ms, 90° pulse length of 4 μs, and a sample spinning rate of 12 kHz. 4k scans were signal-averaged for each spectrum using high power ^{1}H decoupling during data acquisition. It should be noted that this is not a quantitative NMR method. For the analysis of oligomer before and after annealing, the sample was annealed directly in the ceramic sample rotor.

3.4 Results and Discussion

Based on the thermodynamics of blends presented in Section 3.2.1 and the potential for diacetylene stabilization of membranes presented in Sections 3.2.2 and 3.2.3, the

properties of diacetylene-functionalized oligomers and their blends with Matrimid have been investigated. The oligomer chemical structure is pictured in Figure 3.1. The BTDA unit is present in the backbone as an enthalpic contributor to phase mixing with Matrimid and other BTDA-based polyimides. The oligomeric nature of the crosslinking agent is intended as an entropic contributor to miscibility. Evaluation of the 1,1-BTDA-DIA oligomer and blend morphology with Matrimid is presented in this section.

3.4.1 Oligomer Solubility

Solubility tests of the crosslinking agents were performed to find a solvent suitable for film casting of blends. The solvents investigated were limited to those that are known to dissolve the host polymers Matrimid and P84. Although solubility tests have been conducted with oligomers possessing the same repeat unit in prior studies,[3,19] the low molecular weight of the materials in this work encouraged reexamination.

The results of the solubility tests for Oligomer 1 are shown in Table 3.3. Solubility of the oligomer was limited; even strong organic solvents such as DMAc and DMF did not dissolve the crosslinking agent despite its low molecular weight. Some solubility was observed in DMSO and NMP, with a solubility limit of approximately 5 wt% oligomer for each. However, these are low volatility casting solvents. For polymer films to be cast from these solvents, the solutions must have a fairly high polymer concentration of around 20 wt% to achieve sufficient solvent evaporation to form solid films in a reasonable amount of time. Therefore, the remaining option was to use HFIP as the casting solvent for film formation as in the previous work. Unfortunately, in addition to

being toxic and hydrophilic, HFIP forms a complex with BTDA polyimides[3] that requires heating in excess of 150 ºC to break.

Table 3.3: Survey of oligomer solubility in various solvents. All tests conducted at ambient temperatures. Highly polar solvents (DMAc, DMF, DMSO, NMP, HFIP) were tested in a nitrogen atmosphere to eliminate exposure to atmospheric water.

Solvent	Polymer Dissolved	Oligomer Solubility
Methylene Chloride	Matrimid	None
Choloroform	Matrimid	None
DMAc	Matrimid, P84	None
DMF	Matrimid, P84	None
DMSO	Matrimid, P84	5 wt%
NMP	Matrimid, P84	5 wt%
HFIP	Matrimid, P84	Soluble

3.4.2 Activation of Oligomer Crosslinking

The crosslinking reaction was activated using thermal treatment under vacuum. Although polyimides are robust polymers, vacuum conditions provide an inert environment that excludes oxidative side reactions that may occur when heating polymers. Thermal treatment studies were performed on the oligomers in the powder form. After thermal treatment, the oligomers changed color from light brown to dark red. The change in color is a result of the highly conjugated structure formed in the 1,4-addition diacetylene reaction (Figure 3.4).

DSC of the oligomers was conducted for the purpose of monitoring the reaction of the active groups (diacetylenes and terminal acetylenes) on the crosslinking agents. Reactions should be displayed as exothermic peaks in the DSC spectrum, with the area

under the peak representing the heat of reaction. In the DSC of Oligomer 1 shown in Figure 3.5, two exotherms are apparent on the DSC spectrum. An initial strong exotherm at approximately 240 °C attributed to diacetylene reaction is followed by a shoulder peak at 280 °C attributed to the reaction of terminal acetylenes. The assignment of these peaks is described below. Thermogravimetric analysis[3] has shown 1,1-BTDA-DIA to be stable (no weight loss) to temperature of 400 °C, indicating that neither of the exotherms in Figure 3.5 are the result of a degradation reaction. Furthermore, an exotherm in the DSC of the oligomer corresponding to the degradation is present at 410 °C and is not shown in Figure 3.5 for the purpose of highlighting the reaction exotherms.

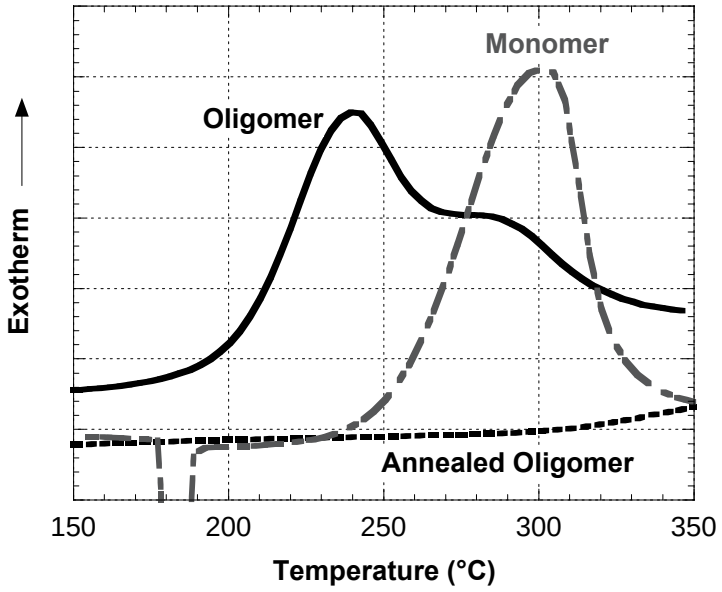

Figure 3.5: DSC of Oligomer 1 and monomer before and after crosslinking. "Annealed Oligomer" denotes a sample that has been heated at 250 °C for 24 hours under vacuum. DSC traces have been shifted along the y-axis for clarity.

As shown in Figure 3.1, the 1,1-BTDA-DIA oligomer is ethynyl (acetylene) terminated, as is the monomer used to form the oligomer. Thermally initiated reaction of ethynyl functionalities is known to occur at approximately the same temperatures as the exotherms observed for Oligomer 1.[3,20,35] Since the ratio of terminal acetylene groups to internal diacetylenes is high for Oligomer 1 (2.0:1.2), the contribution of their reaction could be significant and present as an exotherm in the DSC thermogram. Therefore the DSC of the monomer group has been included in Figure 3.5 for comparison. The monomer does not contain any diacetylene functionalities, so the reaction of these groups is restricted to the oligomer. It appears that the monomer exotherm at 300 °C is due to the reaction of its terminal acetylenes. The presence of this exotherm on the monomer DSC also suggests that the shoulder peak of the oligomer is due to the reaction of its terminal acetylene groups. Therefore, the reaction of diacetylenes is concluded to be the source of the exotherm at 240 °C. A monomer extraction step in the oligomer synthesis as well as the absence of the monomer crystalline melting endotherm at 182 °C in the oligomer DSC can be used to rule out monomer impurities as the source of the shoulder peak.

Further verification of the reaction of the terminal acetylene and diacetylene groups was found using ^{13}C-NMR solid-state spectroscopy. Figure 3.6 shows the ^{13}C-NMR CP/MAS spectra of the oligomer before and after thermal treatment at 250 °C, termed "annealing". The peaks in the "original oligomer" spectrum between 60 and 75 ppm represent the terminal acetylenes and internal diacetylenes. After thermal treatment, these acetylene peaks essentially vanish suggesting significant reaction of the diacetlyene and terminal acetylene groups. This supports the DSC interpretation of both acetylene

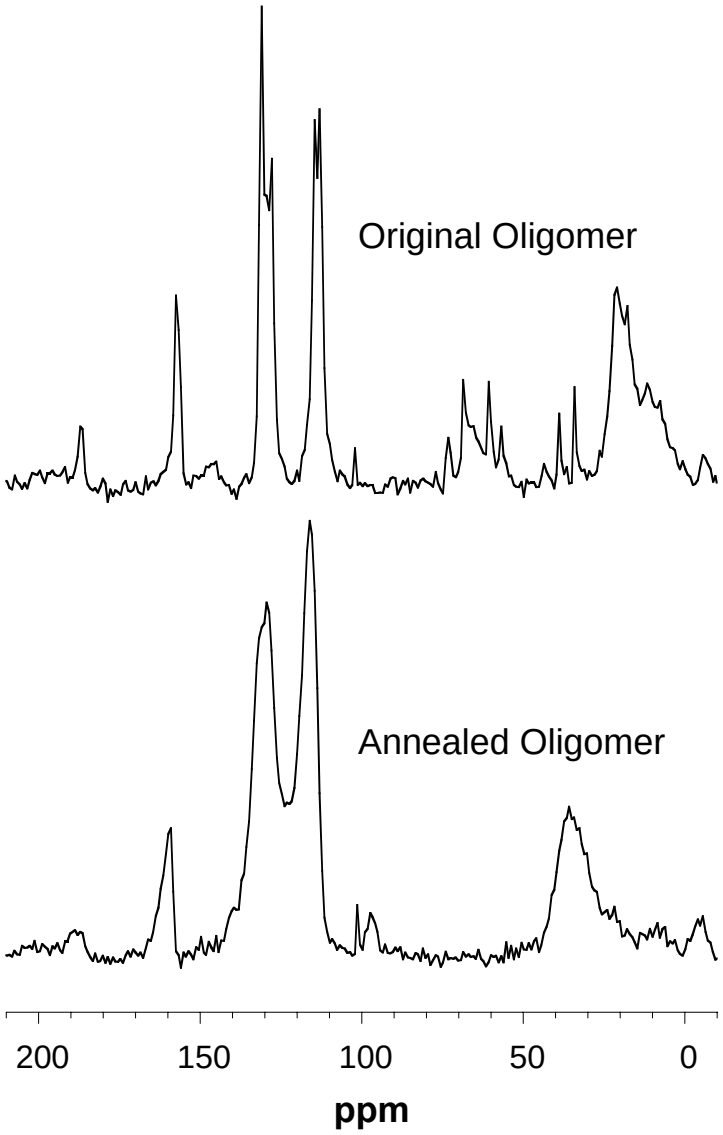

Figure 3.6: ^{13}C-NMR CP/MAS solid-state spectra of annealed and original oligomer. The annealing process is thermal treatment of the oligomer at 250 °C for 24 hours under vacuum.

reactions occurring with thermal input and indicates that the terminal acetylenes are reacting even though the heat treatment of the oligomer did not reach the peak exotherm temperature for terminal acetylene reaction of 280 °C. The reaction of the terminal acetylenes under these conditions is also supported by the absence of any further exotherms in the DSC of the post-treated oligomer ("Annealed Oligomer") in Figure 3.5.

Further investigation of Figure 3.6 shows the formation of a peak at 96 ppm. This is consistent with the diacetylene 1,4-addition (Figure 3.4), as the ^{13}C-NMR chemical shift represents the conjugated acetylene carbons formed during the reaction. Also, there is an increase in the integrated area for carbons in the aromatic region (110 – 135 ppm) relative to a group assumed to be unaffected by annealing – the imide ring carbonyls at 162 ppm. A review of reactions in ethynyl-terminated imide oligomers by Alam et al.[35] found a predominance of phenyl groups in the crosslinked structures. A mechanism that was proposed for this reaction is a trimerization shown in Figure 3.7. Although one could view this reaction as one that is entropically hindered in the solid-state (due to the limited probability of three acetylene groups meeting for reaction), the work of Bos et al.[20] with thermally treated acetylene terminated oligomers showing changes in transport properties commensurate with a crosslinked network combined with Alam's review points to this reaction occurring to an extent that can be measured through transport and spectrographic studies. In addition to the terminal acetylene reactions contributing to the annealed oligomer spectrum between 110 and 135 ppm, the formation of carbon-carbon double bonds in the diacetylene 1,4-addition also fall in this region. Finally, the shift of methylene carbons from 22 to 36 ppm after annealing is a product of the change in bonding environment of its nearest neighbor due to reaction.

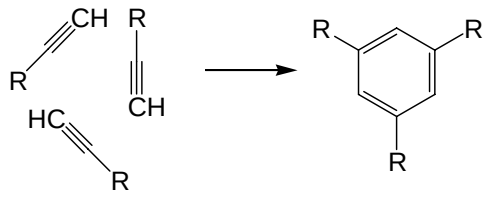

Figure 3.7: Proposed mechanism for the thermally initiated reaction of ethynyl-terminated imide oligomers in the solid-state.[35]

A final note on the ^{13}C-NMR spectrum of Figure 3.6 is the notable decline in spectrum "clarity" after annealing. In comparison to the original oligomer, the carbon peaks in spectrum are not as sharp. This can be attributed to the more heterogeneous bonding environment of the annealed oligomer. The proximity of the carbon nuclei to bonds formed in diacetylene crosslinking, terminal acetylene reaction, or unreacted groups can cause upfield or downfield shifts in the spectrum that result in broader peak shapes.

DSC of Oligomer 2 was performed (Figure 3.8) to determine the effects of oligomer chain length on the crosslinking reactions. A notable difference between the DSC of Oligomer 2 and Oligomer 1 is the absence of the exotherm attributed to terminal acetylene reactions in Oligomer 2. One cause of this is that the ratio of terminal acetylenes to internal diacetylenes (~1:3) in Oligomer 2 is approximately one fourth of that in Oligomer 1; there are simply a greater number of internal diacetylenes reacting and their exotherm dominates in magnitude. Another contributor to the absence of a terminal acetylene exotherm is the reduced mobility of the longer Oligomer 2 chains. Solid-state reactions are dependent on diffusion and orientation of the active sites, which are both inhibited by longer chain length. Therefore, the interpretation of the DSC thermogram is that the predominant reaction in Oligomer 2 is diacetylene reaction with terminal acety-

lenes reaction limited by concentration and diffusion, although the occurrence of the terminal acetylene reaction cannot be completely ruled out.

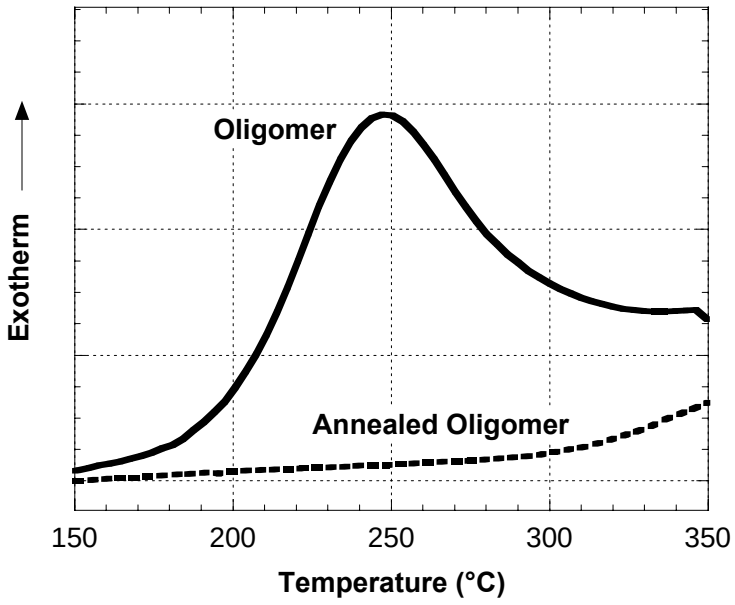

Figure 3.8: DSC of annealing process for Oligomer 2. "Annealed Oligomer" denotes a sample that has been heated at 250 °C for 24 hours under vacuum.

A rough quantification of the extent of reaction in the two oligomers is obtained from the integration of the exothermic peaks in the DSC, shown in Table 3.4. The effect of mobility restriction of the higher molecular weight oligomer on reactivity is emphasized by the lower value of its reaction exotherm (especially when considering the sum of exotherms in Oligomer 1). In addition to the exotherm value, the higher peak temperature of the diacetylene reaction exotherm suggests a higher activation energy requirement for increasing molecular weights. This is consistent with previous studies of diacetylene-functionalized polyimides[3] and poly(aromatic diacetylenes).[36]

Table 3.4: Summary of thermal properties of Oligomers 1 and 2 obtained in DSC. The content of terminal acetylenes relative to internal diacetylenes is provided to support the difference in reaction energy.

Oligomer	DP	Ratio of terminal acetylenes to diacetylenes	Peak Center of DIA Exotherm (°C)	Enthalpy of Reaction (J/g)
1	2.2	1.67	240	-213[a], -93[b]
2	6.1	0.39	249	-189

[a]Heat of reaction for reaction centered at 240 °C

[b]Heat of reaction for reaction centered at 280 °C

Attempts to analyze blends of crosslinking agent with the host polymers for the presence of the same reactions as the pure oligomers were attempted with DSC, ^{13}C-NMR and infrared spectroscopy (IR). In all cases, the dilute nature of the blends – especially in terms of the concentration of reactive functionalities – resulted in the inability to detect the presence of the acetylene functionalities or their reaction products within the resolution of the above listed characterization methods. However, the thermal treatment of the blends has been presumed to still affect the same type of reactions as the oligomers. The reader is referred to the subsequent chapters of the thesis for corroboration of formation of a crosslinked network in terms of the altered transport properties of the blends.

3.4.3 Macroscopic Phase Behavior of Matrimid Blends

The host polymers and 1,1-BTDA-DIA crosslinking agent both contain the same dianhydride unit in their structure to promote compatibility. Following the thermodynamic development for polymer blending in Section 3.2.1, this chemical similarity enthalpically contributes to phase mixing. Additionally, the oligomeric nature of the

crosslinking agent should entropically enhance blend compatibility. Support for this approach can also be found in polyimide blending literature. From their work studying structure effects on polyimide blending Tang et al.[37] concluded that structure matching of the components strongly affected blend miscibility. In the study of Bos et al.,[38] imide oligomers were blended with Matrimid at levels of up to 30% (w/w) oligomer and heat treated without evidence of phase separation. Rezac et al.[1,2] demonstrated the ability to blend diacetylene-functionalized imide oligomers with linear polyimides.

The blends in this study were formed by combining the host polymer with the crosslinking agent in solution with the solvent HFIP and solution casting films (~ 20 – 25 μm). Prior to drying and heat treatment, all films were yellow in color as were the solutions they were cast from. Films containing 5% (w/w) and 10% oligomer were transparent, while films containing greater than 10% oligomer were opaque and often of variable macroscopic morphology. Opacity is a good indicator that two components are phase-separated.

After annealing the films for 24 hours at 250 °C under vacuum, all films except the neat polyimides developed red coloring, its intensity varying with crosslinking agent concentration. Formation of conjugated bonds via the diacetylene 1,4-addition (Figure 3.4) is the source for the red coloration[31] of the annealed blends. Photographs of the 0, 5, and 10% blends are shown in Figure 3.9. Films that were transparent prior to annealing remained so afterwards and remained mechanically tough. The opaque films (>10 wt% crosslinking agent) became brittle after crosslinking, leading to the conclusion that these materials were phase-separated and the blend components were incompatible at concentrations in excess of 10% (w/w) oligomer.

a.) Matrimid

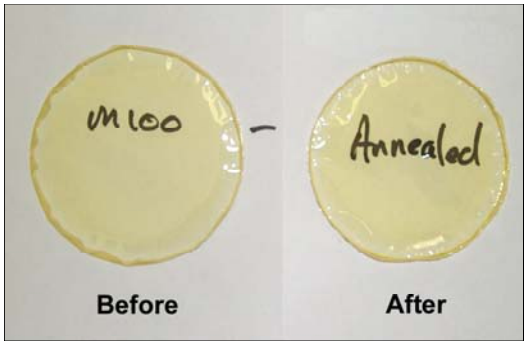

b.) 5% Oligomer 1

c.) 5% Oligomer 2

d.) 10% Oligomer 1

e.) 10% Oligomer 2

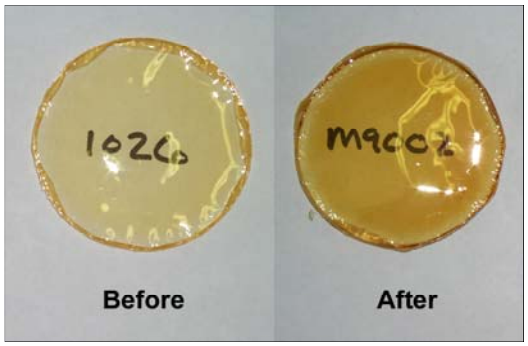

Figure 3.9: Photographs of polymer film appearance before and after annealing at 250 °C for 24 hours. All films were cast in HFIP and dried at 180 °C for 3 days prior to annealing. Text underneath the films is present to illustrate transparency of the films.

3.4.4 Microscopic Phase Behavior of Matrimid Blends

On the basis of optical clarity and qualitative mechanical strength, the blends of crosslinking agent up to and including 10% oligomer are miscible. This section endeavors to investigate the morphology of these materials.

The term "miscible" is often used to describe polymer mixtures that exhibit behavior expected of single-phase systems.[39] However, this does not imply that the components of the mixture have mixed in an ideal manner, but that the level of mixing on a microscopic scale is adequate to yield macroscopic properties expected of a single-phase material. The microscopy data presented in the proceeding paragraphs suggests that the 10% oligomer in Matrimid blend falls into the category of a multiphase material possessing single-phase behavior (e.g. optical clarity & single glass transition). In this document, "miscible" multi-phase mixtures will be differentiated from single-phase mixtures by terming it a "compatible" mixture.

Analysis of the microstructure of 0%, 5% and 10% blends of Oligomer 1 in Matrimid was performed using atomic force microscopy (AFM). AFM has proven to be an effective tool for analyzing transparent, yet multiphase polymer blends – particularly when operating in the phase imaging mode. Phase images utilize the AFM stylus in the "tapping" mode to detect differences in mechanical properties as the instrument maps the specimen surface. Using this technique, Borsig et al.[40] determined the morphology of a transparent interpenetrating network of butylmethacrylate-co-styrene blended with polyethylene with resolutions that identified domain sizes of 300 nm as well as the lamellae of the crystallized polyethylene.

Both height and phase images of neat Matrimid (Figure 3.10a & b) are unremarkable and suggest a homogeneous morphology, as expected. In addition to verifying the purity of the polymer and the AFM technique, these scans provide the baseline for the "Matrimid" phase in the analysis of the other blends.

The phase image of the 5% blend (Figure 3.11b) reveals what appears to be a networked structure (light) surrounding the Matrimid phase (dark). Scans of various areas of the sample were conducted and this morphology was consistent throughout. The morphology strongly suggests the formation of a semi-interpenetrating network. Although the films remained transparent after crosslinking, clear delineation of two phases is apparent in Figure 3.11b. Most likely, this is due to the instrument detecting variations in the toughness (modulus) arising from crosslink formation rather than a multiphase morphology. The average domain size of the continuous Matrimid phase (>1 μm) is large enough to refract light and cause opacity in the films if multiple phases are present and it is known from the macroscopic phase studies through opacity of phase-separated films that the refractive indices of the two phases differ.

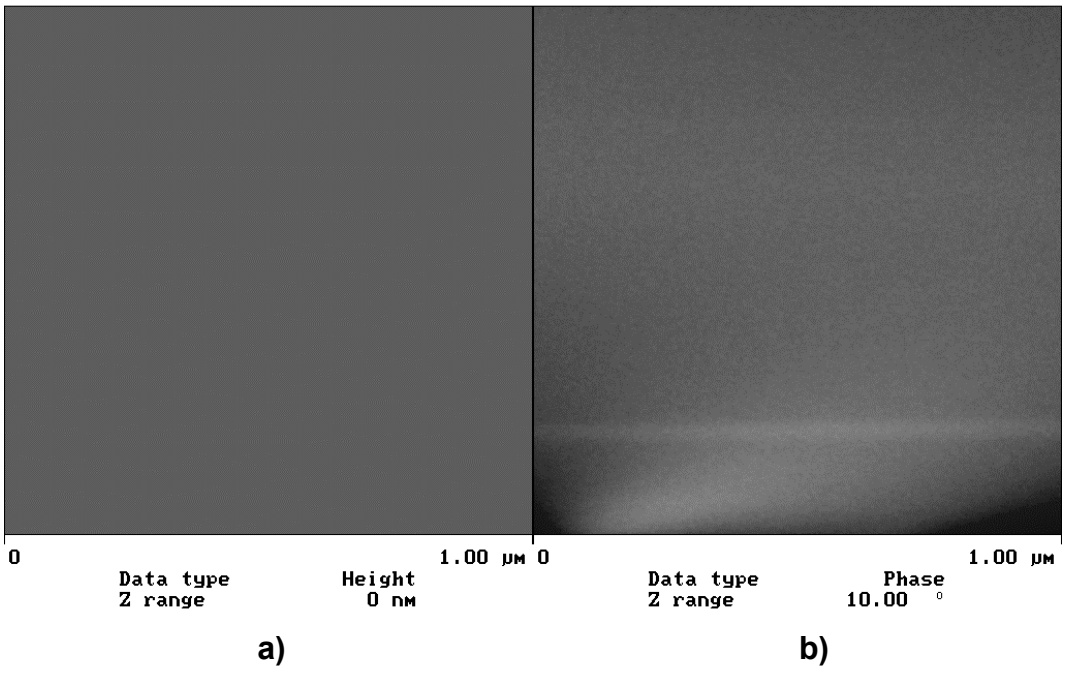

Figure 3.10: Height (a) and phase (b) AFM micrographs of solution cast film of Matrimid.

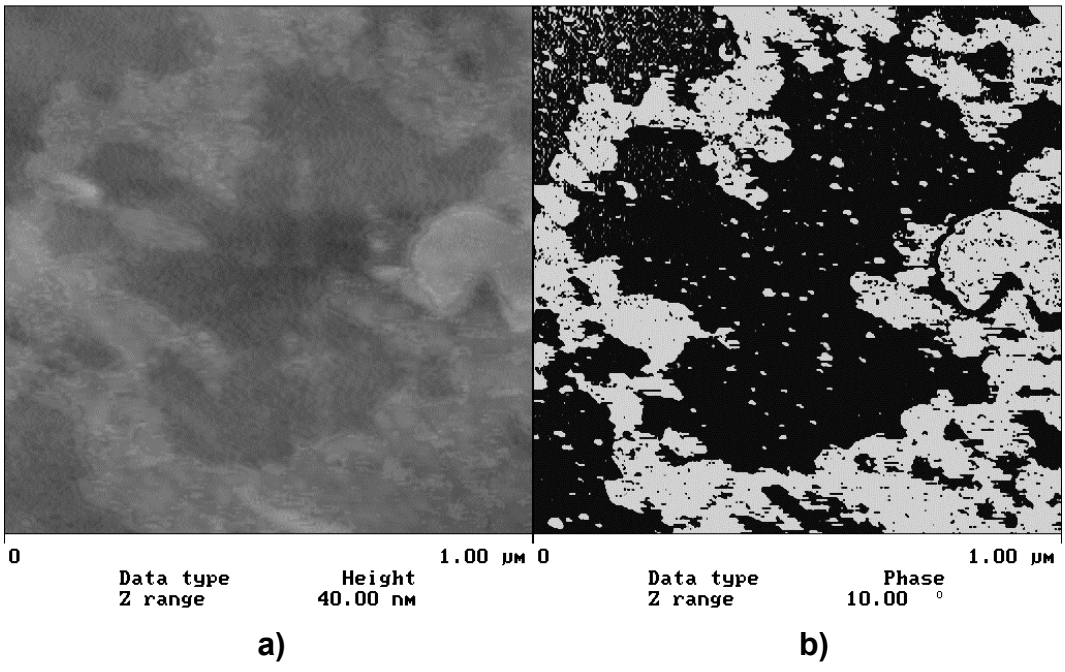

Figure 3.11: Height (a) and phase (b) AFM micrographs of solution cast film of Matrimid blended with 5 wt% Oligomer 1.

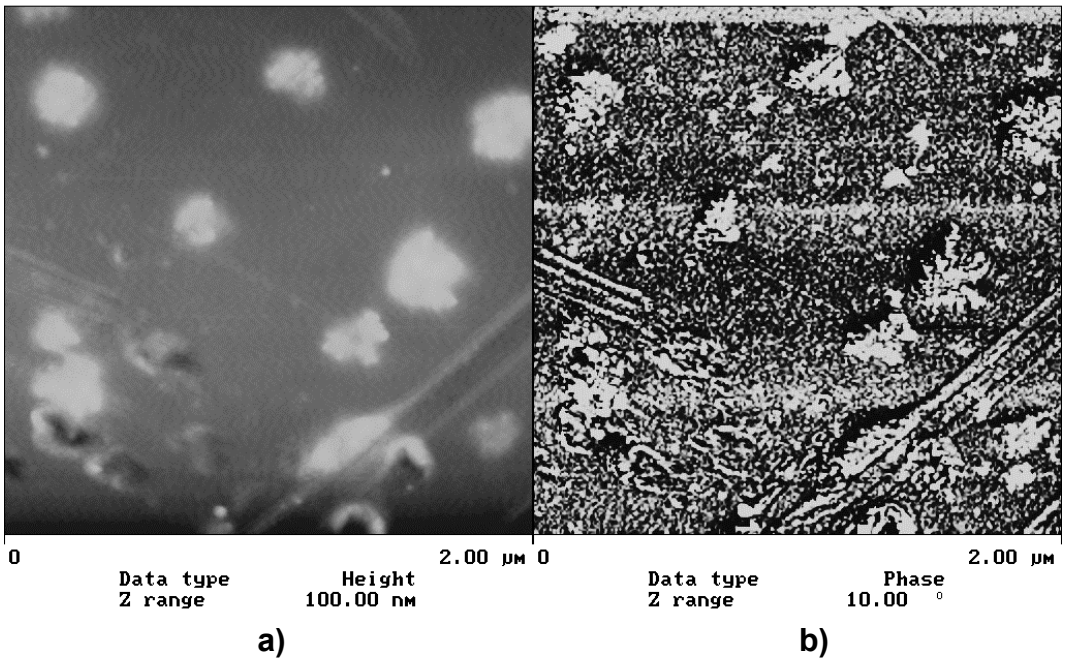

Figure 3.12: Height (a) and phase (b) AFM micrographs of solution cast film of Matrimid blended with 10 wt% Oligomer 1.

Table 3.5: Analysis of AFM micrographs of Oligomer 1 blended with Matrimid.

Wt% Oligomer in Blend	Apparent Morphology	% Secondary Phase	Average Phase Domain Size
0	Homogeneous	-	-
5	Network	36 ± 9	Continuous
10	Phase Separated	8.4 ± 1.3	220 ± 60 nm

Image analysis of the network domain in the 5% blend AFM shows that it occupies approximately 36% of the mixture, based on an average of several scans at different locations on its surface. Obviously, this value far exceeds the 5% by weight of crosslinking agent in the blend. Density differences between the crosslinking agent and Matrimid cannot be the cause of the discrepancy due to the extremely large decrease in density that would be required of the crosslinking agent. There are two probable causes for this discrepancy. One is the inherent error associated with trying to extrapolate three-dimensional information (volume) from two-dimensional data (area). Domains below the surface could well be influencing the phase detection, thus enlarging the area. Secondly, since the crosslinking occurs in the solid-state, Matrimid chain segments near reactive sites on the crosslinking agent may become entangled in the network and stressed. Incorporation of these Matrimid chain segments could be included in the "hardened" phase.

The AFM micrographs of 10 wt% Oligomer 1 blended with Matrimid (Figure 3.12a & b) are quite different than those of the 0% and 5% blends. These AFM scans suggest that the morphology of the 10% blend is a continuous Matrimid phase containing randomly dispersed domains of crosslinking agent. The volume fraction of the dispersed domains is approximately 8.4%, consistent with these being concentrated pockets of the crosslinking agent. Further evaluation of the phase-separated domains reveals an average diameter (assuming a spherical shape) of 220 nanometers. The domain size is smaller than the wavelength of visible light, which can explain the optical clarity of these materials despite their apparent phase separation.

Lack of resolution in the phase diagram for the continuous phase of the 10% blend (Figure 3.12b) does not offer any conclusive information for that phase. The network structure of the 5% blend is not apparent, and the domain size of 8.4% suggests a minimal concentration of crosslinking agent in the continuous phase, though the shortcomings of the image analysis in 5% blend are applicable here as well. However, it is clear that the morphology for the 10% is different than the other materials and presumably categorizes this blend as one that is compatible, yet not ideally phase mixed.

3.4.5 Thermo-mechanical Properties of Matrimid and Blends

Thermo-mechanical analyses of the host polymer Matrimid and blends with the crosslinking agent have been conducted to determine the influence of the crosslinking agent. All information in this section has been obtained through dynamic mechanical analysis (DMA) testing. DMA is powerful technique in the measurement of polymer mechanical properties and thermal transitions.[41] It is a rapid analysis method that can accurately measure multiple quantities simultaneously. Samples are stressed sinusoidally; the elastic modulus of the materials (*E'*) is determined from the in-phase strain response to the stress and the viscous modulus (*E''*) is determined from the out of phase response.

The mechanical properties yielded from DMA for the blends of Oligomer 1 and Oligomer 2 relative to neat Matrimid are shown in Figure 3.13a & Figure 3.13b respectively. Generally speaking for both cases, the blends retain the mechanical properties of the host Matrimid. This lack of improvement in mechanical performance is not necessarily an indication of inadequate network formation. It is possible that unreacted oligomer

units and incomplete network segments in the blend are diminishing the mechanical strength through plasticization, balancing gains imparted by the network. The 10% Oligomer 2 blend has the most significant impact on the mechanical strength, showing a measurable increase in its modulus.

Another item of note in the DMA studies is that the instrument was unable to continue the tests beyond the glass transition temperature for Matrimid. This was caused by elongation of the Matrimid sample beyond the maximum extension of the instrument armature, which on average was a sample elongation exceeding 150%. Matrimid's drastic drop in modulus before test termination can be seen in Figure 3.13. A lack of chemical crosslinks in a polymer in the rubbery state can lead to this tremendous elongation. As Matrimid is known to have no covalent crosslinks, this facet of the DMA is considered to be an indication of the absence of network formation. With this interpretation in mind, the only blend material other than Matrimid that failed at temperatures above the glass transition was the 10% Oligomer 1 blend. The failure of this material supports its phase-separated morphology observed using AFM (Section 3.4.4). Since a large portion of the crosslinking agent constitutes the dispersed phase, it is likely that little network formation occurred and failure similar to Matrimid would be probable.

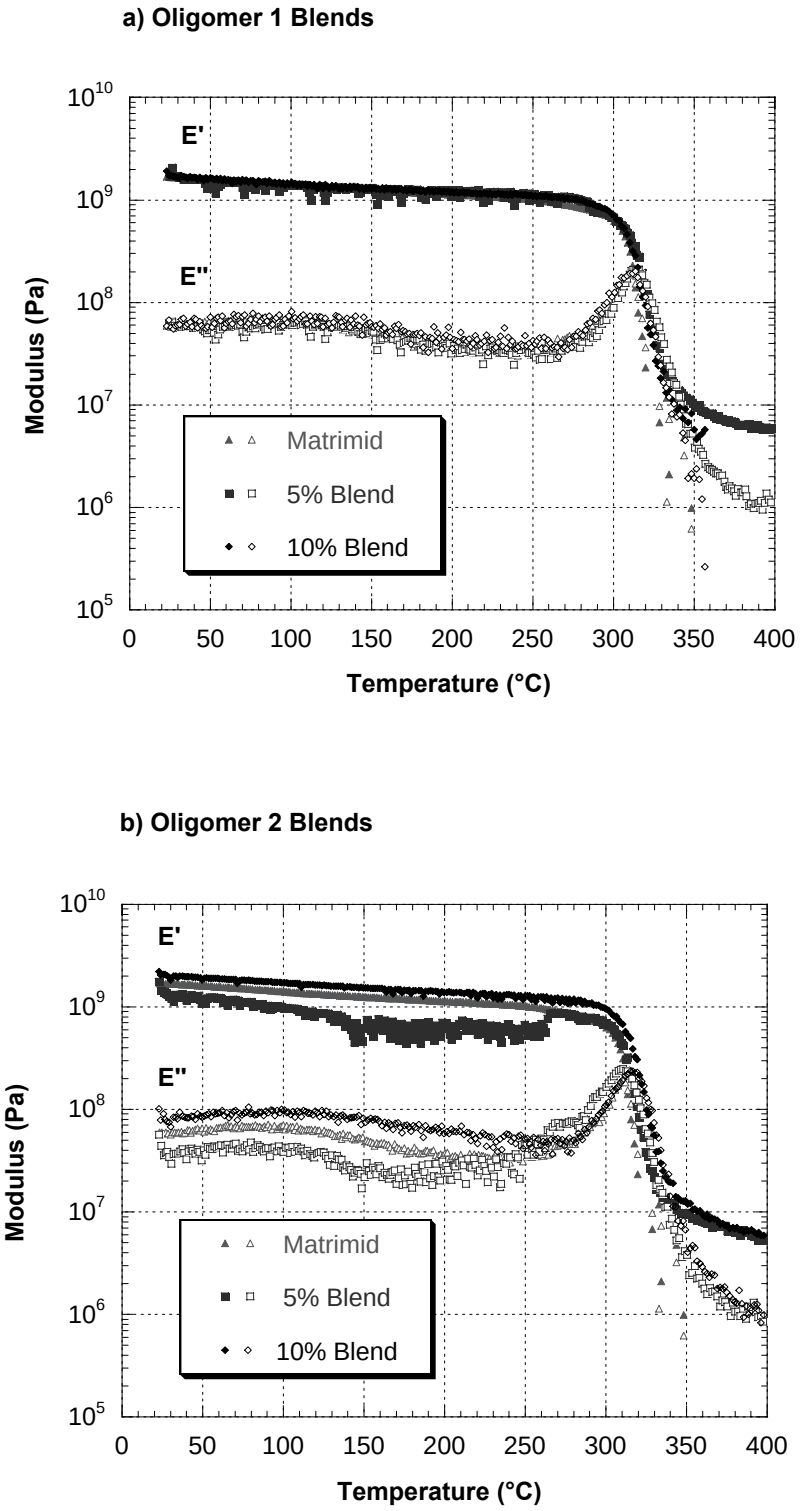

Figure 3.13: Elastic (E') and viscous (E'') modulus for films of Matrimid and blends yielded from dynamic mechanical analysis. All films annealed prior to testing

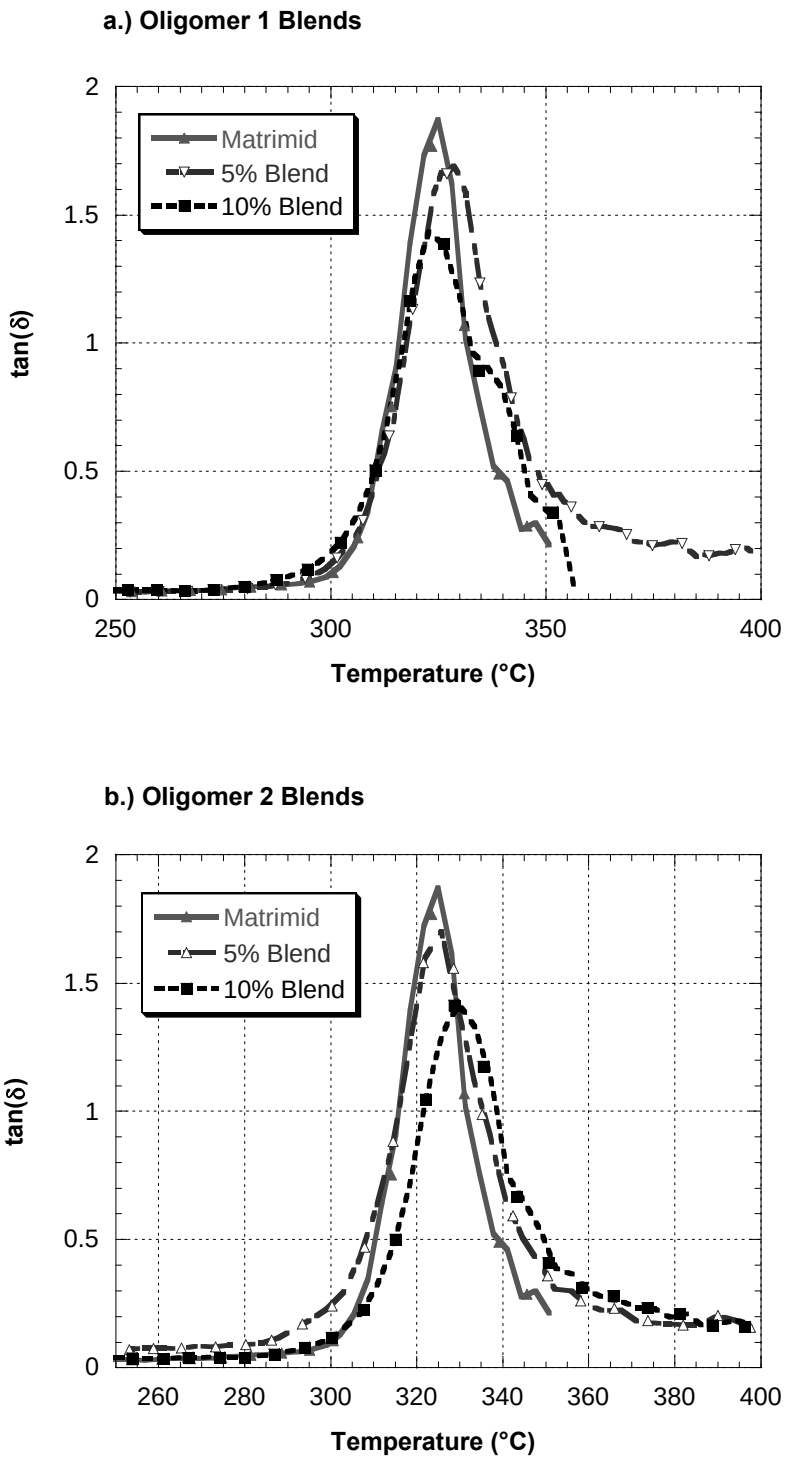

Figure 3.14: tan(δ) plots for Matrimid and Blends from dynamic mechanical analysis. All films annealed prior to testing.

Thermal transitions of the polymers can also be evaluated from DMA. The ratio of viscous modulus to elastic modulus, known as the quantity *tan(δ)*, shows a maximum during these transitions. A marked thermal transition in polymers is the glass transition temperature, a point at which segmental motion of the polymer chains occurs. A crosslinked polymer would be expected to have a higher glass transition temperature than an uncrosslinked analog due to increased energy requirements for the mobility-restricted polymer chains, though this is not necessarily true for the blends evaluated here due to the addition of a secondary component.

tan(δ) plots at temperatures near the glass transition for the blends are provided in Figure 3.14. The maximum in *tan(δ)* shows an increase in temperature relative to Matrimid for the 5% Oligomer 1 blend and the 10% Oligomer 2 blend, suggesting restriction of polymer chain mobility. In the *tan(δ)* plots, the 10% Oligomer 1 blend again exhibits similar properties to the neat Matrimid.

A final piece of information about the polymer blends that can be gleaned from the DMA study is a relative estimate of the crosslink density. From the theory of rubber elasticity for a Gaussian network, the crosslink density, v, can be determined using the following equation:[42]

$$E = \phi v R T \tag{3.2}$$

where E is the modulus of the material in the rubbery plateau region (T_g + 40 °C)[43], ϕ is a quantity known as the front factor, R is the gas constant, and T is the absolute temperature. The front factor, ϕ, is a term related to: 1) the mean square end-to-end distance between chains and 2) the molecular weight between crosslinks relative to the average molecular weight of the original material. It is often acceptable to assume a value of

unity for the front factor,[41] and this assumption is applied here. For the s-IPN's in this study, there is a considerable deviation from ideal rubber behavior and this calculation is presented only as a means to obtain relative crosslink densities for the materials in question.

Calculation of the crosslink densities is provided in Table 3.6. Values for the materials that exhibited a rubbery plateau do not vary greatly, but the trend of increasing crosslink density can be seen for the Oligomer 2 blends, though the values fall with in the measurement error.

Table 3.6: Glass transition temperatures, T_g, and crosslink densities, v, for Matrimid and blends. T_g's determined from maximum in E''.[41] v calculated using Eq. 3.2 for modulus data averaged over 380 – 400 °C.

Material	$\mathbf{T_g}$ (°C)	$\boldsymbol{v}$ (x 10^3) (mol wt. between crosslinks/cm^3)
Matrimid	313	-
5% Oligomer 1	314	1.12 ± 0.03
10% Oligomer 1	312	-
5% Oligomer 2	311	1.19 ± 0.06
10% Oligomer 2	317	1.23 ± 0.05

3.5 Conclusions

Blends of crosslinkable oligomers with a BTDA-based polyimide, Matrimid, have been formed. The post-processing crosslinking of these materials provides a route to obtain semi-interpenetrating network structures in the solid-state. The crosslinked blends have properties that make them interesting as materials for studies in membrane separa-

tions, particularly in the application of focus in this thesis: a highly aggressive environment in which polymer stabilization can enhance membrane performance.

Thermal analysis studies show that the activation of the reactive groups in the crosslinking agent can be achieved through heating at 250°C for 24 hours (termed "annealing"). Two functional groups on the crosslinking agents are reacted under these conditions: internal diacetylene functionalities and terminal acetylenes on the oligomer chain ends. Both of these reactions are suspected to form distributed network structures and further polymerization of the oligomers. In terms of the membrane properties desired in the overall goals of this research, the network formation incurred through reaction of both functionalities is beneficial. DSC indicates that the annealing procedure converts all reacting functionalities that are not diffusion limited. For the purposes of this work, it is not of interest to tune the extent of crosslinking through varying annealing temperature or time, but to obtain the highest extent of reaction for a given blend concentration. Therefore, the annealing procedure presented will be maintained for the remainder of the work.

In the analysis of the influence of molecular weight on the crosslinking agent properties, it was found that the lower molecular weight oligomer (Oligomer 1) was more reactive on a mass basis due to the higher concentration of reactive groups. As a result of the higher reactivity combined with their interesting blend morphology, some emphasis will be placed on Oligomer 1 blends in the subsequent work presented.

AFM studies reveal three morphologies for the materials of interest: a homogeneous morphology for the Matrimid homopolymer, a network morphology for the 5% Oligomer 1 / Matrimid blend, and a phase-separated morphology for the 10% Oligomer 1 / Matrimid blend. The phase separation of the 10% blend is on the nanoscale and the

material still possesses the properties of a "compatible" blend. Though the initial objective of these blends was to achieve network morphologies, the 10% blend provides an interesting third morphology for study and will continue to be featured in transport analysis. Multiphase membranes such as zeolite mixed-matrix membranes and membranes combined with inert fillers such as fumed silica have received significant attention in membrane research because they can be relatively simple means to alter membrane properties.

3.6 References

1. Bayer, B., B. Schoberl, K. Nagapudi, M. E. Rezac and H. W. Beckham, "Crosslinked diacetylene-functionalized polyimides for gas separation membranes: polymer reactivity and resultant properties," *ACS Symp. Ser.*, **733**, 244 (1999).

2. Rezac, M. E., E. T. Sorensen and H. W. Beckham, "Transport properties of crosslinkable polyimide blends," *J. Memb. Sci.*, **136**, 249 (1997).

3. Sturgill, G. K., "Stabilization of polyimide blends through solid-state crosslinking," *Ph.D. Thesis*, Georgia Institute of Technology (1999).

4. Beckham, H. W. and M. F. Rubner, "Synthesis and optical properties of a new class of polyamides containing reactive diacetylene groups," *Macromolecules*, **22**, 2130 (1989).

5. Koros, W. J., M. R. Coleman and D. R. B. Walker, "Controlled permeability polymer membranes," *Annu. Rev. Mater. Sci.*, **22**, 47 (1992).

6. Hiryama, Y., T. Yoshiniga, Y. Kusuki, K. Nimoyima, T. Sakakibara and T. Tamari, "Relation of gas permeability with structure of aromatic polyimides I," *J. Memb. Sci.*, **111**, 169 (1996).

7. Hiryama, Y., T. Yoshiniga, Y. Kusuki, K. Nimoyima, T. Sakakibara and T. Tamari, "Relation of gas permeability with structure of aromatic polyimides II," *J. Memb. Sci.*, **111**, 183 (1996).

8. Ohya, H., V. V. Kudryavtsev and S. I. Semenova, *Polyimide membranes: applications, fabrications, and properties*, Gordon and Breach: Tokyo (1996).

9. White, L. S. and A. R. Nitsch, "Solvent recovery from lube oil filtrates with a polyimide membrane," *J. Memb. Sci.*, **179**, 267 (2000).

10. White, L. S., "Transport properties of a polyimide solvent resistant nanofiltration membrane," *J. Memb. Sci.*, **205**, 191 (2002).

11. Xu, W. Y., D. R. Paul and W. J. Koros, "Carboxylic acid containing polyimides for pervaporation separations of toluene/iso-octane mixtures," *Journal of Membrane Science*, **219**, 89 (2003).

12. Tanihara, N., K. Tanaka, H. Kita and K. Okamoto, "Pervaporation of organic liquid mixtures through membranes of polyimides containing methyl-substituted phenylenediamine moieties," *J. Memb. Sci.*, **95**, 161 (1994).

13. Ren, J., C. Staudt-Bickel and R. N. Lichtenthaler, "Separation of aromatics/aliphatics with crosslinked 6FDA-based polyimides," *Sep. Purif. Tech.*, **22-23**, 31 (2001).

14. Fang, J., K. Tanaka, H. Kita and K. Okamoto, "Pervaporation properties of ethynyl-containing copolyimide membranes to aromatic/non-aromoatic hydrocarbon mixtures," *Polymer*, **40**, 3051 (1999).

15. Hao, J., K. Tanaka, H. Kita and K. Okamoto, "The pervaporation properties of sulfonyl containing polyimide membranes to aromatic/aliphatic hydrocarbon mixtures," *J. Memb. Sci.*, **132**, 97 (1997).

16. Kim, J., B. Chang, S. Lee and S. Y. Kim, "Incorporation effect of fluorinated side groups into polyimide mebranes on their pervaporation properties," *J. Memb. Sci.*, **169**, 185 (2000).

17. Okamoto, K., H. Wang, T. Ijyuin, S. Fujiwara, K. Tanaka and H. Kita, "Pervaporation of aromatic/non-aromatic hydrocarbon mixtures through crosslinked membranes of polyimide with pendant phophonate ester groups," *J. Memb. Sci.*, **157**, 97 (1999).

18. Wallace, D., "Crosslinked Hollow Fiber Membranes for Natural Gas Purification and Their Manufacture," *Ph.D. Thesis*, University of Texas, Austin (2004).

19. Karangu, N. T., "Synthesis Characterization and Properties of Diacetylene-Functionalized Polyimides," *Ph.D. Thesis*, Georgia Institute of Technology (1998).

20. Bos, A., I. G. M. Punt, M. Wessling and H. Strathmann, "Suppression of CO_2-plasticization by semiinterpenetrating polymer network formation," *J. Polym. Sci. B: Pol. Phys.*, **36**, 1547 (1998).

21. Lloyd, D. R. and T. B. Meluch, "Selection and evaluation of membrane materials," *Mat. Sci. of Synth. Membr.: ACS Symp. Ser.*, **269**, 47 (1985).

22. Lee, W. M., "Selection of barrier materials from molecular structure," *Polym. Eng. & Sci.*, **20**, 65 (1980).

23. Park, J. Y. and D. R. Paul, "Correlation and prediction of gas permeability in glassy polymer membrane materials via a modified free volume based group contribution method," *J. Memb. Sci.*, **125**, 23 (1997).

24. Kapantaidakis, G. C., S. P. Kaldis, X. S. Dabou and G. P. Sakellaropoulos, "Gas permeation through PSF-PI miscible blend membranes," *J. Memb. Sci.*, **110**, 239 (1996).

25. Cabasso, I., "Organic liquid mixtures separation by permselective polymer membranes. 1. Selection and characteristics of dense isotropic membranes employed in the pervaporation process," *Ind. Eng. Chem. Prod. Res. Dev.*, **22**, 313 (1983).

26. Villaluenga, J. P. G. and A. Tabe-Mohammadi, "A review on the separation of benzene/cyclohexane mixtures by pervaporation processes," *J. Memb. Sci.*, **169**, 159 (2000).

27. Kwei, T. K. and T. T. Wang. In *Polymer Blends Vol. 1*, D. R. Paul and S. Newman, Eds.; Academic Press: New York (1978).

28. Flory, P. J., *Principles of polymer chemistry*, Cornell University Press: Ithaca (1953).

29. Lipatov, Y. S. and A. E. Nesterov, *Thermodynamics of Polymer Blends*, Technomic Pub.: Lancaster, PA (1997).

30. Rodriguez, F., *Principles of Polymer Systems*, Hemisphere Publishing Co.: New York (1989).

31. Wegner, V. G., "Topochemische reaktionen von monomeren mit konjugierten driefachbindungen II. A topochemical synthesis and reaction of polymers with conjugated acetylene groups in the backbone," *Die Makromolekulare Chemie*, **134**, 219 (1970).

32. Baughman, R. H., "Solid-State Polymerization of Diacetylenes," *J. Appl. Phys.*, **43**, 4362 (1972).

33. Baughman, R. H., "Solid-State Synthesis of Large Polymer Single-Crystals," *J. Polym. Sci. B: Pol. Phys.*, **12**, 1511 (1974).

34. Bos, A., I. G. M. Punt, M. Wessling and H. Strathmann, "Plasticization-resistant glassy polyimide membranes for CO_2/CH_4 separations," *Sep. Purif. Technol.*, **14**, 27 (1998).

35. Alam, S., L. D. Kandpal and I. K. Varma, "Ethynyl-terminated imide oligomers," *J. Macromol. Sci. and Rev. Macromol. Chem. Phys.*, **C33**, 291 (1993).

36. Kwock, E. W., T. Baird and T. M. Miller, "Synthesis and Characterization of Soluble, High-Molecular-Weight Poly(Aromatic Diacetylenes)," *Macromolecules*, **26**, 2935 (1993).

37. Tang, H., L. S. Dong, J. Zhang, M. X. Ding and Z. L. Feng, "Miscibility and crystallization behavior of thermosetting polyimide thermoplastic polyimide blends," *Macromol. Chem. Phys.*, **197**, 543 (1996).

38. Karangu, N. T., T. E. Girardeau, G. K. Sturgill, M. E. Rezac and H. W. Beckham, "Solution polymerization of an a,w-diethynyl diimide to a diacetylene-containing polymide via oxidative coupling," *Polymer*, **42**, 2031 (2001).

39. Olabisi, O., L. M. Robeson and M. T. Shaw, *Polymer-polymer miscibility*, Academic Press: New York (1979).

40. Borsig, E., R. Thomann, A. Fiedlerova and R. Mulhaupt, "Morphology of the transparent IPN-like system PE: (BMA-co-S)," *J. Appl. Polym. Sci.*, **81**, 2615 (2001).

41. Nielsen, L. E. and R. F. Landel, *Mechanical properties of polymers and composites*, M. Dekker: New York (1994).

42. Tobolsky, A. V., D. W. Carlson and N. Indictor, "Rubber elasticity and chain configuration," *J. Polym. Sci.*, **54**, 175 (1961).

43. Shen, S. B. and H. Ishida, "Dynamic mechanical and thermal characterization of high-performance polybenzoxazines," *J. Polym. Sci. B: Polym. Phys.*, **37**, 3257 (1999).

CHAPTER 4

SORPTION AND SWELLING BEHAVIOR OF MATRIMID AND BLENDS IN TOLUENE

The stability of Matrimid and polymer blends in toluene and their sorption characteristics are presented in this chapter. Blends of Matrimid with the diacetylene-functionalized crosslinking agents introduced in Chapter 3 have been investigated as a test of one of the hypotheses of this work: that the incorporation of a diacetylene crosslinking agent can stabilize the material. Furthermore, the material properties evaluated in this chapter can have a profound impact on their membrane performance in homogeneous catalyst recovery. Therefore, analysis with some perspective on their final application is provided.

4.1 Introduction

It has been well established at this point that a robust membrane material is required for homogeneous catalyst recovery. The crosslinkable diacetylene-functionalized oligomers characterized in Chapter 3 displayed some promising properties that make them an interesting candidate for membrane materials in this application. In this chapter we will be evaluating the solvent resistance of the host polymer, Matrimid, with varying concentrations of crosslinking agent. The probe solvent chosen is toluene, the solvent for the model hydroformylation reaction under consideration in this work. Through experiments monitoring toluene sorption in these materials, further interpretation of the mor-

phology of the blends will be made as well as an assessment of their potential as membrane materials.

Sorption characteristics also provide insight into the transport properties of these materials. The solution-diffusion model reviewed in Section 2.1.1 governs the permeation rate of toluene. Enhanced toluene solubility in the membrane can lead to higher permeation rates and greater membrane productivity. However, the plasticization that accompanies the faster permeabilities may decrease the ability of the membrane to retain the catalyst due to increased polymer mobility. It is the design intent of the diacetylene crosslinking agent to provide a means to balance the goals of membrane stability and productivity.

4.1.1 Blend Morphology

The properties observed in these sorption investigations are sensitive to the polymer structure. To gain an understanding of the structure impact on sorption, interpretation of the sorption results will be made using the blend morphologies suggested in Chapter 3. For review, schematic representations for the 5% and 10% blend morphologies are shown in Figure 4.1. The 5% blend is in the form of a semi-interpenetrating network (s-IPN). The 10% blend is phase-separated with small domains of the crosslinking agent dispersed in a continuous phase. In the proceeding analysis, it will be assumed that the continuous phase of the 10% blend has the properties of Matrimid due to the small amount of crosslinking agent present in that phase (~1.6%). Application of these representations of the blends to the sorption data will provide information on the structure

influence on their observed sorption behavior as well as enable further refinement of this interpretation of their structure.

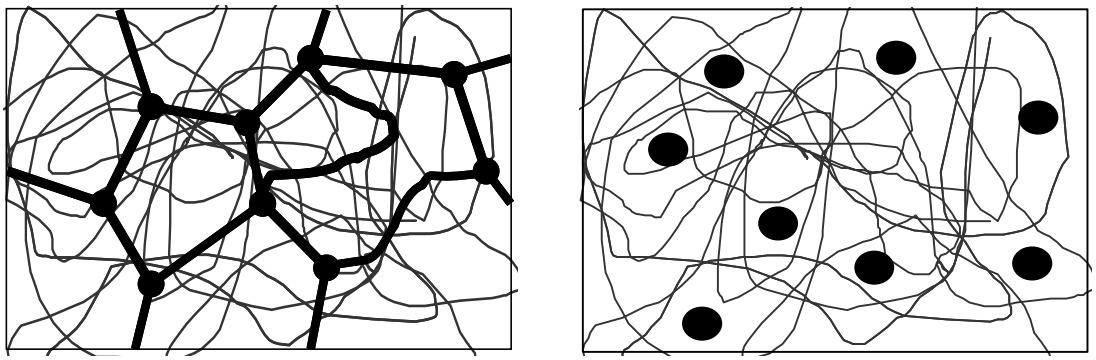

5% Blend **10% Blend**

Figure 4.1: Schematic pictures of blend morphologies. The crosslinking agent is shown as the dark lines with the host Matrimid is shown as the lighter, continuous lines.

4.2 Background

Due to the aggressive nature of toluene and other reaction solvents towards polymers, it is typically necessary to implement some stabilization strategy for membrane materials. Not only is dissolution a potential problem, but membrane selectivity for rejecting the catalyst can also be compromised by polymer plasticization. However, increases in selectivity through stabilization are often accompanied by reductions in flux and some balance between the two is necessary to obtain a productive, yet effective membrane separation process.

One approach to stabilization of polymeric membranes in literature for pervaporation and other organic liquid feed applications is to use either copolymers or blends with alternating components of strong / weak interactions with the permeable compound or hard / soft segments.[1-3] This group of polymers is typically solubility selective and is

used for separations involving feed mixtures with compounds of varying degrees of solubility in the membrane. The success of a homogeneous catalyst recovery membrane is more dependent on size selectivity, with the membrane selectively permeating the smaller structures of the feed and restricting permeation of the large catalyst molecules. Polymer crosslinking via covalent, charge transfer, or plasma-graft crosslinks in the polymer is an approach that can stabilize membranes and impart mobility selectivity.[4-10] Consequently, this work has pursued stabilization via covalent crosslinking.

Polyimides have shown promising properties as membrane materials for gas and liquid mixtures. All of the above listed references for crosslinking are studies utilizing polyimides, some of which have involved separation of organic compounds in the liquid phase. Applications of polyimides in reverse osmosis / nanofiltration have also had some success. In the removal of higher hydrocarbons from toluene feed streams, White[11,12] and Ohya et al.[13] were able to achieve moderate fluxes and selectivities with polyimide membrane materials. However, in each instance, asymmetric membranes were used and little information about permeability or swelling in the polymer medium could be obtained.

This research uses the approach of blending a commodity polymer, Matrimid, with a crosslinking agent. This type of polymer blending could help the membrane process economics because the specialty component is in low concentration. Formation of an s-IPN or nanophase-separated blend between the two components has been a demonstrated way to gain thermal and solvent stability for gas separations.[14] Their applicability to swelling reduction in toluene, the solvent for the model homogeneous catalysis, is presented in this chapter.

4.3 Experimental

4.3.1 Materials

The polymeric materials (Matrimid and crosslinking agent) utilized in sorption experiments can be found in Section 3.3.1. ACS grade toluene (99.5+%, Aldrich, Inc.) was used as received.

The blend concentrations studied in the sorption experiments of this chapter are listed in Table 4.1. Matrimid was evaluated in two states. The "Untreated" films were solvent-cast and dried according to the procedures listed in Section 5.3.2, but not subjected to the "Annealing" conditions (heating to 250 °C for 24 hours) required to activate crosslinking of the oligomers in the blends. "Annealed" Matrimid films, as the name would suggest, were subjected to the same thermal treatment as the blends. This procedure was followed to establish a basis of comparison between the neat Matrimid and blends and also to determine if the annealing alone would affect the swelling and plasticization of Matrimid, as suggested in previous work with this polymer.[5,15] All blends of Matrimid with crosslinking agent are by weight percent and this should be considered implicit in further references to the blends as "5% blend" or "10% blend."

Table 4.1: Blend formulations and Matrimid states studied in sorption experiments.

Material	States Investigated
Matrimid	Untreated, Annealed
Matrimid / Oligomer 1 Blends	5%, 10% by weight
Matrimid / Oligomer 2 Blends	5%, 10% by weight

4.3.2 Film Casting

Matrimid and blends were evaluated as dense films cast using the procedure outlined in Section 5.3.2. Sorption of raw oligomers was performed on the as-received powders. For the blends of Matrimid with crosslinking agent, all films were annealed prior to testing to activate crosslinking.

4.3.3 Vapor Sorption

Thermodynamics dictates that if a component in the vapor phase and liquid phase possess the same activity, the chemical potential of the two states is equal. Because the chemical potential is the driving force for sorption, the amount of penetrant sorbed into a polymer for a given activity will be the same whether it is being fed from the liquid or vapor state. This allows the use of vapor sorption to determine the sorption isotherms and apply them to a liquid separation, which is quite useful due to the comparative ease of gathering accurate sorption data of vapors versus liquids.

The sorption of toluene in polymers or oligomers of interest were studied using a gravimetric sorption apparatus. In this method, a sample is exposed to toluene vapor at a constant partial pressure and the kinetics of sorption and solubility of toluene in the sample is determined by observing the rate of weight gain. Weight of the sample was measured by a computer-controlled microbalance that is connected to a vacuum system. A schematic of the entire experimental apparatus is shown in Figure 4.2.

As the specific workings of the apparatus have been detailed in a prior publication,[16] only a brief overview of the operation will be provided here. A sample to be tested was placed in the electronic microbalance, accurate to 1 μg, (Cahn Instruments

Inc., Model D-200) connected to a vacuum system and toluene vapor supply with a ballast volume of 12 L to minimize pressure fluctuation during measurements. Toluene vapor was supplied from a liquid reservoir in the flask. The balance was housed in a temperature-controlled chamber. All experiments were run at 35 ± 0.1 °C.

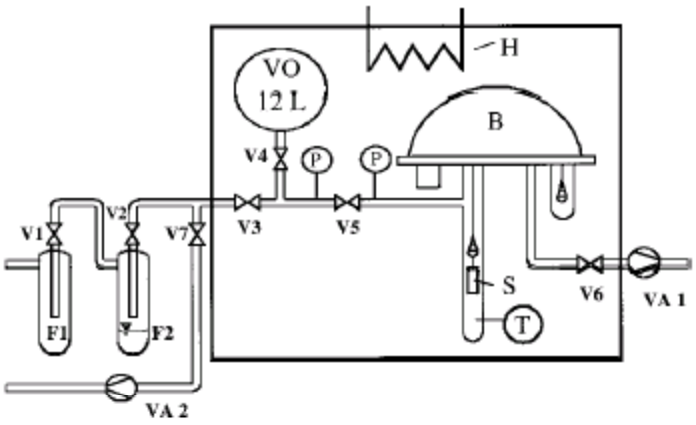

Figure 4.2: Diagram of gravimetric vapor sorption apparatus. Key components are: (B) electronic microbalance, (S) sample, (VO) ballast volume, (VA) vacuum pump, (P) pressure transducer, and (F) flask.[16]

To start a series of sorption runs on a particular material, a sample of known thickness (if a film) was placed on the balance weighing pan and the system was put under vacuum overnight to degas the polymer and sorption apparatus internals. Toluene liquid was then poured into the connected vapor supply flask. To degas the toluene and reduce the inert vapor presence in the system, the toluene liquid was subjected to three freeze / thaw cycles using liquid nitrogen. After that the system was allowed to fill with toluene vapor, with the sample still isolated in vacuum, until the desired vapor pressure for the sorption test was reached, with heating of the toluene liquid provided when necessary. The mass of the sample prior to toluene exposure was recorded. Once the

sample was exposed to toluene (which is $t = 0$ for kinetic experiments), the entire system was allowed to reach the pressure for that run and maintained at it until conclusion. Buoyancy adjustments were not necessary at the low pressures (the vapor pressure of toluene, $p^0_{Tol.}(35\ ^\circ\text{C}) = 46.3$ mm Hg) and high amounts of toluene sorbed by our polymers.

The adjustable parameter of the experiments was toluene partial pressure, p, expressed as its thermodynamic activity, which because of the low pressure conditions can be assumed to behave ideally (Eq. 4.1). The weight fraction of toluene sorbed by the polymer, $w^P_{Tol.}$, was the output variable (Eq. 4.2). Utilizing the sorption versus activity relationships generated by sorption experiments is a useful way of predicting sorption behavior.[17]

$$a_{Tol} = \frac{p}{p^0_{Tol}} \tag{4.1}$$

$$w^P_{Tol} = \frac{M_f - M_d}{M_f} \tag{4.2}$$

In Eq. 4.2, M_d is the dry mass of the sample measured after polymer degassing. M_f is the final mass of the polymer plus sorbed toluene measured by the balance after equilibrium is achieved.

The polymers studied exhibited significant non-ideal sorption characteristics, such as non-Fickian sorption kinetics (to be reviewed in Section 4.4.1) and some history dependence of the final sorption values. For the purpose of establishing that the procedure for obtaining sorption data minimized the impact of history effects, some of the effects that were observed in the materials will be briefly presented as well as the procedures used to maintain uniform histories from sample to sample. It is not uncommon to

observe history effects in glassy polymers sorbing organic compounds.[18-21] Some factors that influence these effects are the thickness of the sample, preswelling of the sample, and whether the sorption pressure was reached in sorption (increasing pressure) or desorption (decreasing pressure). In order to minimize these history effects each sample was subjected to the same conditions.

The sorption conditions for each sample are listed in Table 4.2. As thickness dependence has been observed for organic vapors in glassy polymers,[18] a uniform thickness for all materials was maintained. This also has the added benefit of keeping the time for equilibration on the same order of magnitude for all samples. The state of the material prior to the sorption test was ensured with a rigorous routine of equal pressure steps preceded by an initial sorption at a toluene pressure of 35 mm Hg (p/p^0 = 0.76) to preswell the sample. Experimental evidence depicted in Figure 4.3 confirmed that this was an adequate procedure to get reproducible sorption. A final note is that the length to equilibration was quite long for each pressure step, with an average value of 4 days. Equilibration was considered to be achieved when $\Delta M/\Delta t \leq 1$ μg/hr.

Table 4.2: Experimental parameters for sorption experiments. These are all values that can influence results due to history effects.

Experimental Parameter	Experimental Value
Film thickness	~ 25 μm
Initial preswelling p_{Tol}	35 mm Hg
Equilibration time	4 days
Sorption mode	Sorption

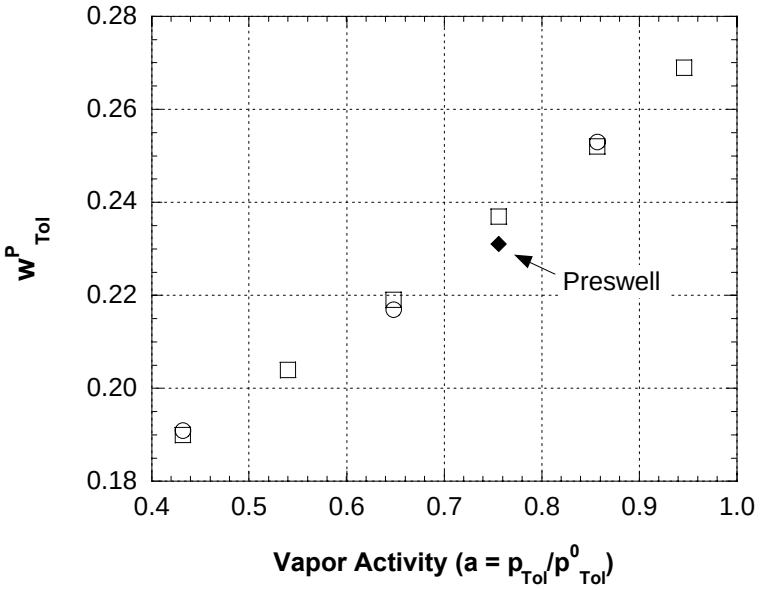

Figure 4.3: Confirmation of $p_{Tol}/p^0_{Tol} = 0.76$ as a suitable preswelling condition. After initially exposing the 10% Oligomer 2 sample to 35 mmHg toluene (♦), isotherm data points were sequentially collected (□) and then points at $p/p_0 = 0.43$, 0.65 and 0.86 (○) were confirmed within +/- 1% of the originally recorded sorption values.

4.4 Results and Discussion

A discussion of the sorption kinetics observed in the Matrimid and blends will be followed by analysis of the equilibrium sorption of toluene in the materials. The influence of annealing the neat Matrimid and incorporation of the crosslinking agent are the core interests of these studies.

4.4.1 Sorption Kinetics

Sorption of toluene in all the materials tested exhibits so-called non-Fickian sorption kinetics.[20,21] When a penetrant with a high affinity for the polymer material sorbs into the polymer matrix, the polymer chains must rearrange (or relax) to accommodate

the penetrant.[22] non-Fickian sorption kinetics are exhibited by glassy polymers when the timescale of diffusion is of the same order of magnitude as that for relaxation of the polymer. Numerical solutions of Fick's law for diffusion into a plane sheet[23] show that the initial gradient in the fractional uptake (M_t / M_∞) of a diffusant is a linear function of ($t^{0.5} / l$), where t is the time of the sorption measurement and l is the thickness of the sheet. Deviations from this relationship are an indication of non-Fickian sorption kinetics. From the sorption curves for toluene in films of Matrimid and Oligomer 1 blends taken for a pressure step of $p = 0 \rightarrow p = 35$ shown in Figure 4.4, the classic "S"-shaped curve indicative of non-Fickian sorption kinetics is exhibited for all of the materials. (Although the untreated Matrimid film looks like it may be linear, on an expanded scale it has the same characteristic non-Fickian shape)

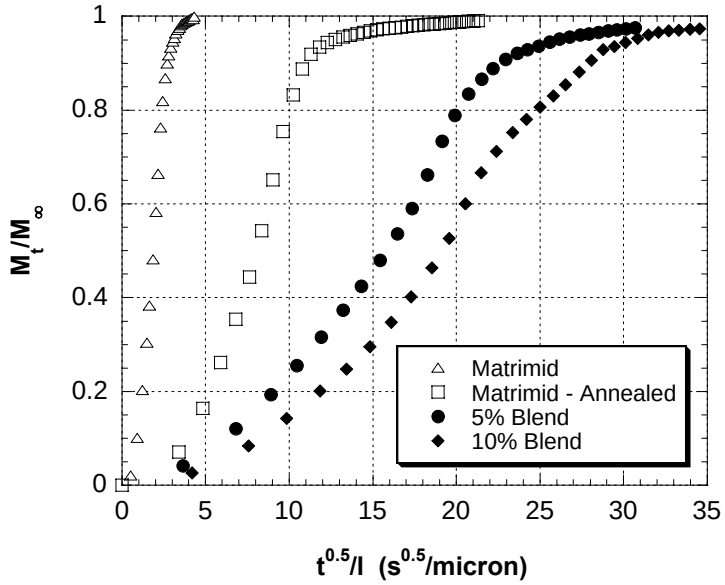

Figure 4.4: Sorption kinetics of toluene in thin films of Matrimid and blends with Oligomer 1 recorded for a $p = 0 \rightarrow 35$ mm Hg sorption step. M_t is mass of penetrant sorbed at time t; M_∞ is the mass of penetrant sorbed at equilibrium. The time scale has been normalized by polymer thickness. All materials display non-Fickian kinetics.

The type of anomalous kinetics exhibited by Matrimid and the blends is quite complex and there are many possible mechanisms that govern them.[21,24,25] The interest of this thesis is in the steady-state behavior of the polymers as membrane materials, so a rigorous analysis of the non-Fickian transient behavior is not within the scope of the research. Attempts to follow the approach of Berens and Hopfenberg[24] to separate the diffusion and relaxation components in the kinetic analysis resulted in toluene diffusivities that were several orders of magnitude lower than those measured in permeation studies, which may be an indicator of the dominance of relaxation in the toluene sorption kinetics. However, qualitative analysis of the kinetic results yields some interesting information. The analysis of the results will follow the generally accepted physical interpertation[22,24] that the factors contributing to the kinetic sorption response are penetrant diffusion within the polymer and polymer relaxation to accommodate the sorbed penetrant molecules.

First, from Figure 4.4 we see that the annealing procedure has significantly affected the kinetics of Matrimid in comparison to the untreated material. Researchers performing heat treatment of polyimides in temperature ranges corresponding to annealing conditions have attributed reductions in sorption to the formation of charge transfer complexes.[26] Charge transfer complexes are formed by electron transfer between an electron-rich donor group and an electron-poor acceptor group.[27] Polyimides contain conjugated structures that can potentially have alternating localizations of charges on the polymer backbone. If groups with opposite charges come into close proximity, the charge transfer complexes can be formed. The formation of the charge transfer complexes may limit the polymer mobility, which would have the dual effect of reducing the

rate of penetrant diffusion and polymer chain relaxation. However, it should be noted that a variable temperature infrared (IR) spectroscopy experiment exposing Matrimid to temperatures up to 350 °C in nitrogen (an inert environment similar to the vacuum conditions of annealing in this research) observed no changes in the spectrum.[14] Other investigations including IR and density measurements in this study yield no conclusive evidence of a structural change after the annealing process. But the charge transfer complexes remain the most likely explanation for the fairly significant change in sorption kinetics observed here as well as the toluene sorption results of this chapter and the permeabilities presented in Chapter 5.

Figure 4.4 also shows that the incorporation of the diacetylene-functionalized crosslinking agents in blends has slowed the uptake of toluene relative to both annealed and untreated Matrimid, with the 5% blend possessing faster kinetics than the 10% blend. From the morphological picture of the 5% blend obtained in the atomic force microscopy (AFM) and other studies of Chapter 3, this material is in the form of a semi-interpenetrating network (s-IPN) with the diacetylene oligomer forming a crosslinked network surrounding the Matrimid after heat treatment. The restricted mobility of the polymer chains in the s-IPN should retard the sorption kinetics of toluene in this polymer. Reduced diffusion, though its contribution has not been quantified relative to polymer relaxation, is one cause for the reduced kinetics relative to the host Matrimid. Mobility restriction from crosslinks can also have a significant impact on the relaxation rate of the polymer blend. Although mechanical analysis of the materials (Section 3.4.5) did not indicate any measurable changes in their modulus with the addition of crosslinking agent, prior work has demonstrated the extreme sensitivity of anomalous sorption kinetics not

only to history[18,21] of the sample, but also to structural changes[28,29] in the polymer. The kinetic data may be exhibiting some smaller-scale mechanical strengthening of the blend due to s-IPN formation that is not apparent in the mechanical analysis.

AFM studies indicate that the 10% blend is a phase-separated material with concentrated domains of crosslinking agent surrounded by Matrimid. Though it is uncertain whether the phase-separated domains consist entirely of crosslinked oligomer and behaves like the pure oligomer, this will be assumed for this portion of its analysis. As indicated by the sorption results to be presented in Figure 4.9 of Section 4.4.2, the crosslinking agent does not measurably sorb any toluene after annealing. Based on the relative sorption between it and Matrimid combined with the probability that the phase-separated domains are highly crosslinked, they are going to be considered as impermeable structures dispersed within the Matrimid. This morphology can affect both the diffusion and relaxation dynamics of the polymer during the uptake of toluene. In terms of diffusion, the crosslinked domains will act as obstacles and add tortuosity to the penetrant diffusion path. The domains may also act like a filler in composite polymer materials, strengthening the Matrimid by restricting chain mobility and extending the relaxation time of the blend. One widely accepted mechanism for polymer relaxation during penetrant uptake is the exertion of a swelling stress by the penetrant on the polymer chains.[22] In this case, the crosslinked domains may absorb some of that stress, causing discontinuities in the stress gradient through the polymer also extending the relaxation time.

Also, it is interesting to note that this is virtually the only characterization of the 10% Oligomer 1 blend performed in this research that displays marked differences

between itself and the 5% Oligomer 1 blend other than the catalyst rejection. Though not shown here, blends with Oligomer 2 exhibit the same kinetic characteristics.

.

4.4.2 Sorption in Matrimid

Sorption tests have a twofold purpose. First, the stability and swelling of the membrane materials at various concentrations of toluene can be determined. Also, the approach to accomplishing the homogeneous catalyst recovery is through the use of nonporous membrane materials, which follow the solution-diffusion model (Section 2.1.1). Penetrant solubility is one of the two factors governing transport in this model and the solubility contribution to flux can be determined from these studies. Furthermore, the influence of the addition of crosslinking agent on the sorption behavior can be observed.

The host polymer, Matrimid, is insoluble in toluene. This was confirmed by soaking Matrimid in a toluene bath for seven days and observing no weight loss in the material after drying under vacuum. The blends also exhibited the same insolubility under this test. A host material that is insoluble in the permeating species is a good starting point for the blend approach, because tuning of the swelling resistance versus flux tradeoff can be achieved with a smaller fraction of crosslinking agent in the blend.

Although insoluble, Matrimid sorbs a considerable amount of toluene, as shown in Figure 4.5. As an activity of one is approached the weight fraction of toluene sorbed, w_{Tol}^{P}, exceeds 0.35. Liquid dip tests of the Matrimid films and blends were attempted and the sorption in the pure liquid could not be determined due to extremely rapid desorption

upon removal of the sample from the toluene bath. However, extrapolation from the sorption isotherm yields a $w_{Tol}^{P} = 0.37$ for an activity of one.

From the dual-mode theory of sorption in polymers,[30] penetrant sorption in glassy polymers occurs via two concurrent mechanisms. One is ordinary dissolution and the other is "hole filling," or penetrant occupation of the non-equilibrium microvoids present in glassy polymers due to restricted segmental mobility of the polymer chains. The profile of the sorption curve in Figure 4.5 for low to moderate toluene activities (approximately: $0 \leq a \leq 0.5$) follows this model. At higher activities the isotherm has an upswing that is indicative of swelling. In these stages of sorption, the swelling of the polymer creates new sorption sites and the sorption capacity of the polymer is increased.

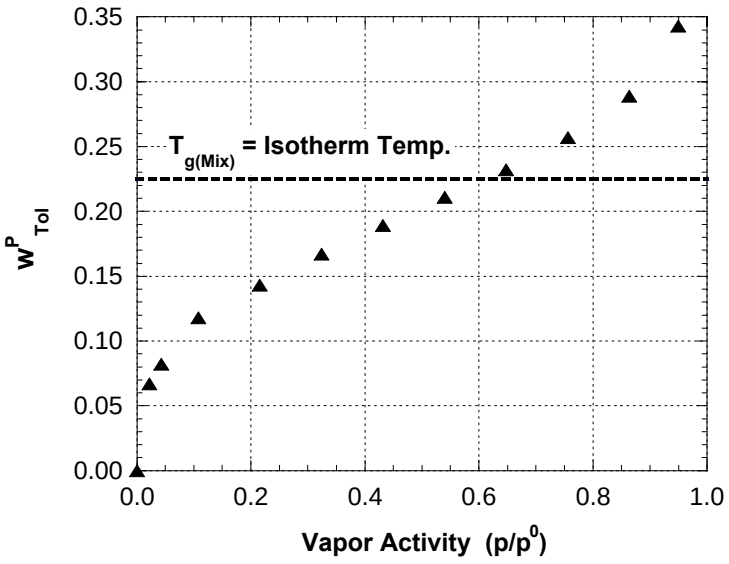

Figure 4.5: Toluene sorption isotherm in untreated Matrimid at 35 °C. The weight fraction of toluene corresponding to a glass transition for the sorbed polymer equal to the isotherm temperature as calculated by the Fox equation[31] shown by the dashed line.

The chemical similarity between Matrimid and toluene is likely causing this high sorption due to strong physicochemical interactions. The backbone structure of Matrimid (and polyimides in general) possesses a high concentration of aromatic structures that could strongly interact with the toluene. This is consistent with other studies investigating toluene sorption in polyimides.[10,32-34]

A consequence of having a high sorption of toluene is plasticization of the polymer and the corresponding reduction in its glass transition temperature (T_g). An estimate of the weight fraction of toluene at which the glass transition temperature is equal to the temperature of the sorption isotherm (35 °C) is shown on Figure 4.5. The Fox equation[31] (Eq. 4.3) can be used to calculate the glass transition of swollen polymer membranes:

$$\frac{1}{T_{g(mix)}} = \frac{w_P}{T_{gP}} + \frac{w_1}{T_{g1}} + ... \tag{4.3}$$

with subscripts 1 and P referring to the toluene and the polymer, respecitvely and the T_g is given in Kelvin. Glass transition temperatures for some common hydrocarbons including toluene have been reported in literature.[35,36] The value for the glass transition temperature of toluene used in the calculation is 117 K. Since the glass transitions of the blends do not vary greatly from the host Matrimid (Section 3.4.5), the value of $w_{Tol}^{P}(T_{g(mix)} = 35°\text{C}) = 0.225$ can be considered the same for all materials presented. It is interesting that the swelling upswing in Figure 4.5 begins very near this concentration, but it is only a fairly crude estimate. The same calculation using the equation of Pochan, Beatty, and Pochan,[37] which uses a logarithmic phase mixing rule, calculates a value for $w_{Tol}^{P}(T_{g(mix)} = 35°\text{C}) = 0.31$ assuming no volume change on mixing. However, permeation studies of toluene presented in Chapter 5 also suggest that at high toluene activities

the polymers behave as materials in the rubbery state. The implications of being in a rubbery state in terms of transport are that gains in flux will be made due to the increased segmental mobility; but transport studies will have to be made to determine if the selectivity of the materials is sufficient (Chapter 5).

4.4.3 Model Interpretation of Sorption

Using the above interpretations of the toluene sorption, the isotherm can be fit to the dual-mode sorption model for lower toluene activities in Matrimid. In the region of the swelling upturn, the Flory-Rehner[38] equation (Eq. 4.4) for crosslinked rubbers provides a good fit. The fits for toluene sorption in untreated Matrimid are shown in Figure 4.6. The Flory-Rehner equation needed to be modified for the "state" change observed in our sorption experiments. If the toluene-swollen Matrimid is considered a rubber the volume fraction terms in Eq. 4.5 need to be modified to make the "0" volume fraction sorbed by the material still contain the toluene necessary to plasticize it. This correction was used as a fitting factor, ϕ'_P, and is shown in Eq. 4.5.

$$\ln a_1 = \ln(1-\phi_P^R) + \phi_P^R + \chi_1(\phi_P^R)^2 + \nu\overline{V}_1\left[(\phi_P^R)^{1/3} - \phi_P^R/2\right] \tag{4.5}$$

$$\phi_P^R = \phi_P + \phi'_P \tag{4.6}$$

The calculated parameters for each of the materials studied are in Table 4.1. Values for the crosslink density, ν, have been taken from those calculated in the dynamic mechanical analysis studies (Section 3.4.5). Equation 4.5 was fit to the sorption data obtained by assuming no volume change on mixing with the sorption isotherms giving ϕ_P and a_1. The χ_1 and ϕ'_P parameters were adjusted to give the best fit. An increasing χ_1, the Flory interaction parameter, indicates decreasing sorption in the polymer.

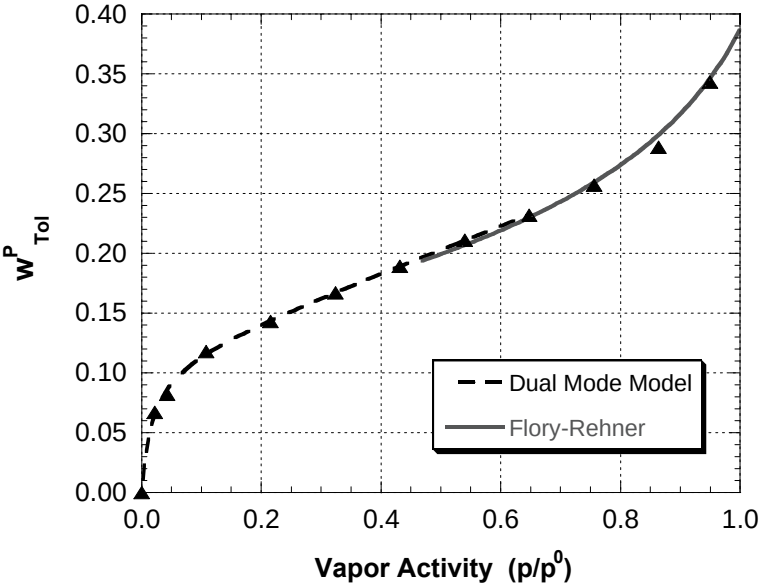

Figure 4.6: Sorption of toluene in Matrimid modeled by the Dual Mode Sorption for low activities and Flory-Rehner at high activities.

Table 4.3: Flory-Rehner parameters (Eqs. 4.5 and 4.6) for toluene sorption in Matrimid and blends at 35°C. All values reported within +/- 5%.

Material	χ	ν (mol xlink/cm^3)	ϕ'_P
Matrimid	1.03	-	0.182
Matrimid – Annealed	1.34	-	0.209
5% Oligomer 1 Blend	1.38	1.12 x10^{-3}	0.208
10% Oligomer 1 Blend	1.37	-	0.197
5% Oligomer 2 Blend	1.30	1.19 x 10^{-3}	0.209
10% Oligomer 2 Blend	1.34	1.23 x 10^{-3}	0.195

4.4.4 Influence of Annealing and Blending on Sorption

The effects of annealing on Matrimid are again seen in the sorption data. Figure 4.7 shows the comparison of the annealed Matrimid to the untreated material. Sorption isotherms in this and the ensuing figures have been plotted in the high vapor activity range to highlight the sorption differences between the materials. Suppression of the swelling upturn visible in the untreated Matrimid has been achieved to some extent through annealing of the Matrimid alone. Similar to the observations in kinetic studies, the sorption of toluene has been suppressed; possibly by the formation of charge transfer complexes restricting the polymer's ability to swell and accommodate more toluene. Bos and coworkers[15] found reproducibly reduced permeabilities of CO_2 in Matrimid after heat treating of Matrimid at 265 °C as well as some reduction in the CO_2-induced plasticization. However, plasticization still occurred in their treated films at the same CO_2 partial pressure. It was not until a crosslinking agent was added that the films were stabilized.

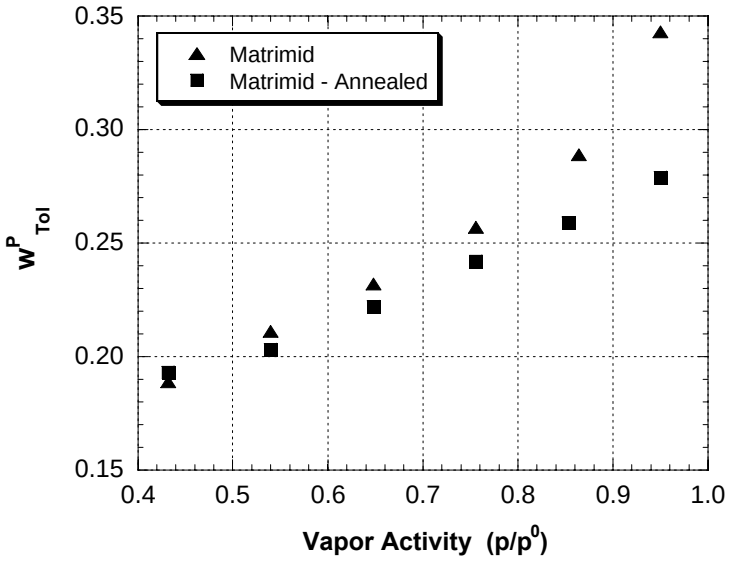

Figure 4.7: Toluene sorption isotherm at 35 °C for annealed Matrimid compared to untreated Matrimid.

The influence of blending Oligomer 1 in 5% and 10% weight fractions is shown in Figure 4.8. Both the 5% and 10% blends show some further reduction of toluene sorption relative to the annealed Matrimid with an average reduction of about 7% of the annealed Matrimid sorption as an activity of one is approached. However, when going from 5% to 10% there is not a marked change in the sorption characteristics. One conclusion of Bos et al.[15] in their work with s-IPN's of Matrimid and crosslinking agents was that the differences in transport behavior were not a strong function of crosslinking agent concentration. Though that may account for the similarity between the 5% and 10% blends of Oligomer 1 here, it is more likely that the two different morphologies for the blends displayed the same sorption characteristics through different mechanisms. Presuming that 5% blend is an s-IPN, the formation of a network around the Matrimid is acting to restrict the mobility of the polymer blend limiting its ability to swell and create more sorption sites for toluene. In this case, it is difficult to have an *a priori* prediction of the sorption values for the blend due to the complexity of the s-IPN.

Viewing the 10% blend as a phase-separated mixture of crosslinked oligomer and Matrimid, the reduction of the toluene sorption in this material should be proportional to the ratio of crosslinked domains to Matrimid multiplied by their corresponding toluene solubilities. With the above considerations in mind, the toluene sorption characteristics of pure Oligomer 1 were tested and the results are shown in Figure 4.9. In the un-crosslinked state, the oligomer displays lower toluene sorption than Matrimid – approximately 10 wt% compared to over 35 wt% at high activities. After annealing of the sample, the crosslinked oligomer displayed no measurable sorption of toluene above the noise level of the gravimetric balance.

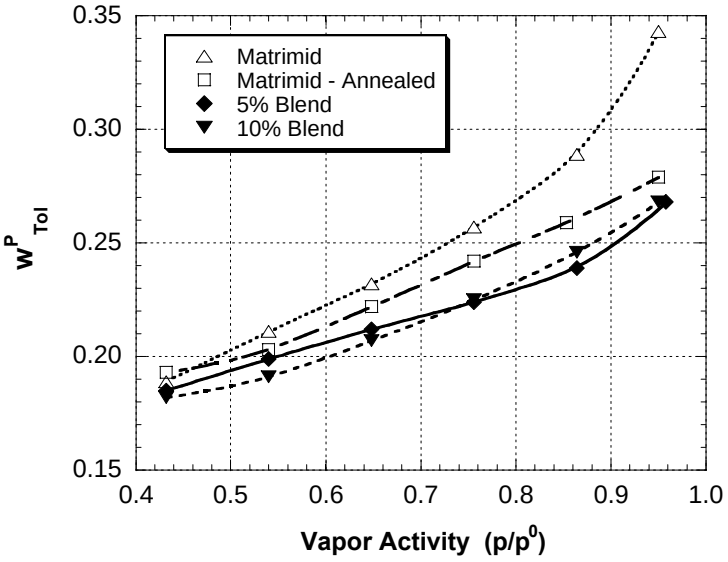

Figure 4.8: Sorption of toluene in Oligomer 1 blends at 35 °C. Untreated and annealed Matrimid included for comparison. Lines have been drawn for clarity.

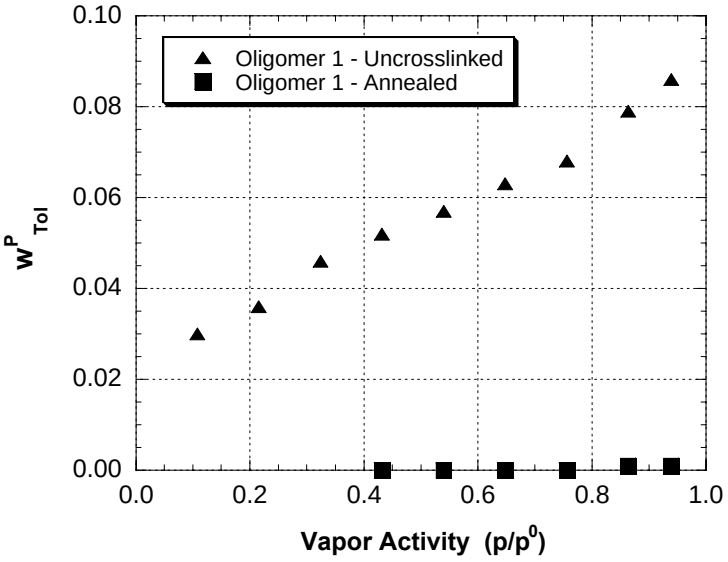

Figure 4.9: Toluene sorption at 35 °C in raw Oligomer 1 crosslinking agent before and after activation of crosslinking. No sorption of toluene was observed after crosslinking above the error limits of the balance.

If it is assumed that the phase-separated domains in the 10% blend behave in the same manner as the crosslinked oligomer, then the blend can be viewed as a composite of annealed Matrimid with a non-sorbing, inert phase. The ~8.4% value for the fraction of the crosslinked domains that was determined from the AFM in Section 3.4.5 along with the sorption values for the annealed Matrimid can be used to predict the sorption in the phase-separated blend. This would approximate the 10% blend as a material composed of 91.6% sorbing phase that has the toluene sorption properties of annealed Matrimid and the remainder is non-sorbing. This morphological interpretation of the 10% blend gives a fairly good representation of the experimentally observed toluene sorption, with the prediction of sorption shown by the line in Figure 4.10.

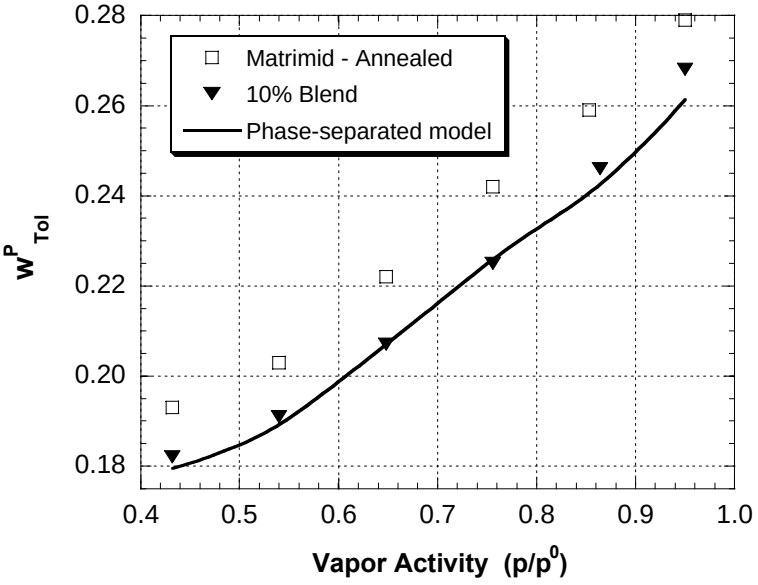

Figure 4.10: Plot of 10% Oligomer 1 blend toluene sorption with a fit based on interpreting the phase morphology as annealed Matrimid containing 8.4% inert, non-sorbing material.

Finally, toluene sorption for the blends of Matrimid with Oligomer 2 has been performed and is presented in Figure 4.11. The 5% blend of Oligomer 2 with Matrimid has less sorption reduction than the same concentration of Oligomer 1, possibly due to the fewer reactive sites present on the Oligomer 2 crosslinking agent. The 10% blend behaves in a manner similar to that of Oligomer 1. Due to these similarities between the two crosslinking agents, transport studies in Chapter 5 will be primarily focused on the Oligomer 1 species.

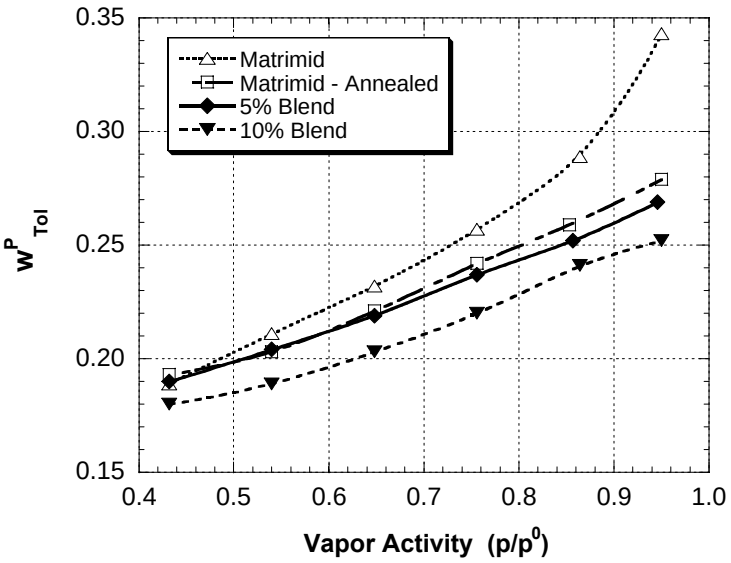

Figure 4.11: Sorption of toluene in Oligomer 1 blends at 35 °C. Untreated and annealed Matrimid included for comparison. Lines have been drawn for clarity.

4.5 Conclusions

Addition of the crosslinking oligomers has the effect of reducing the solubility and swelling of Matrimid in the reaction solvent toluene. Heat treatment (annealing) of Matrimid alone at a temperature of 250 °C reduces its swelling in high concentrations of

toluene. Incorporation of crosslinking agent can provide further reduction in sorption and swelling. The diacetylene crosslinking agents were able to stabilize the membrane materials, but still maintain significant sorption, which may be able to promote productive membrane fluxes, but the transport studies of Chapter 5 must be reviewed for membrane selectivity to determine if the materials are suitable for the homogeneous catalyst recovery.

The non-Fickian kinetics of sorption show an interesting delineation of the various states and blends of polymers studied. Uptake of toluene increases in the order of: 10% Blend < 5% Blend < annealed Matrimid < untreated Matrimid. The kinetic response of the annealed Matrimid coupled with its reduced sorption indicates that the polymer network was strengthened as a result of the heat treatment. The reduction in kinetics for the blends is likely due to network formation (5% blend) or the strengthening of the polymer with a high mechanical strength filler (10% blend).

Additional support for the phase-separated morphology of the 10% blend has been garnered from the sorption results. The crosslinked oligomer shows no significant sorption. Using the assumption that the dispersed phase viewed in AFM studies has the same sorption characteristics, a model of the 10% blend as annealed Matrimid with inert filler matches its sorption data well. Because of its similar sorption characteristics, the 5% does not fit this morpholigical model and suggests that network formation can lead to similar reductions in sorption with less crosslinking agent.

4.6 References

1. Cabasso, I., "Organic liquid mixtures separation by permselective polymer membranes. 1. Selection and characteristics of dense isotropic membranes employed in the pervaporation process," *Ind. Eng. Chem. Prod. Res. Dev.*, **22**, 313 (1983).

2. Ho, W. S. W., G. Sartori and D. A. Thaler, "Polyimide copolymers containing polycarbonate soft segment," In *U.S. Patent No. 5,756,643* (1998).

3. Tanihara, N., N. Umeo, T. Kawabata, K. Tanaka, H. Kita and K. Okamoto, "Pervaporation of organic liquid mixtures through poly (ether imide) segemented copolymer membranes," *J. Memb. Sci.*, **104**, 181 (1995).

4. Yamaguchi, T., S. Nakao and S. Kimura, "Plasma-graft filling polymerization - preparation of a new type of pervaporation membrane for organic liquid mixtures," *Macromolecules*, **24**, 5522 (1991).

5. Bos, A., I. G. M. Punt, M. Wessling and H. Strathmann, "Plasticization-resistant glassy polyimide membranes for CO_2/CH_4 separations," *Sep. Purif. Technol.*, **14**, 27 (1998).

6. Okamoto, K., H. Wang, T. Ijyuin, S. Fujiwara, K. Tanaka and H. Kita, "Pervaporation of aromatic/non-aromatic hydrocarbon mixtures through crosslinked membranes of polyimide with pendant phophonate ester groups," *J. Memb. Sci.*, **157**, 97 (1999).

7. Fang, J., K. Tanaka, H. Kita and K. Okamoto, "Pervaporation properties of ethynyl-containing copolyimide membranes to aromatic/non-aromoatic hydrocarbon mixtures," *Polymer*, **40**, 3051 (1999).

8. Staudt-Bickel, C. and W. J. Koros, "Improvement of CO2/CH4 seoparation characteristics of polyimides by chemical crosslinking," *J. Memb. Sci.*, **155**, 145 (1999).

9. Wind, M. M. and H. J. W. Lenderink, "A capacitance study of pseudo-fickian diffusion in glassy polymer coatings," *Prog. in Org. Coat.*, **28**, 239 (1996).

10. Ren, J., C. Staudt-Bickel and R. N. Lichtenthaler, "Separation of aromatics/aliphatics with crosslinked 6FDA-based polyimides," *Sep. Purif. Tech.*, **22-23**, 31 (2001).

11. White, L. S., "Transport properties of a polyimide solvent resistant nanofiltration membrane," *J. Memb. Sci.*, **205**, 191 (2002).

12. White, L. S. and A. R. Nitsch, "Solvent recovery from lube oil filtrates with a polyimide membrane," *J. Memb. Sci.*, **179**, 267 (2000).

13. Ohya, H., I. Okazaki, M. Aihara and S. Tanisho, "Study on molecular weight cut-off performance of asymmetric aromatic polyimide membrane," *J. Memb. Sci.*, **123**, 143 (1997).

14. Sturgill, G. K., "Stabilization of polyimide blends through solid-state crosslinking," *Ph.D. Thesis*, Georgia Institute of Technology (1999).

15. Bos, A., I. G. M. Punt, M. Wessling and H. Strathmann, "Suppression of CO_2-plasticization by semiinterpenetrating polymer network formation," *J. Polym. Sci. B: Pol. Phys.*, **36**, 1547 (1998).

16. Rezac, M. E., T. John and P. H. Pfromm, "Effect of copolymer composition on the solubility and diffusivity of water and methanol in a series of polyether amides," *J. Appl. Polym. Sci.*, **65**, 1983 (1997).

17. Lipnizki, F. and G. Tragardh, "Modelling of pervaporation: Models to analyze and predict the mass transport in pervaporation," *Sep. Purif. Method*, **30**, 49 (2001).

18. Hopfenberg, H. B., "The effect of film thickness and sample history on the parameters describing transport in glassy polymers," *J. Memb. Sci.*, **3**, 215 (1978).

19. Berens, A. R., "Sorption of organic liquids and vapors by rigid PVC," *J. Appl. Polym. Sci.*, **37**, 901 (1989).

20. Sanopoulou, M. and J. H. Petropoulos, "Sorption and longitudinal swelling kinetic behavior in the system cellulose acetate-methanol," *Polymer*, **38**, 5761 (1997).

21. Sanopoulou, M. and J. H. Petropoulos, "Systematic analysis and model interpretation of micromolecular non-Fickian sorption kinetics in polymer films," *Macromolecules*, **34**, 1400 (2001).

22. Crank, J., "A theoretical investigation of the influence of molecular relaxation and internal stress on diffusion in polymers," *J. Polym. Sci.*, **11**, 151 (1953).

23. Crank, J. and G. S. Park, *Diffusion in Polymers*, Academic Press: New York (1968).

24. Berens, A. R. and H. B. Hopfenberg, "Diffusion and relaxation in glassy polymer powders: 2. Separation of diffusion and relaxation parameters," *Polymer*, **19**, 489 (1978).

25. Alfrey, T., E. F. Gurney and W. G. Lloyd, "Diffusion in glassy polymers," *J. Polm. Sci.: Part C*, **12**, 249 (1966).

26. Bos, A., "High pressure CO_2/CH_4 separation with glassy polymer membranes: aspects of CO_2-induced plasticization," *Ph.D. Thesis*, University of Twente (1996).

27. Dinan, F. J., W. T. Schwartz, R. A. Wolfe, D. S. Hojnicki, T. St. Clair. and J. R. Pratt, "^{13}C-NMR spectral evidence for charge transfer complex formation in aromatic diimides and dianhydrides," *J. Polym. Sci., Polym. Chem. Ed.*, **30**, 1992 (1992).

28. Bajpai, A. K. and M. Shrivastava, "Enhanced water sorption of a semi-interpenetrating polymer network (IPN) of poly(2-hydroxyethyl methacrylate) (PHEMA) and poly(ethylene glycol) (PEG)," *J. Macromol. Sci. Pure.*, **39**, 667 (2002).

29. Lin, A. A., V. R. Sastri, G. Tesoro and A. Reiser, "On the cross-linking mechanism of benzophenone containing polyimides," *Macromolecues*, **21**, 1165 (1988).

30. Vieth, W. R., J. M. Howell and J. H. Hsieh, "Dual sorption theory," *J. Memb. Sci.*, **1**, 177 (1976).

31. Billemeyer Jr., F., *Textbook of Polymer Science*, Wiley-Interscience: New York (1984).

32. Hao, J., K. Tanaka, H. Kita and K. Okamoto, "The pervaporation properties of sulfonyl containing polyimide membranes to aromatic/aliphatic hydrocarbon mixtures," *J. Memb. Sci.*, **132**, 97 (1997).

33. Kim, J., B. Chang, S. Lee and S. Y. Kim, "Incorporation effect of fluorinated side groups into polyimide mebranes on their pervaporation properties," *J. Memb. Sci.*, **169**, 185 (2000).

34. Xu, W. Y., D. R. Paul and W. J. Koros, "Carboxylic acid containing polyimides for pervaporation separations of toluene/iso-octane mixtures," *J. Memb. Sci.*, **219**, 89 (2003).

35. Privalko, V. P., "Excess entropies and related quantities in glass-forming liquids," *J. Phys. Chem.*, **84**, 3307 (1980).

36. Angell, C. A., J. M. Sare and E. J. Sare, "Glass transition temperatures for simple molecular liquids and their binary solutions," *J. Phys. Chem.*, **62**, 2622 (1978).

37. Pochan, J. M., C. L. Beatty and D. F. Pochan, "Viscosity and glass transition relations for polymer-diluent systems," *Polymer*, **20**, 879 (1979).

38. Flory, P. J. and J. Rehner Jr., "Statistical mechanics of crosslinked polymer networks. Part 2. swelling," *J. Chem. Phys.*, **11**, 521 (1943).

CHAPTER 5

TRANSPORT OF HOMOGENEOUS REACTION COMPONENTS

Characterizations of the polyimide, Matrimid, and blends with the novel diacetylene crosslinking agent thus far have demonstrated their potential as membrane materials for homogeneous catalyst recovery. A systematic study of the transport characteristics of the 1-dodecene hydroformylation components is presented in this chapter not only to assess the viability of the subject materials of this research in homogeneous catalyst recovery, but also to identify the underlying mechanisms that affect this separation. In this manner, the various polymer states of this research are presented in order to determine their influence.

5.1 Introduction

As outlined in Chapter 2, the function of the membrane in homogeneous catalyst recovery is to retain the catalyst and permeate the products, reactants and solvent. A reactor effluent containing a homogeneous transition metal catalyst is fed to a membrane separator. A catalyst-rich recycle stream is then recycled to the reactor from the membrane retentate (fraction of the feed not permeated through the membrane) for further reaction and catalyst reuse. In terms of the model hydroformylation reaction of focus in this research (Figure 5.1), the components to be permeated are toluene, 1-dodecene and tridecanal (as well as the CO/H_2 syngas reactant). The design intent of the membrane is to selectively restrict permeation of the rhodium triphenylphosphine catalyst complex

while permeating the above components. The permeate stream will have a reduced catalyst content that can then be subjected to further separation steps to separate the reactants and solvent from the product. The benefits of using a membrane for the catalyst recovery step have been outlined in Chapter 2.

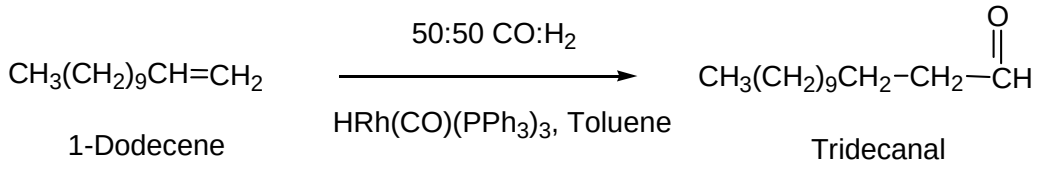

Figure 5.1: The hydroformylation of 1-dodecene to form tridecanal with a rhodium tristriphenylphosphine organometallic catalyst.

A preliminary indication of the dominant mechanisms that drive this membrane separation – and consequently the material design approach for membranes to be applied to it – can be obtained from the physical properties of the feed components (Table 5.1). In membrane material selection, the two mechanisms by which membrane selectivity is attained are differences in penetrant solubility and diffusivity in the membrane material, following the solution-diffusion model for membrane transport (Section 2.1.1). Lloyd and Meluch[1] have shown that membrane solubility selectivity can be correlated to the differences in Hildebrand solubility parameters of the feed components for liquid separations. Although, the solubility parameter of the catalyst is unknown, it is fair to assume that its solubility parameter is fairly close to that of the triphenylphosphine since this functionality is the predominant feature of the catalyst structure. With this in mind, the differences in solubility parameters shown in Table 5.1 for all components are nominal and it appears that this membrane separation will not provide any significant solubility

selectivity. Lack of solubility selectivity is a feature that can likely be applied to the general case of homogeneous catalyst recovery beyond this specific model reaction. A criterion for solvent selection is high solvating ability for the reaction components and the strong interactions between these components will likely inhibit any solubility selectivity.

Table 5.1: Physical properties of membrane feed components.[2]

Component	MW (g/mol)	$\delta^{1/2}$ $(J/cm^3)^{1/2}$	van der Waals Volume (cm^3/mol)
$HRh(CO)(PPh_3)_3$	919	-	517[a]
Triphenylphosphine	262	19.7[3]	161
Tridecanal	198	19.1	149
1-Dodecene	168	16.6	126
Toluene	92	18.2	60

[a]Additive contribution of tristriphenylphosphine, rhodium, carbon monoxide and hydrogen

The large size of the catalyst, shown in terms of molecular weight and van der Waals volume in Table 5.1, relative to the other reaction components must be the means to achieve the separation. Membrane materials that can selectively sieve the catalyst and permeate the smaller reaction components are the objective for this application. The materials under consideration in this research are nonporous, and size selectivity is manifested in the diffusivity of the components in the dense polymer matrix, hence the terms: diffusivity selective or mobility selective membranes.

An analysis of the membrane performance of Matrimid and crosslinked blends is presented in this chapter with the purpose of identifying their suitability for homogeneous catalyst recovery. It will be highlighted in the subsequent background section (Section 5.2) that little fundamental understanding exists of the governing mechanisms of homogeneous catalyst recovery. Therefore, the approach of this chapter is to attempt to

geneous catalyst recovery. Therefore, the approach of this chapter is to attempt to elucidate the relationship of factors such as component diffusivity and solubility to the ultimate catalyst rejections and product fluxes that can be achieved. Furthermore, the influence of the diacetylene crosslinking agent on the transport properties will be investigated to test the hypothesis that these materials can impart stability and selectivity while still maintaining membrane productivity.

In the aim of achieving these goals, the permeabilities of toluene, 1-dodecene (dodecene), and triphenylphosphine in Matrimid and blends with Oligomer 1 have been measured experimentally. Toluene, as the reaction solvent, has significant impact on the catalyst rejection and membrane fluxes that can be achieved. Prior work in solute recovery from liquid streams[4,5] has found that the solute rejection is a strong function of the solvent medium. This fact can aid in increasing the permeability of the product through the membrane, but can be detrimental to achieving significant catalyst rejection levels. Therefore, the permeabilities of model product and catalyst species (dodecene and triphenylphosphine, respectively) have been measured in the toluene-swollen membrane material. The choices of each model component have been dictated by their relative ease of experimental analysis. Dodecene, due to its similar chemical structure and size is assumed to have transport properties commensurate with the product, tridecanal. Triphenylphosphine, the catalyst ligand, has been analyzed to observe the effects of membrane material modification on the catalyst subunit as well as provide a conceptual benchmark for the properties of the larger catalyst molecule. Also, the rejection of triphenylphosphine may be a beneficial side product of the catalyst recovery, due to the

free ligand typically included in industrial reaction formulations.[6] The species studied and their function in the reaction are summarized in Table 5.2.

Table 5.2: Hydroformylation reaction components studied in transport experiments.

Component	Function	Structure
Toluene	Solvent	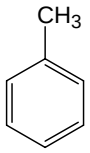
Dodecene	Reactant / Product Analogue	$CH_3(CH_2)_9CH{=}CH_2$
Triphenylphopshine (TPP)	Catalyst Ligand	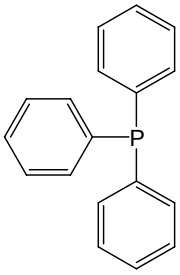
$HRh(CO)(PPh_3)_3$	Catalyst	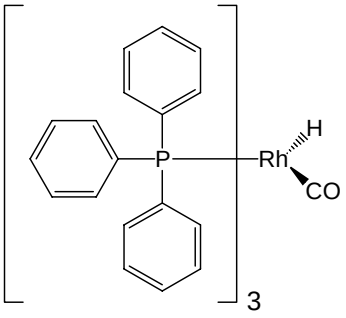

5.2 Background

Synthesis of complex organic compounds often requires the use of soluble transition metal catalysts.[7] However, the expense of these catalysts and intensive separation steps required to recover them from the reaction products often generates waste materials and consumes energy. Membrane recovery of these catalysts has been recognized as a potentially energy efficient means to recover the catalyst in its active state.[3,5,8-16]

To date, the work in implementing membranes for catalyst recovery has focused on proofs of concept utilizing commercial nanofiltration membranes. Hydrogenation,[14,16] Heck coupling,[10-12] oxidation,[9] and hydroformylation[3] are among some of the reactions that the catalyst has been proven to remain active after the recycle step. In the few instances where catalyst recovery is reported, the rejections obtained are fairly good. Miller et al.[3] demonstrated that a PDMS-based (polydimethylsiloxane, a common rubbery membrane material) commercial membrane was able to reject rhodium-organophosphite catalysts at levels >99% in an aldehyde solvent and >93% in acetone. In a study of a Heck coupling reaction using a palladium catalyst, Nair et al.[12] report initial catalyst rejections of 96% with a decline in rejection after recycle to 90% using a commercial polyimide membrane. Catalyst decomposition was cited as the cause for the decline in rejection in this study, but it is also possible that this decline reflects some unsteady-state plasticization occurring during the course of the experiment. An interesting study by Scarpello et al.[5] measured catalyst rejection for three different catalyst species, varying the solvent medium and membrane. A wide range of rejections was observed, from 60% to >99%, which were strongly influenced by membrane type and solvent medium. No conclusive evidence or analysis was provided to explain the observed trends.

In the above-cited instances, the researchers were interested in demonstrating the ability of these membranes in catalyst recovery and not in material design. The interaction between the membrane, catalyst and other diffusing species is not very well understood and may explain some of the variability exhibited when altering solvents or membrane types. Additionally, the composition of the commercial membranes is often unknown and their asymmetric morphology prevents direct measurement of component diffusion rates. The work presented in this research attempts to address this void in information regarding polymer-penetrant properties and their influence on separation characteristics.

5.3 Experimental

5.3.1 Materials

The polymeric materials and crosslinking agents used in this section are identical to those presented in Chapter 3. Unless otherwise specified, the crosslinking agent used in the blends is Oligomer 1. The chemicals studied in transport measurements are listed in Table 5.3. All compounds were used as received.

Table 5.3: Reagents for transport studies and their function in the model reaction.

Chemical	Purity	CAS No.	Supplier
Toluene	≥99.5%	108-88-3	Aldrich
1-Dodecene	≥99%	1121-41-4	Fluka
Triphenylphosphine	99%	603-35-0	Aldrich
$RhH(CO)(P(C_6H_5)_3)_3$	97%	17185-29-4	Aldrich

5.3.2 Film Casting

All transport studies were performed on dense, nonporous films. The benefit of using dense films as opposed to composite or asymmetric membrane materials is their homogeneous structure and quantifiable thickness. From transport studies on the dense films, intrinsic material properties can be found.

Lack of solubility of the crosslinkable oligomer (Chapter 3) made choice of casting solvent difficult. Hexafluoroisopropanol (HFIP) was the only solvent studied that would readily dissolve the host polymer, Matrimid, as well as the crosslinkable oligomers in significant concentrations. At the start of film preparation, Matrimid and crosslinking agents were dried under vacuum without heating for 4 hours to remove residual water. Crosslinking agent and Matrimid were weighed out in the proper ratios for a given blend prior to addition of solvent. All subsequent steps in film formation were performed in a nitrogen purged glovebag due to the hygroscopic nature of the HFIP solvent and the resultant polymer precipitation that would occur if the solutions were exposed to ambient moisture. HFIP was added to the dry polymer / oligomer to give solutions containing 1 – 2 wt% polymeric material. Approximately one hour of mixing was sufficient time for dissolution. Films were cast in 2.25" stainless steel rings on mirrors. The polymer solution was filtered through a 0.45 μm (PTFE, Cole-Parmer) syringe tip filter into the casting ring. 5 mL of solution in a ring would result in a final, dried film thickness of approximately 25 μm, which was the standard thickness used in all experiments. A slight nitrogen purge was maintained in the glovebag while the solvent evaporated over the course of 2 days.

After solid films were formed in the casting rings, the mirror was removed from the glovebag and the nascent films were removed from the mirror by floating off with deionized water. Drying steps to remove residual HFIP were complicated by complex formation between the solvent and the carbonyl groups of the polyimides.[17] Sturgill[17] found that a heat treatment of 180 °C for 3 days was sufficient to break this complex and remove the remaining HFIP. Therefore, films were dried under vacuum according to this procedure, with a 30 °C/hr ramp from ambient conditions to 180 °C to prevent macrovoid formation.[17] Annealing of the films to activate crosslinking (or anneal neat Matrimid) was then performed at 250 °C for 24 hours.

To get a greater appreciation of the influence of annealing, untreated Matrimid films were cast in chloroform (ACS Grade, Aldrich) to avoid complex formation and exposure of the films to the 180 °C temperature of HFIP decomplexation. Casting conditions were the same as the HFIP-cast materials with the exception of a 3-day drying period of 100 °C. Solvent exchange of any residual chloroform in the material after the drying step occurred in preswelling of the films in toluene performed before transport studies.

5.3.3 Toluene Diffusion and Hydraulic Permeability

Toluene diffusion and hydraulic permeability have been measured in hydraulic permeation experiments. In this membrane operation, a pure liquid is fed to a polymer film and permeation is induced through the application of pressure on the feed. Details of the experimental apparatus and parameter calculation from these tests are given in

Appendix A. All experiments were run at 35 °C with motive pressure supplied as a nitrogen pressure head on the liquid.

Due to the high sorption of toluene in the polymers studied, films were preswelled in toluene prior to testing to reduce dimensional changes that may occur. This reduced the possibility of film failure due to swelling once placed in a membrane test cell and its area was constrained. An added benefit of preswelling is a reduction in the time needed to achieve steady-state diffusion in the polymer due to the slow kinetics of the material. Based on the kinetic studies of Chapter 4, the films were soaked in toluene at least 4 days before testing in hydraulic permeation.

5.3.4 Dialysis Permeability Measurements

The permeabilities of 1-dodecene and triphenylphosphine were determined in dialysis experiments. Dialysis is the transport of a solute through a membrane that separates solutions of different solute concentration. Each dialysis experiment began with a "feed" solution of the compound of interest in solution with toluene and a "permeate" solution of toluene, each 100 mL. The initial feed concentrations used were 6 mmol/L for triphenylphosphine and 50 mmol/L for dodecene for each dialysis experiment.

Solute (triphenylphosphine and dodecene) permeabilities were determined using the experimental apparatus and calculation methods detailed in Appendix A. In dialysis, the sole driving force is the difference in solute concentration in the two solutions separated by the membrane set at the start of a run. The basic apparatus of the hydraulic permeation tests was used, except with the known permeate volume of toluene connected to the permeate side of the membrane test cell. The feed and permeate volumes were

well-mixed and the increase in solute concentration in the permeate volume was monitored with respect to experiment time to determine permeability. An Agilent Model 6890 gas chromatograph (GC) equipped with a 5% phenyl methyl siloxane capillary column (Agilent HP-5, 30m long x 0.25 μm nominal diameter) and a flame ionization detector (FID) was used to detect solute concentration via reference to the solvent peak area. Again, all polymer films tested in dialysis were preswelled in toluene and the experiment was conducted at 35 °C.

5.3.5 Solute Rejection

The ability of the polymer films to retain dissolved solutes was tested in rejection studies. In these studies, the permeation apparatus was run in a similar manner to hydraulic permeability, collecting liquid permeate for analysis. A flow diagram of the apparatus is shown in Figure 5.2. Feeds of solute in solution with toluene were fed to the membrane test cell, with the liquid permeate collected and analyzed for solute concentration. The 100 mL Parr reactor unit feeding the membrane was agitated at 400 rpm and feed pumps to the membrane test cell circulated the fluid at 100 mL/min to limit concentration polarization, a factor that can reduce the apparent membrane rejection due to mass transfer limitations at the membrane surface.[18] The low fluxes through the polymer films and the turbulence generated through fluid recirculation is sufficient to render concentration polarization negligible. A purge volume of 3 mL (holdup volume of the membrane test cell x 2) was allowed to permeate before a sample to be analyzed was collected to ensure steady state concentrations. The GC was used to determine the solute concentra-

tions in the feed and permeate. The rejection, $\Re$, was determined using the standard calculation:

$$\Re = \left(\frac{c_{jo} - c_{jl}}{c_{jo}} \right) \times 100 \tag{2.11}$$

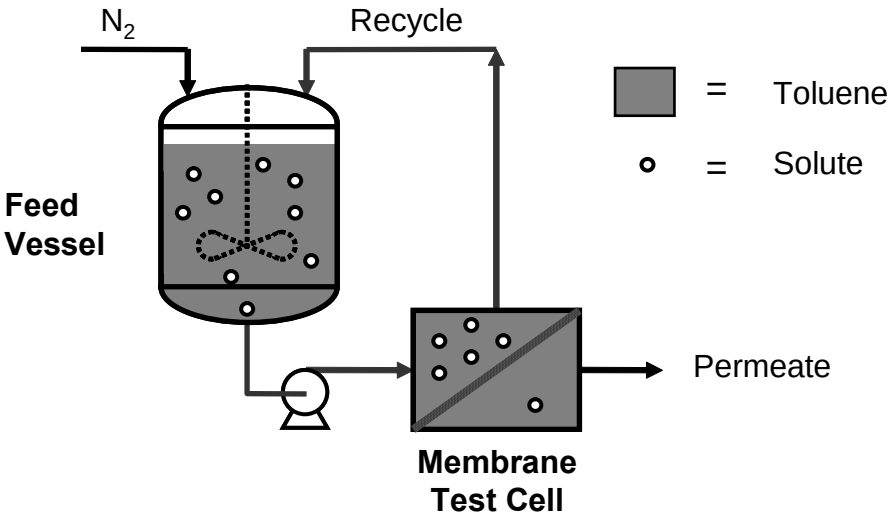

Figure 5.2: Diagram of experimental apparatus employed in rejection studies.

In these experiments as well as catalyst rejection (Section 5.3.6), the influence of the osmotic pressure, π, of the solute has been evaluated using the van't Hoff equation (Eq. 5.1). It is typical in analysis of solute rejection to account for osmotic pressure effects by reducing the pressure driving force by osmotic pressure ($\Delta p - \pi$), which has been applied here. However, because of the low concentrations (c_S) used in each of the experiments (as well as in practice), this osmotic pressure effect is negligible with the maximum experimental $\pi < 0.25$ atm.

$$\pi = c_S RT \tag{5.1}$$

5.3.6 Catalyst Rejection

Catalyst rejection experiments were conducted in the same manner as solute rejection experiments. Due to the air and moisture sensitivity of the rhodium catalyst, solutions were prepared in a nitrogen-purged glove box. The permeation apparatus was dried under vacuum prior to the rejection experiments and run with an inert nitrogen atmosphere. Detection of the catalyst concentration was performed using inductively coupled plasma (ICP) atomic emission spectroscopy. A Perkin-Elmer Optima 3000-DV was used to analyze rhodium content. The Analytical Chemistry Group at the Institute of Paper Science and Technology at Georgia Tech conducted sample preparation and analysis.

Due to incompatibilities of the instrument internals with the organic solvent toluene, an aqueous based solution had to be prepared. The procedure for sample preparation is as follows: A metered amount (500 μL) of a catalyst solution was put into a sample vial and the toluene was allowed to evaporate, leaving the nonvolatile catalyst behind. 5 mL of nitric acid (HNO_3) was added and the solution was boiled for 30 minutes. 5mL hydrogen peroxide (H_2O_2) was added to that and boiled again for 30 minutes. A final boiling step followed the addition of hydrochloric acid (HCl, 5 mL). To bring the final sample volume up to 5 mL, deionized water was added. Samples of known rhodium concentration were referenced to an internal standard to confirm complete recovery of the rhodium by this procedure.

5.3.7 Solute Solubility in Polymers

Determination of solute solubility in the polymeric materials serves two functions in this research. First, according to the solution-diffusion model, solute permeability is a function of solubility and an understanding of its influence on solute flux can better characterize this system. The other function of solubility measurement is a more practical matter. Since permeability is the only measured quantity in the dialysis experiments, the solubility can then be used to determine solute diffusivity in the polymers.

The solubility of the solutes in the polymers can be related to their liquid composition through an equilibrium partitioning coefficient, K_i. This value should be a constant at the small solute concentration ranges investigated in the toluene-swollen polymers.[19] K_i has been measured by a method of sorption followed by solvent extraction.

A polymer sample is placed in an adsorption solution of known solute concentration (c_{iA}) in toluene. The volume of this solution (20 mL) is quite large relative to the polymer sample (100 mg, or ~0.08 mL) so that its concentration can be assumed constant during the sorption step, although measurements of concentration by GC were performed at the start and end of each solubility test to confirm this. Equilibration of the solution and polymer was allowed to occur over 10 days in a sealed container: a conservative estimate based on the toluene sorption kinetics of Chapter 4 and low solute diffusivity in the material. After this, the polymer film was removed from the sorption solution, patted dry to remove excess solvent and placed in a desorption bath of pure toluene. Potential exists for inaccuracy due to the presence of residual solution on the films and ambient desorption before transfer from bath to bath. Multiple tests showed a reproducibility of ±15% for the solute concentration in desorption. Care was taken to perform this step in a

glovebag that was toluene-saturated by open beakers of toluene to prevent excess desorption from the films. Furthermore, the solutes investigated in this manner, dodecene and triphenylphosphine, have very low volatilties and little loss of the sorbed components should have occurred through the vapor phase. The volume of the desorption bath (4 mL) was dictated by the detection limits for the solutes in the GC. After another 10 days was allowed for the solute to desorb to its equilibrium partitioning between the toluene solution and the polymer, the solute concentration of the desorption bath (c_{iD}) was measured. A mass balance on the solute is then used to determine the value of its partition coefficient, K_i:

$$K_i = \frac{c_{iD}}{c_{iA} - c_{iD}} \left(\frac{v_D}{v_M} \right) \tag{5.2}$$

where v_D is the volume of the desorption bath and v_M is the volume of the toluene-swollen polymer sample, determined from the sorption relationships of Chapter 4. The concentration of solute in the liquid phase is related to that in the polymer phase by:

$$c_i^M = K_i c_i \tag{5.3}$$

5.4 Results and Discussion

Transport data is presented here in the interest of characterizing the effects of changes in material properties of Matrimid and blends induced by thermal treatment and blending and their impact on separation characteristics for homogeneous catalyst recovery. The separation of factors contributing to component flux has been performed with the objective of identifying their influence on the material efficacy. For a uniform basis of comparison, the transport properties in annealed Matrimid will be compared to the

blends. Though not shown, the untreated Matrimid shows uniformly higher transport for all components relative to the other materials.

5.4.1 Toluene Transport

Toluene thickness-normalized flux in the polymer films at a 10 atm pressure driving force (Δp) is shown in Table 5.4. Flux decreases as the crosslinking agent content of the blends increases, nearly by a factor of two for each additional step in blend concentration.

Table 5.4: Thickness normalized fluxes of toluene in Matrimid and Oligomer 1 blends for a feed pressure of 10 atm at 35 °C.

Material	**Flux** (L-μm/m^2-hr)
Annealed Matrimid	13.8 ± 0.8
5% Blend	8.7 ± 0.4
10% Blend	4.7 ± 0.4

The diffusivity and hydraulic permeability of toluene in Matrimid and the blends with Oligomer 1 is shown in Figure 5.3. Diffusivities and permeabilities were determined at various applied pressures and it was found that an average value over the pressure ranges studied described the system well (Appendix A.2). These averages are the values reported in Figure 5.3.

The hydraulic permeability relates flux to driving force, so the permeability trend in the materials matches the fluxes shown in Table 5.4. Permeabilities for the materials decrease in the same order: annealed Matrimid > 5% Blend > 10% Blend. Following the solution-diffusion model, the factors affecting this trend are the sorption and diffusion of

toluene in the polymer films. The observations in the sorption studies of Chapter 4 were that sorption of toluene was reduced in blends of Matrimid with the crosslinking agent. Thus, it appears that one factor affecting the decline in flux of these materials is reduced toluene sorption. This is a predictable result based on the relatively high toluene sorption levels in the polymers and its subsequent reduction upon blending and thermal treatment.

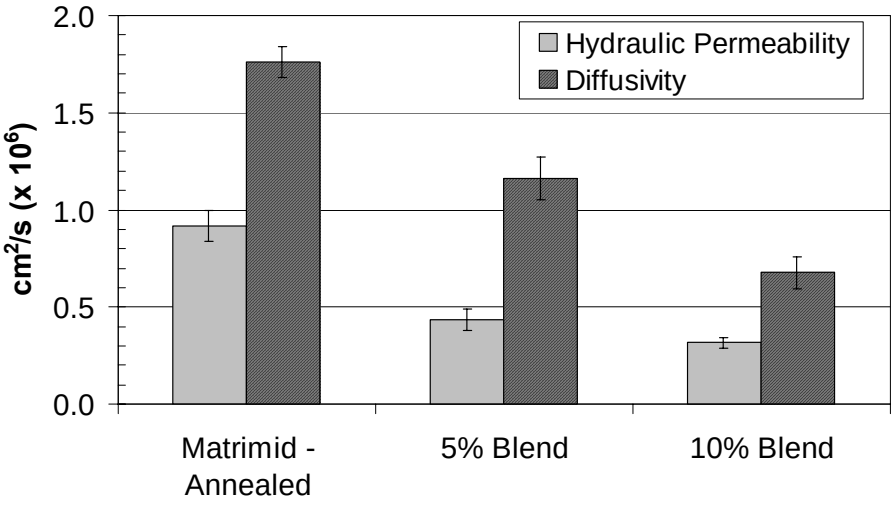

Figure 5.3: Hydraulic permeability and diffusivity of **toluene** in Matrimid and blends with Oligomer 1 measured at 35 °C. Transport data was obtained in hydraulic permeation.

Toluene sorption can also indirectly affect flux through reduction of polymer chain mobility or plasticization as toluene content in the polymer decreases. Additionally, polymer mobility is reduced through network formation and increased polymer-polymer interactions such as those suggested to occur in the annealing of Matrimid (charge transfer complex formation, Chapter 4). These two factors affecting polymer mobility are manifested in the diffusivities of toluene in the polymer. The diffusivities

shown in Figure 5.3 show a declining trend with the addition of crosslinking agent suggesting that reductions in both sorption and diffusion are influencing the toluene permeability.

An interesting facet of the toluene diffusivities in these materials is that they suggest the polymers are in the rubbery state. Similar to thermal and mechanical properties, transport properties in polymers are significantly affected by the enhanced segmental mobility which occurs when the polymer transitions from a glassy to rubbery state.[18] This is observed as a marked difference in penetrant diffusion rates in glassy versus rubbery polymers. The toluene diffusivities in Matrimid and blends are on the same order of magnitude as those measured by Paul and Ebra-Lima[20] for several solvents in natural rubber. As it was introduced in Chapter 4, the degree of toluene sorption in these materials is sufficient to indicate suppression of the glass transition temperature below the experimental temperature of 35 °C. In terms of homogeneous catalyst recovery, the rubbery state of these materials can have the effect of enhancing flux of the desired components, increasing the productivity of the membrane. This is quite desirable due to the large portion of the membrane feed that is required to permeate in these applications. The solute permeabilities and catalyst rejections presented in the subsequent sections of this chapter suggest that it is possible achieve selective materials for this separation with these polymers in the rubbery state.

Impact of Blend Phase Morphology

Continuing with the same morphological understanding of the materials that has been developed in Chapters 3 and 4, the s-IPN structure of the 5% Blend should have

mobility restriction due to the formation of crosslinks. The reduction in toluene diffusivity in the 5% Blend relative to the annealed Matrimid supports this interpretation.

A model of the 10% Blend as a two-phase material with a continuous phase that possesses essentially the same properties as annealed Matrimid and a non-sorbing secondary phase of crosslinked oligomer was put forth in Chapter 4. If we extend that model to assume that the phase separated domains are not only non-sorbing, but also impermeable to toluene (a valid assumption considering the extremely low sorption of toluene in the crosslinked oligomer as well as its highly crosslinked structure) the diffusion characteristics in this idealized material can be predicted. The effective diffusion coefficient, D_{eff}, of a small solute through a medium containing impermeable spheres periodically arrayed can be predicted by[21,22]:

$$\frac{D_{eff}}{D} = \frac{1-\phi_I}{\left(1+\frac{\phi_I}{2}\right)} \tag{5.4}$$

where D is the diffusion coefficient of the material without the spheres and ϕ_I is the volume fraction of the impermeable spheres. Applying Eq. 5.4 to the above morphology with $\phi_I = 8.4\%$ (based on AFM analysis of the dispersed domains in the 10% Blend, Section 3.4.4) predicts that the effective diffusivity of the blend would be 88% of the host polymer (annealed Matrimid in this case). In contrast, the measured toluene diffusivity in the 10% Blend is only 39% of the annealed Matrimid diffusivity. This discrepancy suggests that the simplified morphology of annealed Matrimid with impermeable domains that was assumed is not entirely accurate. One possible explanation for the discrepancy is that because the dispersed phase does not contain the entirety of crosslinkable oligomer in the blend (8.4% versus 10%), the continuous phase may possess some s-IPN

character, which will lower the diffusivity through mobility restriction in addition to the tortuosity of diffusion path introduced by the crosslinked domains.

5.4.2 1-Dodecene and Triphenylphosphine Transport

The equilibrium partitioning of the solute between liquid solution and polymer provides the sorption contribution to transport. The values for the partition coefficient, K_i, are shown in Table 5.5. For each solute measured, the sorption increases with the addition of crosslinking agent. This is a somewhat unfortunate and unanticipated result for the triphenylphosphine, which is assumed to be representative of the sorption characteristics of the catalyst. Since it is the design intent of these membrane materials to reject the catalyst, the increase in permeability that accompanies this sorption increase is counterproductive. The influence of the increased sorption is compounded when taking into account the flux coupling effects observed in similar systems,[4,5] reviewed in Chapter 6. In a system with flux coupling, collisions with the faster moving component – toluene in the model case – drag the solute through the membrane reducing rejection and these effects are generally enhanced with increasing solute sorption. However, in regards to dodecene, these effects are useful in increasing its flux through the membrane.

The origins of the higher blend sorption of triphenylphosphine and dodecene may be attributed to the increase in concentration of unsaturated and conjugated bonds through addition of the crosslinking agent. As presented in Chapter 3, the reactions of the diacetylene and terminal acetylene functionalities in the crosslinking oligomer both form highly conjugated structures. This increases the opportunities of the double bond of

the dodecene and the unpaired electrons of triphenylphosphine to interact with the polymers.

Table 5.5: Partition coefficients for dodecene (DOD) and triphenylphosphine (TPP) in Matrimid and blends with Oligomer 1 relative to solutions in toluene.

Material	K_{DOD}	K_{TPP}
Annealed Matrimid	0.33 ± 0.01	0.39 ± 0.05
5% Blend	0.39 ± 0.01	0.73 ± 0.12
10% Blend	0.45 ± 0.01	0.55 ± 0.09

The augmented sorption of dodecene in the blends results in enhanced permeabilities, as shown in Figure 5.4. Dodecene permeability remains relatively unchanged when the crosslinking agent is added to Matrimid. However, dodecene diffusion coefficients (obtained by dividing permeability by the partition coefficient following Eq. 2.7) are reduced. This follows the trend of the crosslinking agent reducing mobility in the manner that has thus far been established. Therefore, it seems that the rise in sorption negates the drop in diffusion resulting in minimal permeability changes for the blends. Figure 5.5 shows similar behavior for triphenylphosphine permeabilities. Increases in sorption of triphenylphosphine counteract the reduced diffusivities accompanying blending.

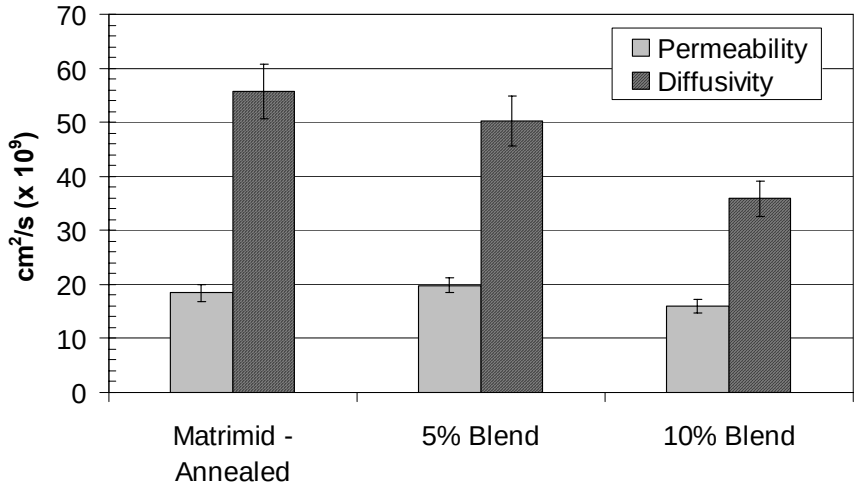

Figure 5.4: Permeability and diffusivity of **dodecene** in Matrimid and blends with Oligomer 1 measured at 35 °C. Transport data was obtained in dialysis through toluene-swollen polymer.

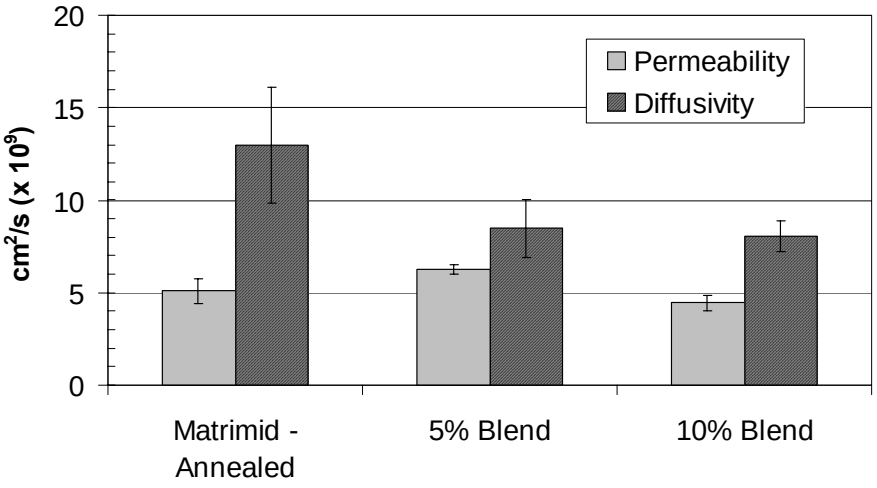

Figure 5.5: Permeability and diffusivity of **triphenylphosphine** in Matrimid and blends with Oligomer 1 measured at 35 °C. Transport data was obtained in dialysis through toluene-swollen polymer.

There is a marked difference in the permeabilities of the reaction components that enables selective separation. The plot in Figure 5.6 shows that permeability is a strong function of penetrant size. This confirms the original assertion that this separation is based strongly on mobility selectivity. Toluene permeabilities are on average 100 times greater than that of triphenylphosphine. In terms of product selectivity, the permeabilities indicate an average of 3.5 times greater transport rate for the dodecene over the triphenylphosphine. Though this value is low, the catalyst is over three times larger than the triphenylphosphine molecule and the trend of Figure 5.6 indicates that it will have a much lower permeability than triphenylphosphine with a commensurate increase in the rejection.

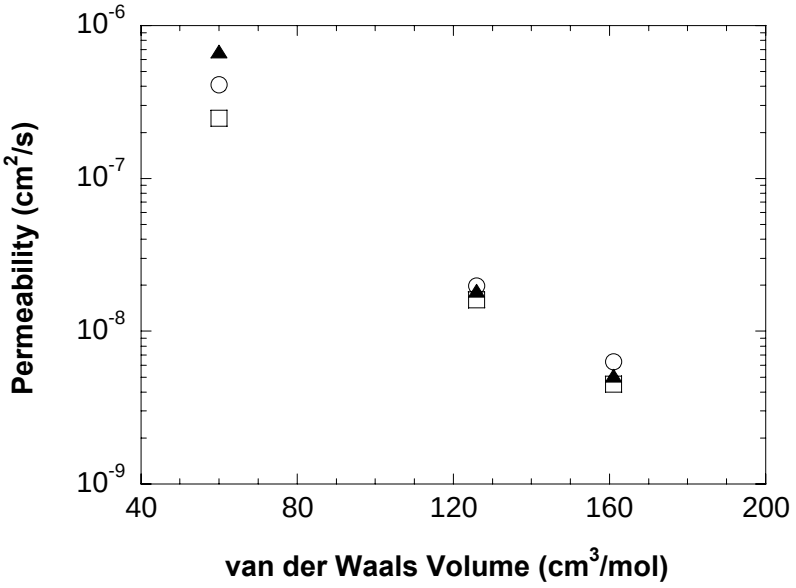

Figure 5.6: Plot of single component permeability as a function of molar volume for hydroformylation components in annealed Matrimid (▲), 5% Oligomer 1 blend (○), and 10% Oligomer 1 blend (□).

Figure 5.6 also shows that addition of the crosslinking agent has little impact on enhancing the ideal selectivity of Matrimid. It has already been seen that solute sorption characteristics contribute to the minimal effect of the crosslinking agent on selectivity. Another factor that may diminish the effects of blending is the fairly large fraction of toluene sorbed by these materials, with each of the materials sorbing over 25 wt% toluene. It has been observed in similar systems[19] that the solute diffusivity is a strong function of the solvent content in the membrane, thus reducing the impact of mobility restriction. However, viewing the permeability alone does not account for the flux coupling effects that are present in this system. This feature of penetrant transport in these materials is apparent in the mixed component permeation of the rejection studies presented in the following section.

5.4.3 Rejection Studies

In the rejection studies of the various reaction components, experimental conditions simulate the catalyst recovery step. It follows a reverse osmosis mode of operation with a liquid mixture fed to the membrane under an applied pressure. The concentration gradient for all penetrants lies in the same direction unlike the dialysis experiments. Therefore, interactions of the permeating components can be seen in this operation, particularly the influence of the faster permeating toluene on the slower solutes. Because of the high levels of sorption, a significant probability exists that toluene can "drag" the solutes through the membrane and reduce the rejection.

The rejection of dodecene and triphenylphosphine by Matrimid and Oligomer 1 blends is shown in Table 5.6. Dodecene, shown to have a higher permeability in dialysis,

has a consistently lower rejection than triphenylphosphine for all of the materials. Triphenylphosphine rejection increases with crosslinking agent content with the highest rejection given by the 10% Blend, retaining about 43% of the triphenylphosphine fed to it. If we neglect the interactions between toluene and the solute, the solution-diffusion model (using Eqs. A.17 and A.20) predicts significantly higher rejections than those experimentally observed, shown in Table 5.7. In fact, because the toluene permeability is decreasing with increasing crosslinking agent content and solute permeability is minimally changed, the rejection trend is opposite what we observe experimentally for triphenylphosphine.

Table 5.6: Experimentally measured rejections for dodecene and triphenylphosphine in solution with toluene for Matrimid and Oligomer 1 Blends for a feed pressure of 7 atm at 35 °C. Rejection values reported as mean values with deviation as error.

Material	$\Re_{DOD}$ (%)	$\Re_{TPP}$ (%)
Annealed Matrimid	14 ± 3	20 ± 2
5% Blend	23 ± 3	28 ± 4
10% Blend	16 ± 2	43 ± 2

Table 5.7: Predicted values for the rejections for dodecene and triphenylphosphine using the solution-diffusion model equations neglecting interactions between the solvent and solute in the membrane.

Material	$\Re_{DOD}$ (%)	$\Re_{TPP}$ (%)
Annealed Matrimid	67	91
5% Blend	56	84
10% Blend	49	81

It appears that pentrent-penetrant interactions are indeed influencing the solute fluxes observed in the rejection studies. A simplified look at the transport will explain the origins of this occurrence. Fluxes observed in membrane systems are relative to a stationary frame of reference, usually defined by the membrane. The flux of a component relative to a stationary frame of reference, n_i, can be expressed as:

$$n_i = w_i \sum_{j=1}^{nc} n_j + j_i \tag{5.4}$$

with the typical[23] j and n notation for flux relative to the mass average velocity and stationary frame of reference, respectively. Typically membrane separations are based on the diffusive contribution to the flux j, which is what has been calculated in Table 5.7. However, when solute sorption is substantial, as in the solute rejection studies, the contribution of the first term on the left hand side of Eq. 5.4 (termed "bulk flux" here) affects the solute flux. As the solute sorption increases so does the contribution of the bulk flux, diminishing the benefits gained by the large differences in diffusion between the solute and the solvent. The increased solute flux that results reduces the membrane rejection of the solute. Additionally, the much larger flux of the solvent dominates the total flux through the membrane, the other factor influencing the bulk flux. Increases in the solvent diffusion through the membrane may also lead to reduced solute rejections.

This generalized analysis can explain some of the previously cited solvent-solute coupling effects as well as the trend in triphenylphosphine rejection observed here where the triphenylphosphine rejection is higher for the materials with lower toluene sorption and fluxes. A more detailed analysis of the coupled transport using the Maxwell-Stefan transport formulation is provided in Chapter 6.

5.4.4 Catalyst Rejection

The expectations that the membrane rejection of the catalyst would exceed that of the other components in the model reaction mixture were confirmed in the rejection studies of catalyst in solution with toluene, shown in Table 5.8. All of the materials studied show higher rejection relative to the rejections of dodecene and triphenylphosphine. The behavior of permeability relative to penetrant size from Figure 5.6 suggests that this is largely due to the large size of the catalyst relative to the other components. This effect of catalyst size on rejection is particularly emphasized when considering that its solubility characteristics should be similar to those of triphenylphosphine, which would indicate that mobility selectivity is the primary means to achieve permeability differences between these two components.

Table 5.8: Rejection of $HRh(CO)(PPh_3)_3$ catalyst for various materials for a feed pressure of 7 atm at 35 °C. Feed for rejection experiments was a 2 mmol/L catalyst solution in toluene.

Material	$\mathfrak{R}_{Cat}$ (%)
Annealed Matrimid	40 ± 4
5% Oligomer 1 Blend	76.3 ± 1.7
10% Oligomer 1 Blend	**91.5 ± 0.6**
10% Oligomer 2 Blend	87.3 ± 1.3

The catalyst rejection behavior of the materials relative to crosslinking agent content behaves in a similar manner as triphenylphosphine, with catalyst rejection increasing as crosslinking agent content in Matrimid is increased. The 10% Oligomer 1 blend showed the highest rejection at 91.5%, which is comparable to the >90% catalyst rejections observed by other researchers cited in Section 5.2. Based on the generalized

approach to flux coupling introduced in Section 5.4.3, the improved performance of the 10% Blend relative to the 5% Blend may be due to the reduced catalyst sorption and toluene permeability in this material, both of which will have the effect of reducing the coupling of the toluene and catalyst flux.

A final test of the higher molecular weight crosslinking agent, Oligomer 2, was conducted in order to determine the presence of any effects of crosslinking agent reactivity or structure in this separation. As in the sorption experiments of Chapter 4, it appears that very little difference in transport is achieved through the use of the higher molecular weight crosslinking agent.

It is interesting that the 10% Blend, with an apparent phase-separated morphology, exhibits the highest catalyst rejection. This may suggest that incorporation of an impermeable, non-sorbing filler into a polymer may be a means to enhance selectivity. However, some caution must be exercised in this interpretation, both practically and in phenomenological terms. The small size of the phase-separated domains as well as their chemical similarity to the host polymer are likely enhancing the compatibility of the phases at their interface. When the domain size and concentration of the dispersed phase increases, nonselective interfacial gaps occur between the continuous phase and filler.[24] This can result in embrittlement of the material such as in the phase-separated blends above 10 wt% oligomer observed in Chapter 4 as well as losses in selectivity such as those viewed by Merkel et al.[25] when combining fumed silica with poly(1-trimethylsilyl-1-propyne) or Barrer's work with rubbers.[24] Furthermore, the simple analysis of the 10% Blend as Matrimid with filler in Section 5.3.3 did not adequately account for its drop in diffusivity relative to annealed Matrimid, suggesting that the continuous phase properties

are different than those of Matrimid. This characteristic may be influencing the rejections achieved with the 10% Blend as well.

5.4.5 Homogeneous Catalyst Recovery Application

An estimate of the membrane area required for the model hydroformylation reaction has been performed to assess the feasibility of utilizing the 10% Oligomer 1 / Matrimid blend for this application. The high fluxes of toluene and product through this material offer the ability to operate with a two-stage membrane recovery, with the permeate from the first stage feeding the second stage, as shown in Figure 5.1. Based on the rejection reported in Table 5.8, this should give an overall catalyst rejection exceeding 99% for the recovery step. Values for the component rejections and permeabilities measured in the above experiments are the input values for this estimate.

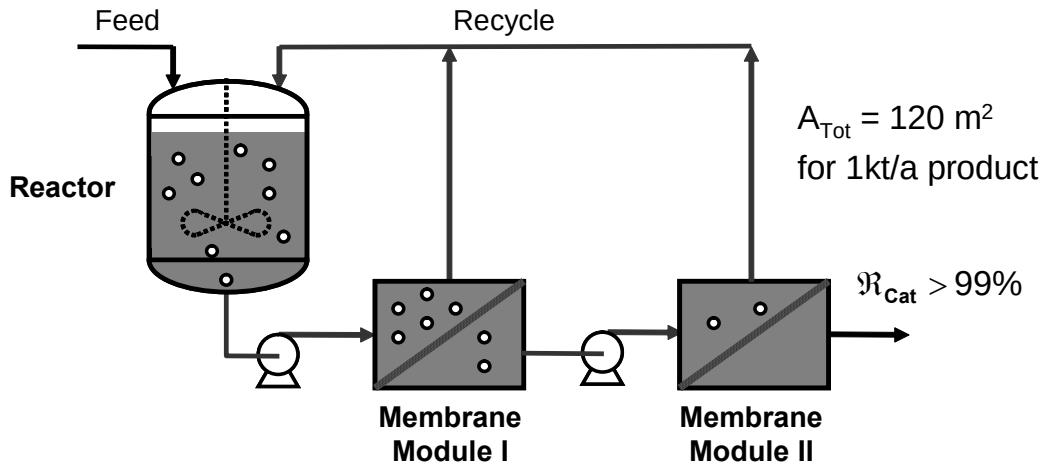

Figure 5.7: Process flow diagram for two-stage membrane recovery of a homogeneous catalyst. Based on the catalyst rejection of the 10% Blend this results in catalyst rejections exceeding 99%.

The productivity of commercial membranes is typically optimized by reducing their thickness (e.g. asymmetric and composite membranes). In the determination of area requirements for this estimate, this optimization has been assumed and a conservative value of the membrane thickness of 0.5 μm has been assumed (typical values for asymmetric membrane thickness range from 0.1 – 0.2 μm[18]). Reaction conditions employed in the estimate are within the range typically found in industrial hydroformylation of higher alkenes.[6,26] The reactor operating pressure of 15 atm is used as the motive force for permeation in the first stage; the second membrane stage operates at the same feed pressure of 15 atm, which requires repressurization, schematically shown as a booster pump in Figure 5.7. The catalyst and product content of the reactor effluent are 250 ppm and 20 mol%, respectively.

On the basis of the above input values, the total membrane area requirement for an aldehyde production of one kiloton per year is 120 m^2. A typical 8 inch diameter by 40 inch long spiral wound reverse osmosis membrane module contains 20 – 40 m^2 of membrane area.[18] Therefore, a process with this production capacity would require somewhere between 3 and 6 of these modules. To put this in perspective of reactor volume, the kinetic model of Bhanage et al.[27] indicates that a reactor volume of approximately 10 m^3 (~ 2600 gallons) is required for this production rate at a reactor conversion of 98%.

5.5 Conclusions

Matrimid and blends of Matrimid with the novel diacetylene-functionalized crosslinking agent, glassy polymers in the dry state, undergo a transition to rubbery

material as evidenced by the diffusivity of toluene in the materials. The rapid diffusion of toluene in these materials combined with high sorption provides a high flux membrane material. Blending of Matrimid with crosslinking agent reduces flux, but increases the ability of these materials to selectively restrict permeation of large molecular weight solutes such as the rhodium-triphenylphosphine catalysts used in hydroformylation reactions.

The relative permeabilities of toluene, dodecene, and triphenylphosphine are functions of their molecular size, supporting the initial assertion that this would be the dominant mechanism of separation. However, the rejection studies of the solutes show flux coupling effects that increase the solute flux through interactions with toluene in the polymer phase, effectively reducing rejection. There is a correlation between these coupling effects and the solute sorption as well as toluene sorption and flux. The material with the lowest toluene sorption and flux, the blend of 10% crosslinking agent and Matrimid, exhibited superior catalyst rejection indicating that the reduction in coupling effects in this material has aided the separation.

It appears that the chemistry of the crosslinking agent enhances the solubility of the catalyst ligand, triphenylphosphine, and likely the catalyst itself. To a certain extent, the increased catalyst sorption counters the design intent of the crosslinking agent because it inhibits the decrease in solute permeability that would aid in restricting its rejection. Future membrane materials following the blending approach of this research may want to consider alternate crosslinking agent chemistries to inhibit this effect and gain better selectivity.

The 10% Blend material has a >90% rejection of a rhodium transition metal catalyst used in hydroformylation, which is comparable to membrane rejections measured for other catalysts in other research.[3,5,12] Analysis of the required membrane area based on the measured transport properties of this material suggests the feasibility of using the membrane in a catalyst recovery process. However, to fully address a membrane unit operation for such a process, additional factors such as long-term stability of the material, membrane fouling, membrane fabrication, and catalyst stability must be examined. Furthermore, opportunity exists for membrane material optimization in terms of flux and rejection behavior following the observations made in this research.

5.6 References

1. Lloyd, D. R. and T. B. Meluch, "Selection and evaluation of membrane materials," *Mat. Sci. of Synth. Membr.: ACS Symp. Ser.*, **269**, 47 (1985).

2. Poling, B. E., J. M. Prausnitz and J. P. O'Connell, *The properties of gases and liquids*, McGraw-Hill: New York ; London (2001).

3. Miller, J. F., D. R. Bryant, K. H. Hoy, N. E. Kinkade and R. H. Zanapalidou, "Membrane separation process," In *US Patent No. 5,681,473* (1997).

4. Bhanushali, D., S. Kloos and D. Bhattacharyya, "Solute transport in solvent-resistant nanofiltration membranes for non-aqueous systems: experimental results and the role of solute-solvent coupling," *J. Memb. Sci.*, **208**, 343 (2002).

5. Scarpello, J. T., D. Nair, L. M. F. dos Santos, L. S. White and A. G. Livingston, "The separation of homogeneous organometallic catalysts using solvent resistant nanofiltration," *J. Memb. Sci.*, **203**, 71 (2002).

6. Arnoldy, P. In *Rhodium Catalyzed Hydroformylation*, P. W. N. M. van Leeuwen and C. Claver, Eds.; Kluwer Academic: Dordrecht (2000).

7. Beller, M. and C. Bolm, *Transition metals for organic synthesis : building blocks and fine chemicals*, Wiley-VCH: Weinheim ; New York (1998).

8. Bahrmann, H., M. Haubs, W. Kreuder and T. Meuller, "Process for separating organometallic compounds and/or metal carbonyls from their solutions organic media," In *U.S. Patent No. 5,174,899* (1992).

9. Langhendries, G., G. V. Baron, I. F. J. Vankelecom, R. F. Parton and P. A. Jacobs, "Selective hydrocarbon oxidation using a liquid-phase catalytic membrane reactor," *Catal Today*, **56**, 131 (2000).

10. Nair, D., J. T. Scarpello, L. S. White, L. M. F. dos Santos, I. F. J. Vankelecom and A. G. Livingston, "Semi-continuous nanofiltration-coupled Heck reactions as a new approach to improve productivity of homogeneous catalysts," *Tetrahedron Lett*, **42**, 8219 (2001).

11. Nair, D., J. T. Scarpello, I. F. J. Vankelecom, L. M. F. Dos Santos, L. S. White, R. J. Kloetzing, T. Welton and A. G. Livingston, "Increased catalytic productivity for nanofiltration-coupled Heck reactions using highly stable catalyst systems," *Green Chem.*, **4**, 319 (2002).

12. Nair, D., S. S. Luthra, J. T. Scarpello, L. S. White, L. M. F. dos Santos and A. G. Livingston, "Homogeneous catalyst separation and re-use through nanofiltration of organic solvents," *Desalination*, **147**, 301 (2002).

13. Livingston, A., L. Peeva, S. J. Han, D. Nair, S. S. Luthra, L. S. White and L. M. F. Dos Santos, "Membrane separation in green chemical processing - Solvent nanofiltration in liquid phase organic synthesis reactions," *Adv. Memb. Tech.*, **984**, 123 (2003).

14. De Smet, K., S. Aerts, E. Ceulemans, I. F. J. Vankelecom and P. A. Jacobs, "Nanofiltration-coupled catalysis to combine the advantages of homogeneous and heterogeneous catalysis," *Chem. Commun.*, 597 (2001).

15. Vankelecom, I. F. J., "Polymeric membranes in catalytic reactors," *Chem. Rev.*, **102**, 3779 (2002).

16. De Smet, K., A. Pleysier, I. F. J. Vankelecom and P. A. Jacobs, "Recycling of homogeneous hydrogenation catalysts by dialysis coupled catalysis," *Chem. Eur. J.*, **9**, 334 (2003).

17. Sturgill, G. K., "Stabilization of polyimide blends through solid-state crosslinking," *Ph.D. Thesis*, Georgia Institute of Technology (1999).

18. Baker, R. W., *Membrane Technology and Applications*, McGraw-Hill: New York (2000).

19. Paul, D. R., M. Garcin and W. E. Garmon, "Solute diffusion through swollen polymer membranes," *J. Appl. Polym. Sci.*, **20**, 609 (1976).

20. Paul, D. R. and O. M. Ebra-Lima, "Pressure-induced diffusion of organic liquids through highly swollen polymer membranes," *J. Appl. Polym. Sci.*, **14**, 2201 (1970).

21. Falla, W. R., M. Mulski and E. L. Cussler, "Estimating diffusion through flake-filled membranes," *J. Memb. Sci.*, **119**, 129 (1996).

22. Maxwell, J. C., *Treatise on Electricity and Magnetism*, Clarendon Press: London (1881).

23. Bird, R. B., W. E. Stewart and E. N. Lightfoot, *Transport Phenomena*, John Wiley & Sons: New York (1960).

24. Barrer, R. M. In *Diffusion in Polymers*, J. Crank and G. S. Park, Eds.; Academic Press: London, p 165 (1968).

25. Merkel, T. C., Z. He, I. Pinnau, B. D. Freeman, P. Meakin and A. J. Hill, "Effect of nanoparticles on gas sorption and transport in poly(1-trimethylsilyl-1-propyne)," *Macromolecules*, **36**, 6844 (2003).

26. Beller, M., B. Cornils, C. D. Frohning and C. W. Kohlpaintner, "Progress in hydroformylation and carbonylation," *J. Mol. Catal. A: Chem.*, **104**, 17 (1995).

27. Bhanage, B. M., S. S. Divekar, R. M. Deshpande and R. V. Chaudhari, "Kinetics of hydroformylation of 1-dodecene using homogeneous $HRh(CO)(PPh_3)_3$ catalyst," *J. Mol. Catal. A: Chem.*, **115**, 247 (1997).

CHAPTER 6

ANALYSIS OF TRANSPORT AND COUPLING VIA MAXWELL-STEFAN EQUATIONS

The results yielded in the multicomponent separations of Chapter 5 have shown significant deviation in separation performance from that which would be predicted from their single component transport values, or "intrinsic" properties. These differences between the measured and predicted separation have been attributed to flux coupling phenomena. The following chapter endeavors to find a theoretical explanation for the observed phenomena through application of the Maxwell-Stefan formulation for multi-component mass transfer to a membrane process.

6.1 Introduction

It is often acceptable in membrane separations, particularly in the prevailing research area of gas separations, to determine membrane permeabilities using a moving frame of reference. This can be illustrated using the n and j[1] notations for flux relative to a stationary frame of reference and the average velocity, respectively:

$$n_A = w_A(n_A + n_M) + j_A \tag{6.1}$$

where

$$j_A = -\rho D_{AM} \frac{dw_A}{dz} \tag{6.2}$$

In the case of membrane separations, component A is the permeating component, component M would be the membrane, and D_{AM} is the diffusivity of component A in the

membrane. Since $n_M = 0$, omission of the term $w_A(n_A + n_M)$ is adequate when the fraction of the component A sorbed in the membrane, w_A, is quite small and this is true in many cases (particularly simple gases). For single component diffusion in a membrane, Eq. 6.2 can then be used to derive an expression such as Eq. 2.6 to describe the flux for component A through the membrane. If permeation of binary mixtures is being evaluated for components A and B and component B also has a small sorption level, independent calculations of the fluxes of components A and B using Eq. 6.2 can give a good estimate of the membrane selectivity. Because of the dilute concentration of the components in the membrane phase, there are limited interactions between the two components.

For homogeneous catalyst recovery, the solvent sorption is not negligible and the full stationary frame of reference must be utilized, where the point of reference is the membrane or polymer film. Eq. 6.1 has been successfully demonstrated by Paul and Ebra-Lima[2] to describe the single component transport of organic solvents through a highly swollen rubber. As illustrated in Appendix A and Chapter 5, this same approach has been used in this research for the measurement of toluene diffusivity in the membrane.

However, when evaluating membrane permeation of multicomponent mixtures where one or more of the components is highly sorbed, Eq. 6.2 is no longer valid because it contains only binary diffusivities in the expression of each component's flux. The diffusion of a feed mixture in a membrane exceeds the binary conditions implicit in Eq. 6.2 (membrane, components A, B, ...,N). A transport model that accounts for the influence of each component in the membrane on the resulting flux is necessary. The Max-

well-Stefan transport equation considers these factors and will be highlighted in the subsequent sections of this chapter as a means to treat the multicomponent diffusion that is occurring in the membrane permeation of a mixture.

In membrane literature, the influence of different mobile species in a membrane on each other is often called "coupling." This categorization is often broadly assigned. Two prevalent sources of coupling are plasticization and so-called bulk or convective flux effects. In a plasticized membrane, deviations from measured single component permeabilities occur due to the increased polymer mobility (and consequently increased diffusivity) caused by the introduction of a plasticizing component in the feed. Bulk flux effects result directly from penetrant-penetrant interactions. The bulk flux effect is generally viewed as a faster permeating component "dragging" the slower components along with it through the membrane, giving a higher permeability for the slower component than its single component case or for different mixtures. This treatment will focus on the latter case, though "convective effects" is somewhat of a misnomer since transport is still diffusive. The role of plasticization in membrane transport is widely studied, but the coupling effect from penetrant-penetrant interactions is not as well understood.

The high concentration of toluene in the polymers under consideration in this work is a cause to believe that there will be significant penetrant-penetrant interactions between the toluene and solutes. These interactions of the more permeable toluene with the slower permeating solute are a likely cause for the higher solute fluxes observed in rejection experiments compared to dialysis. Examples of flux coupling are evident in other membrane studies. Bhanushali et al.[3] cited solvent-solute coupling as a source for the variability of rejection observed in nanofiltration studies of dyes using different

solvents. In their work with commercial nanofiltration membranes, solvents with higher membrane permeability gave poorer rejections for the same dye. Even in a gas separation study, which has sorption levels that are quite low relative to the solvent in this work, Kamaruddin and Koros[4] found coupling effects in a CO_2/CH_4 separation after separating the flux into bulk and diffusive components.

A question that may be asked at this point is: if high sorption reduces rejection, why not just choose a material with lower sorption? An answer to that is that some swelling may be desirable in order to obtain reasonable flux. In the catalyst recovery application, the component that is rejected represents only a minor fraction of the feed. Therefore, a large portion of the feed must permeate the membrane and a high flux is required to obtain a reasonable membrane area for the separation. It is the objective of the analysis presented here to gain some phenomenological understanding of the trade-off between rejection and flux. This has been performed to aid in the selection and design of materials for this type of application. An introduction to the Maxwell-Stefan transport formulation followed by its application to homogeneous catalyst recovery endeavors to elucidate this relationship.

6.2 Original Maxwell Stefan Formulation

The Maxwell-Stefan formulation has been widely accepted as a means to describe multicomponent transport.[5,6] Use of the Maxwell-Stefan equation has been demonstrated to model phenomena related to coupling, such as transport against a concentration gradient or transport without a driving force that cannot be described through the classical Fickian formulation.[7] In order to provide a groundwork for the application of this

approach to membrane separations such as the homogeneous catalyst recovery, an overview of its basis is provided here. An adaptation of the Maxwell-Stefan formulation for its application to systems involving diffusion in polymers is presented in Section 6.3. The primary source for the development of the general Maxwell-Stefan equations presented is the simple kinetic theory of diffusion given by Taylor and Krishna.[5]

For the purpose of clarity, the origins of the Maxwell-Stefan formulation will be presented in binary form, though the multicomponent system will have the same considerations. The presentation will use mole fractions as opposed to the weight fraction notation of Eqs. 6.1 and 6.2, as its development is dependent on these quantities. Also, the "A, B" notation for various components will be replaced with "1, 2" notation as it lends itself better to index notation.

The Maxwell-Stefan formulation considers diffusion as a force balance. To affect motion of the molecules of one species relative to another, a force must be exerted on the components. In opposition to this force are the collisions with other molecules in the mixture, exerted as a drag force. This concept is shown graphically in Figure 6.1 for a binary system consisting of components 1 and 2. The frictional drag between components balances the force exerted on each. In the case of one dimensional diffusion (as assumed for membranes), the force acting on species i of the mixture is a chemical potential gradient, $\mathrm{d}\mu_i/\mathrm{d}z$.

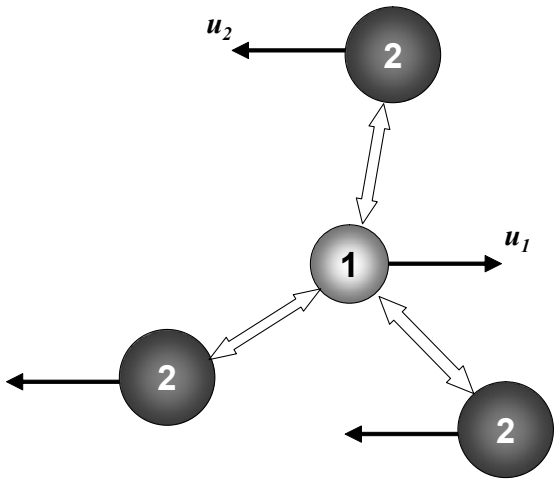

Figure 6.1: Maxwell-Stefan view of diffusion as relative motion of components 1 and 2 caused by the exertion of a force on the two molecules. This force is balanced by frictional drag between the two components.

In the force balance for component 1, the rate at which collisions occur with component 2 is proportional to the concentration of component 2, expressed as its mole fraction, x_2. The drag force in opposition to the chemical potential gradient is expressed as the momentum transfer from a collision between species 1 and 2. This momentum transfer is a function of the velocity of species 1, u_1, relative to component 2, u_2. The resulting equation for the force balance is:

$$-\frac{d\mu_1}{dz} = \frac{RT}{Đ_{12}} x_2 (u_1 - u_2) \tag{6.3}$$

with the applied force (left hand side of Eq. 6.3) equal to the fractional drag force (right hand side). The chemical potential gradient of Eq. 6.3 is negative for transport in the positive z direction to occur with a negative gradient. The remaining factor in Eq. 6.3 that has not been discussed is the term $RT/Đ_{12}$, which has the meaning of a friction factor for the drag exerted in a collision between components 1 and 2. With this interpretation,

the Maxwell-Stefan diffusivity, $Đ_{12}$, has the physical significance of being an inverse drag coefficient and has units of (length)^2/time, just as Fickian diffusion coefficients.

Multiplying both sides of Eq. 6.3 by -1/*RT*, gives the generally presented form of the Maxwell-Stefan equation for binary mixtures:

$$\frac{1}{RT}\frac{d\mu_1}{dz} = \frac{x_2(u_2 - u_1)}{Đ_{12}} \tag{6.4}$$

which can be expanded for multicomponent mixtures as:

$$\frac{1}{RT}\frac{d\mu_i}{dz} = \sum_{j=1}^{n}\frac{x_j(u_j - u_i)}{Đ_{ij}} \tag{6.5}$$

Flux values for the diffusing components can be obtained by multiplying both sides of Eq. 6.5 by x_i and substituting the definition for flux relative to a fixed coordinate system (Eq. 6.6, with c_{tot} as the total molar concentration of the mixture) to give Eq. 6.7.

$$N_i = c_i u_i = x_i c_{tot} u_i \tag{6.6}$$

$$\frac{x_i}{RT}\frac{d\mu_i}{dz} = \sum_{j=1}^{n}\frac{x_i N_j - x_j N_i}{c_{tot} Đ_{ij}} \tag{6.7}$$

The solutions to the generalized equation of Eq. 6.7 have been successfully applied to multicomponent diffusion in various media including gases, nonideal liquids, and microporous media.[7] Values for $Đ_{ij}$ in these equations have been estimated from the same relationships as the Fickian *D*, such as the kinetic theory for gases and the Wilke-Chang Equation for liquids (usually in combination with a relationship for concentration dependence such as the one proposed by Vignes[8]), thus illustrating the similar origins of the Maxwell-Stefan $Đ$ relative to the *D* of Fick's Law.

6.3 Maxwell-Stefan Relationship for Membrane Separations

Now the Maxwell-Stefan relationship will be applied to diffusion in nonporous membranes. Several applications of the Maxwell-Stefan equations have been made to model pervaporation in polymer membranes[9-12] as well as a fairly complex model combining viscous, electrostatic, and diffusional forces for nanofiltration.[13] Here, the separation of a liquid feed containing a dilute solute in a solvent swollen membrane (i.e. reverse osmosis) will be modeled. The initial development (up to Eq. 6.10) of the application to diffusion in polymers follows the treatment of Heintz and Stephan.[9]

When considering the diffusion in nonporous polymers, it can be argued that the use of mole fractions in the Maxwell-Stefan equations is not appropriate. In the development of the general model of Eq. 6.3, the number of collisions with a molecule of species *i* was assumed to be proportional to the mole fraction of that species. In the case of macromolecular species like polymers, it is expected that multiple collisions will occur on the same molecule. A more realistic measure of the polymer contribution to the total friction force on a component is its volume fraction, ϕ_i, and this value will be substituted for mole fraction in the transport equations here. A parallel to this use of volume fractions can be drawn from the well-known thermodynamic treatment of polymer solutions by Flory,[14] where volume fractions are used in a lattice model to account for the macromolecular nature of a polymer.

As described in Appendix A.2.1, pressure is constant throughout the membrane in nonporous membranes. This yields Eq. 6.8 as the expression for the chemical potential gradient in the membrane:

$$d\mu_i = RTd\ln a_i \tag{6.8}$$

where a_i is the thermodynamic activity. Substituting Eq. 6.8 into Eq. 6.3 and replacing the mole fractions with volume fractions gives Heintz and Stephan's modified Stefan-Maxwell relationship for diffusion in polymers:

$$\frac{d\ln\phi_i}{dz} = \sum_{j=1}^{n} \frac{\phi_j (u_j - u_i)}{\widetilde{D}_{ij}} \tag{6.9}$$

with

$$\widetilde{D}_{ij} = Đ_{ij} \frac{d\ln a_i}{d\ln\phi_i} \tag{6.10}$$

where $\widetilde{D}_{ij}$ are diffusion coefficients that are dependent on composition as well as the nonideality of the mixture component interactions, represented by a_i.

In the development of the flux equations for the hydraulic permeation of organic solvents through swollen rubbers, Paul and Ebra-Lima[2] assumed that there was no volume change on mixing in the sorbed polymer. The model developed provided an accurate description of the transport phenomena they were observing in these systems. Since the behavior of the materials under investigation in this study closely resemble those that were modeled in the Paul and Ebra-Lima work (in terms of solvent solubility and diffusivity) the same assumption of no volume change on mixing will be applied here. This leads to the introduction of a volumetric flux, $\hat{n}_i$, which has units of (volume/ area-time) and is defined in a stationary frame of reference as:

$$\hat{n}_i = \phi_i u_i \tag{6.11}$$

which is analogous to Eq. 6.6. Inserting Eq. 6.11 into Eq. 6.9 and keeping in mind that $d\ln\phi_i = d\phi_i / \phi_i$, yields the modified Maxwell-Stefan transport equation for flux in a swollen polymer:

$$\boxed{\frac{d\phi_i}{dz} = \sum_{j=1}^{n} \frac{\phi_i \hat{n}_j - \phi_j \hat{n}_i}{\widetilde{D}_{ij}}} \tag{6.12}$$

6.3.1 Flux Equation for Single Component Transport

For consistency, the rest of the document will use the indices listed in Table 6.1 to designate the same components in each of the transport evaluations presented.

Application of Eq. 6.12 to single component transport in a membrane (a binary system: solvent and membrane) gives a differential equation of the same form as that used by Paul and Ebra-Lima[2] (Eq. 6.13). Since we are using the stationary frame of reference, the membrane flux is equal to zero, $\hat{n}_M = 0$. This condition can be imposed in any membrane process, regardless of the number of components. Another simplification in the solution of Eq. 6.12 is that it is only necessary to specify (n-1) equations for an "n" component mixture, because of the relationship $\sum_{i=1}^{n} \phi_i = 1$.

$$\hat{n}_1 = \frac{\widetilde{D}_{1M}}{(1-\phi_1)} \frac{d\phi_1}{dz} \tag{6.13}$$

Table 6.1: Indices for transport calculations.

Component	Index
Solvent	1
Solute	2
Membrane	M

Eq. 6.13 can be integrated using the boundary conditions that are assumed in Appendix A.2.1 for the hydraulic permeation. That is, we know the solvent volume fraction at the feed of the membrane, $\phi_{10} = f(a_{10})$, from the equilibrium relationship (in our case Flory-Rehner). The permeate volume fraction, ϕ_{1l}, can be determined from the influence of pressure on liquid membrane processes given by Eq. A.7, combined with the equilibrium relationship. After manipulation to account for the thickness as function of the gradient in sorption, this gives essentially the same equation (Eq. 6.14) as Eq. A.16, with $\widetilde{D}_{1M}$ replacing *D* (see Section A.1.2 for development).

$$\hat{n}_1 = \frac{\widetilde{D}_{1M}}{l_{dry}(1-\phi_{10})^{2/3}}\left(\phi_{10} - \phi_{1l}\right) \tag{6.14}$$

The driving force for diffusion in Eq. 6.14 is simply the difference in volume fraction of component 1 across the membrane, as the volume fraction on the feed side is constant due to constant feed fluid activity. A plot of the flux versus driving force for the hydraulic permeation of toluene in an annealed Matrimid film is shown in Figure 6.2. Analysis indicates that it reasonable to replace $\widetilde{D}_{iM}$ with experimentally measured diffusion coefficients, which do not show concentration dependence for the range of pressures studied. The data in Figure 6.2 are well fit by a linear equation with a constant $\widetilde{D}_{1M}$ of 1.8 x 10^{-6} cm^2/s. From the form of Eq. 6.14, any concentration dependence of $\widetilde{D}_{1M}$ would be indicated by nonlinearity in this plot. Due to this absence of concentration dependence, $\widetilde{D}_{1M}$ is constant and equivalent to the diffusivities determined in the toluene transport studies of Chapter 5. It appears that the low driving forces of the hydraulic permeation studies are partly responsible for the absence of concentration dependence.

In some situations, this generalization can be extended beyond the specific toluene diffusion measurements presented in this work. Paul[2,15] has shown that a wide variety of solvents exhibit linear behavior in rubbery membranes when analyzed using Eq. 6.14.

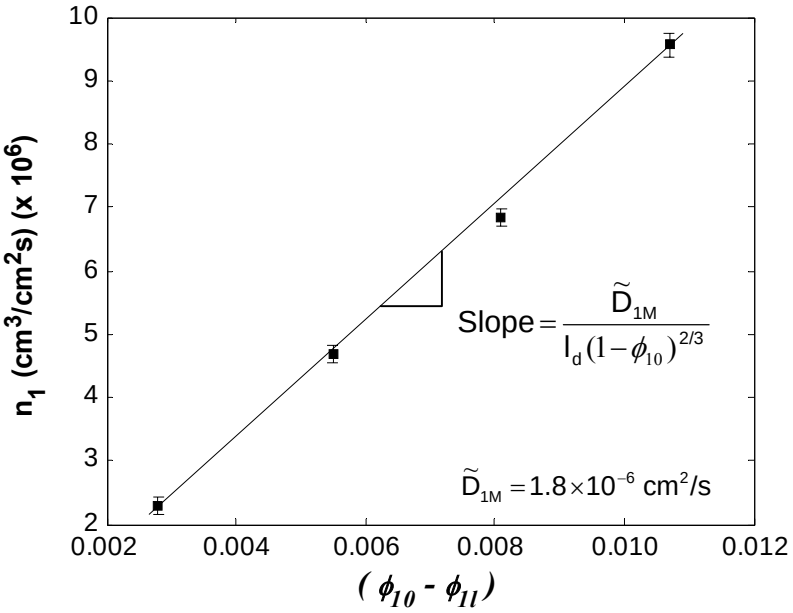

Figure 6.2: Flux-driving force relationship for toluene permeation in an annealed Matrimid film. The linear increase of flux with driving force indicates a constant $\tilde{D}_{1M}$ over this concentration range according to Eq. 6.4. The volume fraction difference data points correspond to pressure driving forces = 25, 50, 75, 100 psi from left to right.

Because of the dilute nature of the solute in the rejection studies of this work, it is assumed that there is no change in solvent diffusivity when going from single component permeation to the binary feed mixtures. This assumption can be applied to similar applications such as reverse osmosis with limited solute concentrations. Similarly, diffusion coefficients determined from solute dialysis in Section 5.4.2 are assumed to be representative of those occurring in the rejection studies since the toluene concentrations in the membrane are nearly the same. This substitution of experimentally measured

diffusivities for $\widetilde{D}_{iM}$ is shown symbolically in the proceeding sections as $\overline{D}_{iM}$ to represent constant diffusivities that are independent of concentration.

6.3.2 Flux Equations for Binary Mixture Transport

As previously stated, we need (n-1) of Eqs. 6.12 for an "n" component system and although the selection is arbitrary, choosing the membrane as one of the components allows for some mathematical simplifications. Because $\hat{n}_M = 0$, this simplifies the differential equations to a point where an analytical solution can be found. Selecting the solute, component 2, as the other component gives:

$$\frac{d\phi_M}{dz} = \frac{\phi_M \hat{n}_1}{\overline{D}_{1M}} + \frac{\phi_M \hat{n}_2}{\overline{D}_{2M}} \tag{6.15}$$

$$\frac{d\phi_2}{dz} = \frac{\phi_2 \hat{n}_1 - \phi_1 \hat{n}_2}{\overline{D}_{12}} - \frac{\phi_M \hat{n}_2}{\overline{D}_{2M}} \tag{6.16}$$

$\overline{D}_{12}$, the diffusivity or inverse friction factor between the solvent and the solute in the membrane phase is the only parameter that cannot be measured from single component permeability experiments. $\overline{D}_{12}$ has been previously described as a coupling parameter between the permeating components.[9,11] Its significance will be examined here by applying the solution of the transport models to our experimentally measured results.

Eqs. 6.15 and 6.16 can be solved for the experimental data. Since the driving force, feed composition, and rejection have been determined, the transport equations can be solved for $\overline{D}_{12}$ using the $\overline{D}_{iM}$ values from the hydraulic permeation and dialysis experiments.

First we need to get Eqs. 6.15 and 6.16 into a tractable form. This can be done by specifying the boundary conditions:

$$\phi_i(z=0) = \phi_{i0}$$

$$\phi_i(z=l) = \phi_{il}$$

Once Eq. 6.15 is solved for ϕ_M using these conditions (Eq. 6.17), it can be inserted into Eq. 6.16 and combined with the relationship $\sum_{i=1}^{n} \phi_i = 1$ to eliminate ϕ_1. The solution to these differential equations is fairly straightforward. The final solutions are:

$$\phi_{Ml} = \phi_{M0} \exp\left[\left(\frac{\hat{n}_1}{\overline{D}_{1M}} + \frac{\hat{n}_2}{\overline{D}_{2M}}\right) l\right] \tag{6.17}$$

$$\phi_{2l} = \phi_{20} e^{Al} + \frac{\hat{n}_2}{\hat{n}_1 + \hat{n}_2}\left(1 - e^{Al}\right) + \frac{\phi_{M0}\hat{n}_2\left(\frac{1}{\overline{D}_{12}} - \frac{1}{\overline{D}_{2M}}\right)}{(B - A)}\left(e^{Bl} - e^{Al}\right) \tag{6.18}$$

where:

$$A = \frac{\left(\hat{n}_1 + \hat{n}_2\right)}{\overline{D}_{12}} \quad ; \quad B = \frac{\hat{n}_1}{\overline{D}_{1M}} + \frac{\hat{n}_2}{\overline{D}_{2M}}$$

Although the math seems a bit messy, it is not as bad as it looks. The same variables remain; they just occur with some more frequency than in the differential equations.

As in the binary case, we can obtain the membrane volume fractions of each component at the membrane boundaries from the equilibrium relationships between the membrane and fluid phases. The feed composition is specified, so that leaves us with five unknowns: the volume fractions on the permeate side of the membrane (ϕ_{1l} and ϕ_{2l}), the solvent and solute fluxes ($\hat{n}_1$ and $\hat{n}_2$), and $\overline{D}_{12}$. Further relationships to describe the permeation process must be provided for solution.

In the homogeneous catalyst recovery studied here and many reverse osmosis applications, there no sweep of the permeate, which means that the permeate composition of a species is simply the ratio of its flux to the total flux through the membrane:

$$\phi_{1l}^{Liq.} = \frac{\hat{n}_1}{\hat{n}_1 + \hat{n}_2} \tag{6.19}$$

$$\phi_{2l}^{Liq.} = \frac{\hat{n}_2}{\hat{n}_1 + \hat{n}_2} \tag{6.20}$$

The values in Eqs. 6.19 and 6.20 are the permeate liquid phase rather than the membrane phase compositions at the permeate side in Eqs. 6.17 and 6.18. If the solubility relationship used to determine ϕ_{il} requires a quantity other than volume fractions (e.g. activity in the Flory-Rehner equation), appropriate conversions must be made using the partial molar volumes or densities of the components in the fluid phase.

The final value to reduce the only unknown to $\overline{D}_{12}$ is the experimentally measured rejection or selectivity. Similar approaches can be used to determine values other than $\overline{D}_{12}$. For example, if the $\overline{D}_{12}$ is specified, membrane selectivities and rejections can be determined for various operating conditions. This has been done in Sections 6.4.2 and 6.4.3 to determine the membrane performance as a function of material properties.

6.4 Application of the Transport Model

Before using the transport model to evaluate the effect of different material properties on the separations that can be achieved, data from triphenylphosphine rejection experiments will be evaluated to determine the applicability of the model. Also, repre-

sentative values of $\overline{D}_{12}$ can be obtained from this exercise for the subsequent analysis of material property effects on separation performance.

6.4.1 Model Description of Experimental Triphenylphosphine Rejection

The equations of Section 6.3.2 and the approach for determination of $\overline{D}_{12}$ have been applied to the triphenylphosphine rejections found in Matrimid and blends with Oligomer 1. In this analysis, data for the individual $\overline{D}_{iM}$'s are taken from the toluene permeability and triphenylphosphine dialysis tests and applied to the results measured in a rejection study of a binary mixture of toluene and triphenylphosphine. All experimental data are taken from Chapter 4 (solubility relationships) and Chapter 5 (diffusion coefficients) for these materials. A nice feature of these values is that they should behave very similarly in the multicomponent analysis. The component concentrations in the rejection measurements are nearly equal to those in the toluene and triphenylphosphine permeability measurements, which limits any changes of the parameters resulting from concentration dependence

Calculation of the transport equations was performed using MATLAB (The MathWorks, Inc.) programming. An initial calculation of two component fluxes for a guess of $\overline{D}_{12}$ was performed by simultaneously solving Eqs. 6.17 and 6.18 giving a rejection. Following that step, a nonlinear least-squares fit was performed to give the $\overline{D}_{12}$ value that best represented the data.

In order to obtain an accurate fit using 6.17 and 6.18, permeation characteristics were measured for a range of driving forces. Therefore, triphenylphosphine rejection was measured as a function of pressure and is shown in Figure 6.3. The fit for the modified

Maxwell-Stefan equations shown by the lines is quite good. Additionally, the model prediction for toluene flux accurately represented experimental measurements. To reiterate, the only adjustable parameter was $\overline{D}_{12}$, the sorption and diffusion values were taken from experimental results. Input values for the transport model are shown in Table 6.2, with toluene sorption in the materials taken from Chapter 4 (Table 4.3).

The values determined for the coupling parameter, $\overline{D}_{12}$, from the Maxwell-Stefan transport modeling of triphenylphosphine rejection in the various materials are shown in Table 6.3. They are roughly on the same order of magnitude (or lower in the case of annealed Matrimid) as the diffusion coefficient for the slowest diffusing component in the feed mixture, triphenylphosphine in this case. The values of $\overline{D}_{12}$ relative to the $\overline{D}_{iM}$ are consistent with previous analyses of membrane transport using the Maxwell-Stefan transport model.[9-12,16] If the $\overline{D}_{12}$ values are viewed as the inverse friction factor of the Maxwell-Stefan model development (Section 6.2), then decreasing values of $\overline{D}_{12}$ indicate increasing friction and interaction between the solvent and solute in the membrane phase. The values in Table 6.3 then indicate that the interaction between the solvent and solute in the annealed Matrimid is much greater than in the blends and consequently the coupling between the triphenylphosphine and toluene fluxes is stronger in this material. The higher toluene sorption in the annealed Matrimid relative to the blends (Chapter 4) may explain the stronger coupling exhibited in this material. Increased concentration of the solvent in the membrane leads to more frequent and possibly more pronounced interaction with the solute, allowing more solute to be dragged along with the flux of the solvent.

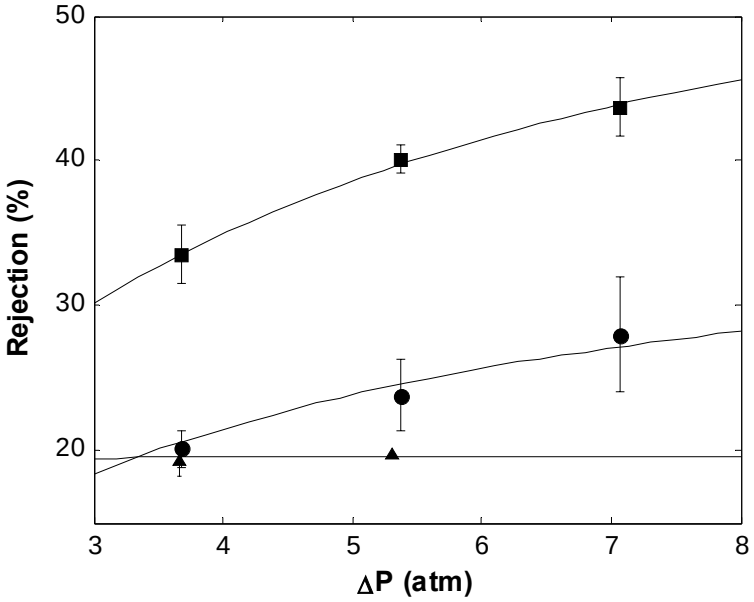

Figure 6.3: Rejection of triphenylphosphine in solution with toluene in annealed Matrimid (▲), 5% Blend (●) and 10% Blend (■) as a function of pressure. Lines are the best fit for the modified Maxwell-Stefan transport equations with $\overline{D}_{12}$ as the adjustable parameter. Error bars are deviation from average values.

Table 6.2: Experimentally measured values for toluene (1) and triphenyl-phosphine (2) used in Eqs. 6.17 and 6.18 to model transport in triphenylphosphine rejection.

Material	K_2 $[(mol/cm^3)_{Mem.}]/[(mol/cm^3)_{Liq.}]$	$\overline{D}_{1M}$ (cm^2/s)	$\overline{D}_{2M}$ (cm^2/s)
Annealed Matrimid	0.39	1.8×10^{-6}	13×10^{-9}
5% Blend	0.74	1.2×10^{-6}	8.5×10^{-9}
10% Blend	0.55	0.68×10^{-6}	8.1×10^{-9}

Table 6.3: $\overline{D}_{12}$ values determined from least-squares fit of Eqs. 6.17 and 6.18 for rejection of triphenylphosphine (2) in solution with toluene (1).

Material	$\overline{D}_{12}$ (cm^2/s)
Annealed Matrimid	2.1×10^{-9}
5% Blend	10×10^{-9}
10% Blend	12×10^{-9}

Interpretation of $\overline{D}_{12}$ as simply the triphenylphosphine diffusion coefficient in toluene does not describe the values observed here and in other membrane studies. One of the best known methods to predict solute diffusivities in solvents, the Wilke-Chang equation,[17] predicts a diffusion coefficient of 1.6×10^{-5} cm^2/s for triphenylphosphine in toluene, which is clearly not the value for $\overline{D}_{12}$ here. An approach to determining the interactions between diffusing components in zeolites via the Maxwell-Stefan model gives some indication of the order of magnitude of the $\overline{D}_{12}$ in dense media. In the model developed by Krishna,[18] the interaction between diffusing components is related to the ability of species *i* to displace species *j* within the zeolite, with *i* and *j* representing the mobile species. The limiting case for this model is that this diffusivity is dictated by the slower moving component, i.e.:

$$\overline{D}_{ij} \propto \lambda^2 \nu_j, \quad \nu_j < \nu_i \tag{6.21}$$

where λ is the displacement or jump length within the material and ν_j is the jump frequency. This model provides some explanation as to why the $\overline{D}_{12}$ is of the same order of magnitude as the triphenylphosphine diffusivity in the polymers. However, there currently does not seem to be a means of obtaining an *a priori* prediction of $\overline{D}_{12}$ from physical property and transport data in membrane separations for a given system.

6.4.2 Modeling of a Membrane with Inert Filler

Throughout the development of the dissertation, it has been observed that the 10% Oligomer 1 blend with Matrimid exhibits some characteristics of a polymeric material combined with an inert filler (with "inert" defined as being both impermeable and non-sorbing). Due to the superior catalyst rejection characteristics of the 10% blend, it is of interest to determine if the addition of filler to a membrane material can enhance its separation characteristics in homogeneous catalyst recovery. To do so, the transport equations developed thus far have been applied to model triphenylphosphine rejection in a composite of annealed Matrimid containing filler. Since the 10% blend may resemble this type of morphology, the model value for the concentration of filler in the composite is the same as the dispersed phase concentration in the 10% blend ($\phi_I = 8.4\,\%$, Section 3.4.4) for comparative purposes.

The transport properties of the model composite can be estimated from those of the host polymer. If the filler is assumed to be randomly distributed and spherical, the change in diffusion coefficient for the composite material relative to the host polymer can be predicted using the same method as in Section 5.4.1:

$$\frac{D_{eff}}{D} = \frac{1-\phi_I}{\left(1+\frac{\phi_I}{2}\right)} \tag{5.4}$$

From Eq. 5.4 the effective membrane diffusivities, $\overline{D}_{iM(eff)}$, for the mobile species in the composite material can be estimated from the $\overline{D}_{iM}$ in the neat membrane material and the volume fraction of inert filler, ϕ_I. The solvent and solute sorption in the membrane are also reduced in proportion to the fraction of filler present. These relationships have been

used to estimate the composite properties for $\phi_I = 8.4\,\%$, giving all the parameters necessary for model solution except for $\overline{D}_{12}$.

As discussed in Section 6.4.1, the variance in the $\overline{D}_{12}$ model parameter with changing material properties in not well understood. From the values of $\overline{D}_{12}$ determined in Section 6.4.1 for the various materials, it does not appear that $\overline{D}_{12}$ for the polymer composite with inert filler will vary following the prediction method of Eq. 5.4. If the coupling of solute and solvent fluxes does indeed decrease with solvent concentration in the membrane, the $\overline{D}_{12}$ in the composite should be increasing rather than decreasing because of the reduction of solvent content. However, assigning a specific relationship to determine $\overline{D}_{12}$ is too much conjecture at this point due to the limited information on its behavior. Therefore, two cases of $\overline{D}_{12}$ will be used in the model: 1) $\overline{D}_{12}$ of the composite is the same as the host polymer, annealed Matrimid, (2.1 x 10^{-9} cm^2/s) and 2) $\overline{D}_{12}$ of the composite is the same as the 10% blend (12 x 10^{-9} cm^2/s). Based on the observations thus far, these are assumed to be the worst and best case scenarios, respectively.

Model results are shown in Figure 6.4. Both $\overline{D}_{12}$ values predict higher rejections for the composite than the annealed Matrimid, suggesting membrane improvement through the addition of filler. The predicted influence of solute sorption on rejection is strong and it is the dominant factor increasing separation performance in this case. The solute rejection of the composite predicted by the higher $\overline{D}_{12}$ exceeds the experimental performance of the 10% Blend. It is evident from the properties in Table 6.2 and observations of Chapter 5 that the 10% Blend does not follow the trends predicted by the idealized filled polymer model in all aspects, particularly solute solubility (increases

rather than decreases in blend). The cause for this, as postulated in Chapter 5, the continuous phase of the 10% blend contains a small concentration of crosslinking agent that influences the blend properties. The predicted influence of these properties on separation performance appears to be fairly strong.

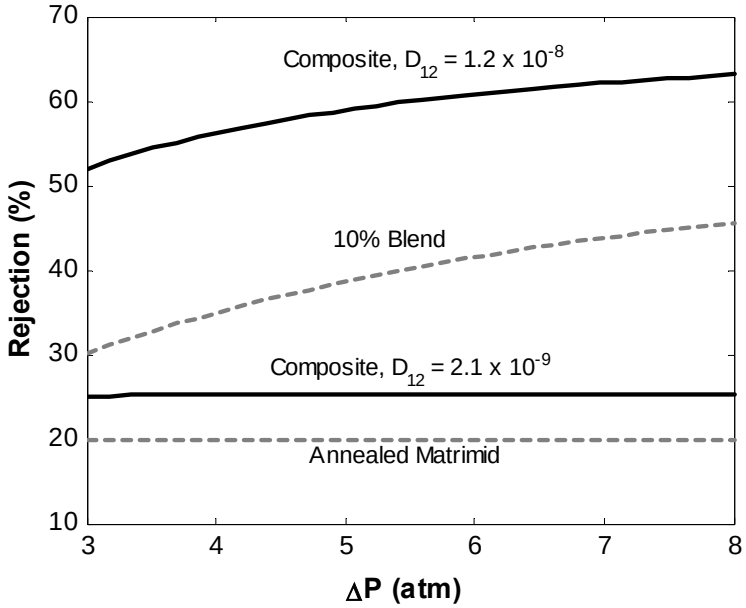

Figure 6.4: Predicted triphenylphosphine rejection for a composite membrane of annealed Matrimid blended with 8.4% filler (—) relative to annealed Matrimid and 10% Oligomer 1 Blend (--).

6.4.3 Generalized Model of Homogeneous Catalyst Recovery

It has observed experimentally and through modeling that membrane properties such as solute sorption, solvent sorption, and the relative diffusivities of the solvent and solute affect the separation performance in varying degrees. Some knowledge of the influence of these properties would aid in the membrane material design for homogeneous catalyst recovery and similar membrane separations. Therefore, a brief overview of the transport predicted by the modified Maxwell-Stefan approach for material properties

beyond the range exhibited by the Matrimid and blended polymers in this research has been performed.

These models are based on the same basic process as the above analysis: recovery of a dilute solute from a binary feed mixture through reverse osmosis. The generalized system used for this analysis varies the solvent sorption, diffusivity selectivity, and solubility selectivity of the membrane material and quantifies their effects on separation performance with the solute rejection. Solubility and diffusivity selectivity are defined in terms of the solvent and shown in Eqs. 6.22 and 6.23. Though the varied properties are not independent (e.g. diffusion in the polymer will be affected by reduced solvent sorption and swelling), correlations relating the properties have been omitted in lieu of a distribution of selectivities and degrees of solvent sorption to account for a variety of material properties.

$$\alpha_D = \frac{\overline{D}_{1M}}{\overline{D}_{2M}} \tag{6.22}$$

$$\alpha_S = \frac{\phi_1^M / \phi_2^M}{\phi_1^{Liq} / \phi_2^{Liq}} \tag{6.23}$$

The range of physical and transport properties is based on the triphenylphosphine rejection in toluene to provide a realistic basis. The general assumptions in the development of the model and its fitting to experimental data are the same. From the observations in the triphenylphosphine rejections and those of other membrane studies using the Maxwell-Stefan approach,[9-12,16] it has been assumed that $\overline{D}_{12} = \overline{D}_{2M}$. Using this assumption it was determined through model calculations that the rejection is influenced by the relative diffusivities and not the absolute values of the diffusivities. Therefore, the

toluene diffusion, $\overline{D}_{1M}$, was maintained at a constant value of 1 x 10^{-6} cm^2/s and $\overline{D}_{2M}$ was varied to obtain the different diffusivity selectivities. The applied pressure drop for all calculations is fixed at 10 atm.

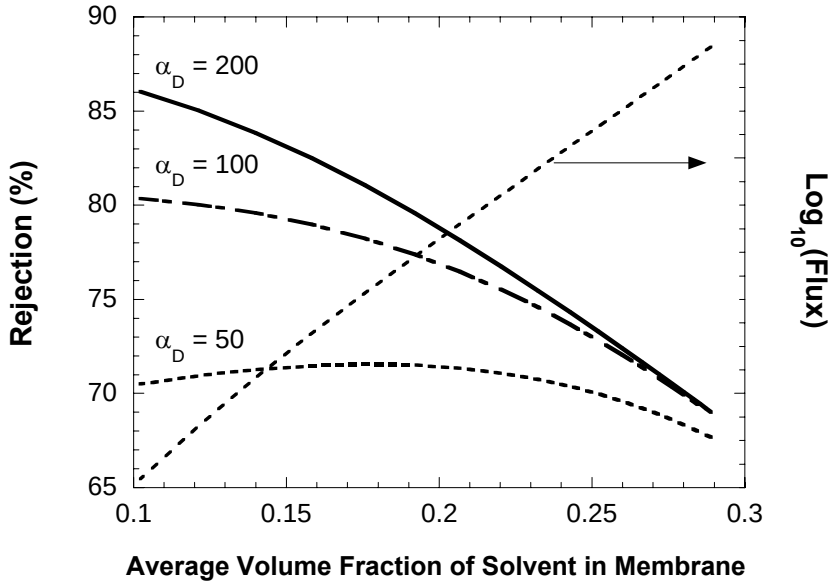

Figure 6.5: Model results showing the effect of diffusivity selectivity (α_D) and solvent content on solute rejection and solvent flux for a solubility selectivity of $\alpha_S = 1$.

Figure 6.5 shows the predicted effects of varying membrane diffusivity selectivity and solvent sorption on the separation with a fixed solubility selectivity of one. A solubility selectivity of one is representative of the triphenylphosphine rejection and the probability is high that similar applications have negligible solubility selectivity because of chemical similarity between the solvent and solute. The general trend is that rejection is increased with decreasing solvent sorption by the membrane material. Solvent flux through the membrane increases exponentially with solvent concentration. This behavior

resembles the tradeoff observed in reverse osmosis when using membranes with lower flux to achieve higher rejection. It also follows the experimental observation in this research of increased catalyst rejection in the blend materials with lower toluene sorption. In terms of the transport model, higher rejections are occurring due to the reduced probability in interaction between solvent and solute due to lower solvent concentration in the membrane. As solvent concentration increases, a point is reached where diffusivity selectivity has minimal or no effect on the rejection achieved, with the rejections for the various α_D's approximately equal as the volume fraction of solvent approaches 0.30 in Figure 6.5.

A recurring theme of the discussions on coupling has been that the solute sorption in the membrane has a profound effect on its membrane flux because sorption controls the quantity that can be dragged through the membrane by the solvent. The influence of solute sorption, shown as solubility selectivity, relative to diffusivity selectivity is depicted in Figure 6.6. It is evident from this graph that the solute sorption has a much stronger influence on rejection than diffusivity selectivity for a coupled system. This indicates that the material design for a separation such as homogeneous catalyst recovery should consider a membrane that preferentially sorbs the solvent. This presents a challenging membrane design problem for two reasons. First, in polymeric membrane separations, it is generally much easier to achieve large differences in component diffusion as opposed to sorption. Secondly, a solvent and solute generally have favorable thermodynamic interactions and little opportunity exists for exploiting solubility differences between the two species.

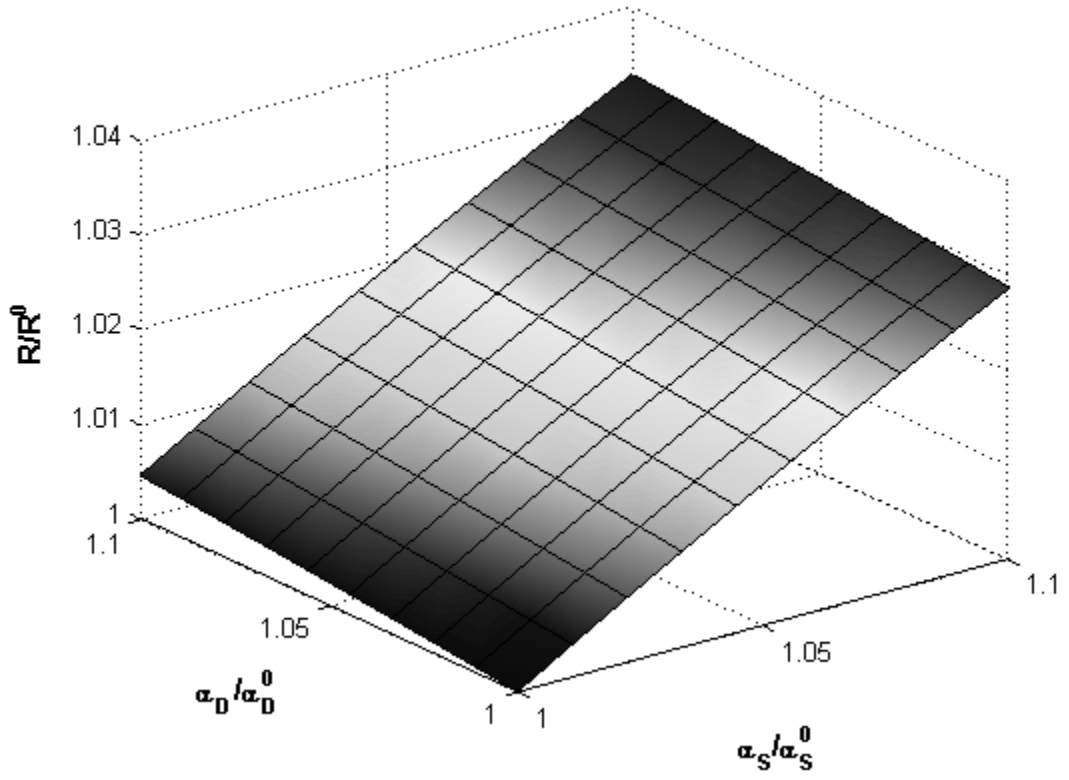

Figure 6.6: Model prediction of the relative change in rejection (R/R^0) as a function of the relative changes in membrane diffusivity selectivity (α_D/α_D^0) and solubility selectivity (α_S/α_S^0).

6.5 Conclusions

Starting from the Maxwell-Stefan equation, modifications appropriate to diffusion in polymers have yielded equations for modeling the transport of multicomponent mixtures in membranes. These equations are a useful tool in the analysis of membrane systems with coupling effects.

Application of the model to experimental data for triphenylphosphine rejection using component diffusivities and solubilities provides a good description of the observed phenomena. The extracted parameters show that coupling is the strongest in the annealed Matrimid. The higher toluene sorption in the annealed Matrimid relative to the crosslinked blends is causing increased interaction between it and the solute. As a consequence, the flux of solvent is dragging more solute through the membrane and reducing the solute rejection in this material.

The accurate representation of the experimental data encourages the extension of the model to hypothetical membrane properties for the purpose of gaining an understanding of their influence on coupled separations. In this manner, the solute recovery of a membrane filled with an inert secondary phase has been investigated. Model results suggest that the incorporation of an impermeable, non-sorbing filler can enhance solute rejection due to the reduced solute sorption. The combination of this performance enhancement with reduced solvent sorption in the phase-separated 10% Oligomer 1 blend is attributed to its superior rhodium-triphenylphosphine catalyst recovery. However, as previously detailed, the chemical compatibility and nano-scale of the phase-separated domains strengthen the interface with the host Matrimid. More detailed experimental

studies are required to determine the benefits of fillers in membrane materials for separations of this type.

There are many challenges in the material selection of polymers for solute recovery from an organic solvent. Generalized modeling of coupled systems shows that sorption of both the solvent and solute are critical to achieving good rejections. Increased solvent sorption can limit the impact of high diffusivity selectivities gained through large solute size due to the coupled fluxes. However, there is a compromise in flux when reducing solvent sorption to gain higher rejection. In terms of the solute, reduction in its sorption relative to the solvent is desirable. Both of these factors should be considered in membrane material development for solute recovery applications. Although the equation development and model results reported here use homogeneous catalyst recovery as their basis, they can be applied to similar applications involving swollen media including recovery of pharmaceutical intermediates, solvent recovery, and polymer-mediated drug delivery.

6.6 References

1. Bird, R. B., W. E. Stewart and E. N. Lightfoot, *Transport Phenomena*, John Wiley & Sons: New York (1960).

2. Paul, D. R. and O. M. Ebra-Lima, "Pressure-Induced Diffusion of Organic Liquids Through Highly Swollen Polymer Membranes," *J. Appl. Polym. Sci.*, **14**, 2201 (1970).

3. Bhanushali, D., S. Kloos and D. Bhattacharyya, "Solute transport in solvent-resistant nanofiltration membranes for non-aqueous systems: experimental results and the role of solute-solvent coupling," *J. Memb. Sci.*, **208**, 343 (2002).

4. Kamaruddin, H. D. and W. J. Koros, "Some observations about the application of Fick's first law for membrane separation of multicomponent mixtures," *J. Memb. Sci.*, **135**, 147 (1997).

5. Taylor, R. and R. Krishna, *Multicomponent Mass Transfer*, John Wiley & Sons: New York (1993).

6. Cussler, E. L., *Multicomponent Diffusion*, Elsevier: Amsterdam (1976).

7. Krishna, R. and J. A. Wesselingh, "The Maxwell-Stefan Approach to Mass Transfer," *Chem. Eng. Sci.*, **52**, 861 (1997).

8. Vignes, A., "Diffusion in Binary Solutions," *Ind. Eng. Chem. Fundam.*, **5**, 189 (1966).

9. Heintz, A. and W. Stephan, "A Generalized Solution Diffusion-Model of the Pervaporation Process through Composite Membranes .2. Concentration Polarization, Coupled Diffusion and the Influence of the Porous Support Layer," *J. Memb. Sci.*, **89**, 153 (1994).

10. Ni, X., X. Sun, D. Ceng and F. Hua, "Coupled diffusion of water and ethanol in a polyimide membrane," *Polym. Eng. & Sci.*, **41**, 1440 (2001).

11. Izak, P., L. Bartovska, K. Friess, M. Sipek and P. Uchytil, "Comparison of various models for transport of binary mixtures through dense polymer membrane," *Polymer*, **44**, 2679 (2003).

12. Izak, P., L. Bartovska, K. Friess, M. Sipek and P. Uchytil, "Description of binary liquid mixtures transport through non-porous membrane by modified Maxwell-Stefan equations," *J. Memb. Sci.*, **214**, 293 (2003).

13. Straatsma, J., G. Bargeman, H. C. van der Horst and J. A. Wesselingh, "Can nanofiltration be fully predicted by a model?," *J. Memb. Sci.*, **198**, 273 (2002).

14. Flory, P. J., *Principles of polymer chemistry*, Cornell University Press: Ithaca (1953).

15. Paul, D. R. and D. H. Carranza, "Pressure-Induced Diffusion in Swollen Butyl Rubber Membranes," *J. Polym. Sci.*, **41**, 69 (1973).

16. Ghoreyshi, S. A. A., F. A. Farhadpour and M. Soltanieh, "Multicomponent transport across nonporous polymeric membranes," *Desalination*, **144**, 93 (2002).

17. Wilke, C. R. and P. Chang, "Correlation of diffusion coefficients in dilute solutions," *AIChE J.*, **1**, 264 (1955).

18. Krishna, R., "A unified approach to the modeling of intraparticle diffusion in adsorption processes," *Gas Sep. Purif.*, **7**, 91 (1993).

CHAPTER 7

CONCLUSIONS AND RECOMMENDATIONS

7.1 Conclusions

There are opportunities in the chemical process industry for the implementation of membranes as the unit operation for catalyst recovery in organic synthesis. This research has been performed to assess the feasibility of this type of membrane separation as well identify the challenges that such a process poses relating to membrane material selection and design. The material design basis was to form blends of Matrimid with a diacetylene-functionalized crosslinking agent for the purpose of achieving polymer stability and membrane selectivity. Therefore, the thrust of the work follows parallel paths of characterization of the influence of the crosslinking agent and determination of the material properties influencing homogeneous catalyst recovery. The conclusions drawn from the research findings will consequently follow this dual perspective.

Blending of Matrimid with the diacetylene-functionalized crosslinking agent and subsequent solid-state crosslinking yields materials with interesting and enhanced properties. The crosslinking agent and Matrimid, which contain matched imide functionalities in their backbones, form compatible blends up to 10 wt% crosslinking agent. Blends of 5 wt% crosslinking agent and 10 wt % exhibit two different blend morphologies. The 5% Blend appears to form a semi-interpenetrating network (s-IPN) with the crosslinking agent forming a network surrounding the host Matrimid. Blends containing 10% crosslinking agent exhibit a phase-separated morphology with domains of crosslinking agent dispersed in a continuous phase that is likely an s-IPN.

The crosslinking agents contain two functionalities that form distributed networks upon thermal activation. Internal diacetylenes react via 1,4-addition to form conjugated crosslinks. Terminal acetylene groups on the oligomeric crosslinking agent form benzenoid structures. Thermal treatment at 250 °C for 24 hours is sufficient for the activation of both reactive groups. Reactivity of the crosslinking agent increases as the number of repeat units is reduced due to a higher concentration of reactive functionalities on a mass basis.

Blending crosslinking agent with Matrimid is a good means of enhancing the material stability as demonstrated by reduction in toluene sorption. Heat treatment of Matrimid alone can also impart increased solvent resistance. The average reduction in Matrimid's sorption of toluene through annealing is 22% with the crosslinking agents adding another 7% reduction beyond that. In the blends, formation of an s-IPN and low sorption in the crosslinked domains contribute to stability. The ordered crosslinking of the diacetylene in the solid-state prevents significant losses in flux and thus allows the blends to be productive membranes for applications such as the homogeneous catalyst recovery.

These materials have proved to be capable of permeating solvent at high fluxes while restricting the permeation of the rhodium-triphenylphosphine catalyst ligand complex used in commercial hydroformylation reactions. Solvent sorption is sufficiently high to cause a transition in the polymers from a glassy to rubbery state as indicated from the sorption studies and toluene fluxes through the materials. This contributes significantly to the productivity of the membrane materials. Despite the high flux of solvent, large differences in the toluene and catalyst permeabilities were observed. Matrimid

blended with 10% crosslinking agent gives 91% rejection of the catalyst. Rejection efficiencies were: 10% Blend > 5% Blend > Matrimid. Similar trends would be expected for the rejection of a large solute from a small and highly sorbing solvent.

In the investigation of separation characteristics of homogeneous catalyst recovery, it was found that flux coupling significantly affects the solute rejections that can be achieved by the membrane. The coupling of fluxes becomes pronounced when sorption occurs to an extent where interactions between permeating components influences the fluxes and consequently the separations that can be achieved. For homogeneous catalyst recovery, this translates into increased catalyst flux due to the faster permeating species dragging the catalyst through the membrane. The mobility selectivity gained by the larger catalyst is diminished by this effect.

An analysis of the membrane transport observed in this work was performed using modified Maxwell-Stefan equations. Following the solution-diffusion model for transport in membranes, the equations were modified into a tractable form that described coupled transport well. Analysis of the rejection characteristics for the separation in this research shows that coupling is greatest in neat Matrimid, which has the highest sorption of toluene. Extension of the model to a generalized case of solute transport shows that sorption of both the solute and solvent are key factors that influence coupling and consequently the level of solute rejection that can be achieved by the membrane. Reduction in the solvent content of the membrane will increase the rejection for applications of this type, but this will be at the cost of flux through the membrane. Reduction in the membrane sorption of the solute can also aid in achieving high rejections. Based on these

model observations, emphasis should be placed on the solute partitioning between the liquid and membrane phases in future studies of membranes for catalyst recovery.

An interesting finding of this work was that a highly permeable polymer combined with impermeable nanoparticles – the morphology of the 10% Blend – showed improved separation characteristics relative to the host polymer alone. Although some characterizations of the materials indicate that there is a modification of the continuous phase due to the presence of the crosslinking agent, experimental observations and modeling suggest that this may be a method of enhancing the rejection characteristics of a high permeability material with coupled flux. It should be noted that strong adhesion of the phases and small size of the secondary phases are almost certainly aiding in the reduction of nonselective gaps at the phase interface. Consideration of these factors should be employed in any future work to modify membranes by this method.

The high rejection of the catalyst by the 10% Blend (91%) combined with high flux show the feasibility of membrane recovery of a homogeneous catalyst. It is likely that membranes with fluxes comparable to those measured here will be required for this application due to the large amounts of feed that must permeate the membrane. Though the materials here show acceptable performance characteristics, opportunities exist for further optimization. Factors such as the increased sorption of catalyst in the materials resulting from the crosslinking agent chemistry can be addressed through material modification (e.g. different crosslinking methods). The work of this dissertation provides a template for understanding the influence of the subsequent modifications and processes on the quality of separation, which can promote the expansion of membranes into a broader application for homogeneous catalyst recovery.

7.2 Recommendations for Future Work

The approach of blending a high-performance polymer with a crosslinking agent was taken as a means to optimize performance and cost. However, the miscibility (or "compatibility") of polymer and crosslinking agent is a limiting factor, and in our case a fairly severe one. Improvement in catalyst recovery (and similar applications relying on mobility selectivity) could be achieved in similar materials with a greater extent of crosslinking. A homopolymer with crosslinkable groups on the polymer backbone can alleviate the miscibility issues associated with blending while providing a more distributed network. The flux rates through the polyimide materials examined in this study are quite high and some compromise in these fluxes due to increased crosslinking could be withstood for the sake of increasing rejection; the compromise in flux is further mitigated when reducing membrane thickness as done in commercial applications. Polyimides investigated for pervaporation of organic solvents such as those by Xu et al.,[1] Ren et al.,[2] and Okamoto et al.[3] possess flux rates comparable to the materials investigated here as well as crosslinkable functionalities in the polymer backbone. Rather than through blending, the extent of crosslinking in these materials can be tailored synthetically (by concentration of crosslinkable groups in the polymer backbone) or through controlled reaction of the crosslinking groups. Investigation of materials such as this or high molecular weight polyimides with diacetylene functionalities for homogeneous catalyst recovery correlating separation selectivity to extent of crosslinking would be interesting.

The interaction of the reaction solvent with the membrane and solute plays a critical role in the separation characteristics. It is to be expected that a change in solvent for a

reaction would affect catalyst rejection. A study of the solvent effects on the separation following the permeation measurement techniques used here could provide a means to optimize not only the membrane material, but also the solvent medium. For example, a lower sorbing solvent may reduce the flux coupling and provide higher rejections, mimicking the effects that could be achieved through increased crosslinking. Again, the polyimides of this study or those cited above would be a good starting material for such a study due to their resistance to many reaction solvents.

A better understanding of flux coupling and its effects on membrane separations would lead to more informed decisions in material selection. A fundamental transport study of solvents and solutes of varying properties combined with a Maxwell-Stefan analysis would provide more detail on the interactions between mobile species in the membrane. The techniques demonstrated in this research can be used to determine rejection as a function of the component solubility and diffusivity. Although the experimental limitation of indeterminate values of the coupling parameter ($\overline{D}_{12}$) in this analysis still exists, the measurement for an array of conditions would be insightful. For example, the concentration dependence of coupling may be demonstrated in solvents of varying degrees of sorption in a membrane material. For the purposes of such a study, an analytically simpler system than the one examined in this research is proposed. A good membrane material to study would be polydimethylsiloxane (PDMS) because it has high fluxes for a number of low molecular weight solvents[4-7] that can be easily measured using the methods outlined in the dissertation. For solutes, an array of dyes (e.g. Sudan IV and Fast Green FCF) and triglycerides of varying molecular weight and chemical nature have been shown to be soluble and detectable using UV-VIS spectrophotometry by Bhanushali

et al.[8] Solvents such as methanol, ethanol, hexane, and toluene can dissolve these solutes and provide an array of interactions with the membrane and solute from which coupling can be observed.[8]

Another area that appears to warrant some further investigation is the influence of filler on reverse osmosis separations with high degrees of solvent sorption. As indicated by the separation characteristics of the 10% Blend, this type of membrane may be able to enhance solute rejection due to reduced sorption. The polymer-filler interface and size of the filler need to be considered in this assessment. Nanoparticles of fumed silica, used as membrane filler by Merkel et al.,[9] combined with PDMS may be good basis for this investigation. Solvents and solutes proposed for the flux coupling system above could be used to determine rejection characteristics of these filled materials relative to the neat polymer.

Finally, the model hydroformylation chosen for study in this research is but one of a host of organic syntheses catalyzed by a soluble transition metal catalyst. Catalytic hydrogenation, Heck coupling, and assymmetric hydroxylation are a few examples of commercially relevant reactions employing large catalyst complexes that could be recovered using membranes. Many opportunities exist for the extension of membranes in the area of homogeneous catalyst recovery.

7.3 References

1. Xu, W. Y., D. R. Paul and W. J. Koros, "Carboxylic acid containing polyimides for pervaporation separations of toluene/iso-octane mixtures," *J. Memb. Sci.*, **219**, 89 (2003).

2. Ren, J., C. Staudt-Bickel and R. N. Lichtenthaler, "Separation of aromatics/aliphatics with crosslinked 6FDA-based polyimides," *Sep. Purif. Tech.*, **22-23**, 31 (2001).

3. Okamoto, K., H. Wang, T. Ijyuin, S. Fujiwara, K. Tanaka and H. Kita, "Pervaporation of aromatic/non-aromatic hydrocarbon mixtures through crosslinked membranes of polyimide with pendant phophonate ester groups," *J. Memb. Sci.*, **157**, 97 (1999).

4. Miller, J. F., D. R. Bryant, K. H. Hoy, N. E. Kinkade and R. H. Zanapalidou, "Membrane separation process," In *US Patent No. 5,681,473* (1997).

5. Bhanushali, D., S. Kloos, C. Kurth and D. Bhattacharyya, "Performance of solvent-resistant membranes for non-aqueous systems: solvent permeation results and modeling," *J. Memb. Sci.*, **189**, 1 (2001).

6. Whu, J. A., B. C. Baltzis and K. K. Sirkar, "Nanofiltration studies of larger organic microsolutes in methanol solutions," *J. Memb. Sci.*, **170**, 159 (2000).

7. Han, S. J., S. S. Luthra, L. Peeva, X. J. Yang and A. G. Livingston, "Insights into the transport of toluene and phenol through organic solvent nanofiltration membranes," *Separ. Sci. Technol.*, **38**, 1899 (2003).

8. Bhanushali, D., S. Kloos and D. Bhattacharyya, "Solute transport in solvent-resistant nanofiltration membranes for non-aqueous systems: experimental results and the role of solute-solvent coupling," *J. Memb. Sci.*, **208**, 343 (2002).

9. Merkel, T. C., V. Bondar, K. Nagai and B. D. Freeman, "Hydrocarbon and perfluorocarbon gas sorption in PDMS, PTMSP, and copolymers of tetrafluoroethylene and 2,2-bis(trifluoromethyl)-4,5-difluoro-1,3-dioxole," *Macromolecules*, **32**, 370 (1999).

APPENDIX A

PERMEATION MEASUREMENT AND CALCULATIONS

The various apparatus in which permeation measurements were performed are presented in this appendix. Methods of calculating the transport properties based on the quantities measured will be reviewed. Example calculations are also presented.

A.1 Experimental Apparatus

To test the volatile organic compounds involved in this research, a completely enclosed permeation system was built. The apparatus is pictured in Figure A.1 and a schematic diagram of the components is shown in Figure A.2. The unit was built to accommodate two operating modes, pressure driven liquid permeation and dialysis (concentration driven) permeability measurements. Two 100 cm^3 stirred reactor systems with integral heating units and temperature control were provided as the liquid reservoir for permeation tests. Each reactor unit was fed to a single membrane test cell by gear pumps that were provided for recirculation of the fluid through the reactor / membrane system. The membrane test cell was the Millipore 47 mm diameter filter housing (Model. No. XX44 047) modified with an additional port on the outlet to provide a crossflow pattern for the feed and permeate sides of the cell. A Teflon O-ring was to seal the feed and permeate sides. The test cell was wrapped in heating tape connected to a temperature control unit for maintaining isothermal conditions (all tests were performed at 35 °C). All components and interconnecting tubing (1/8" diameter OD) that came into

Figure A.1: Membrane permeation apparatus. Diagram of component parts and interconnecting tubing provided in Figure A.2.

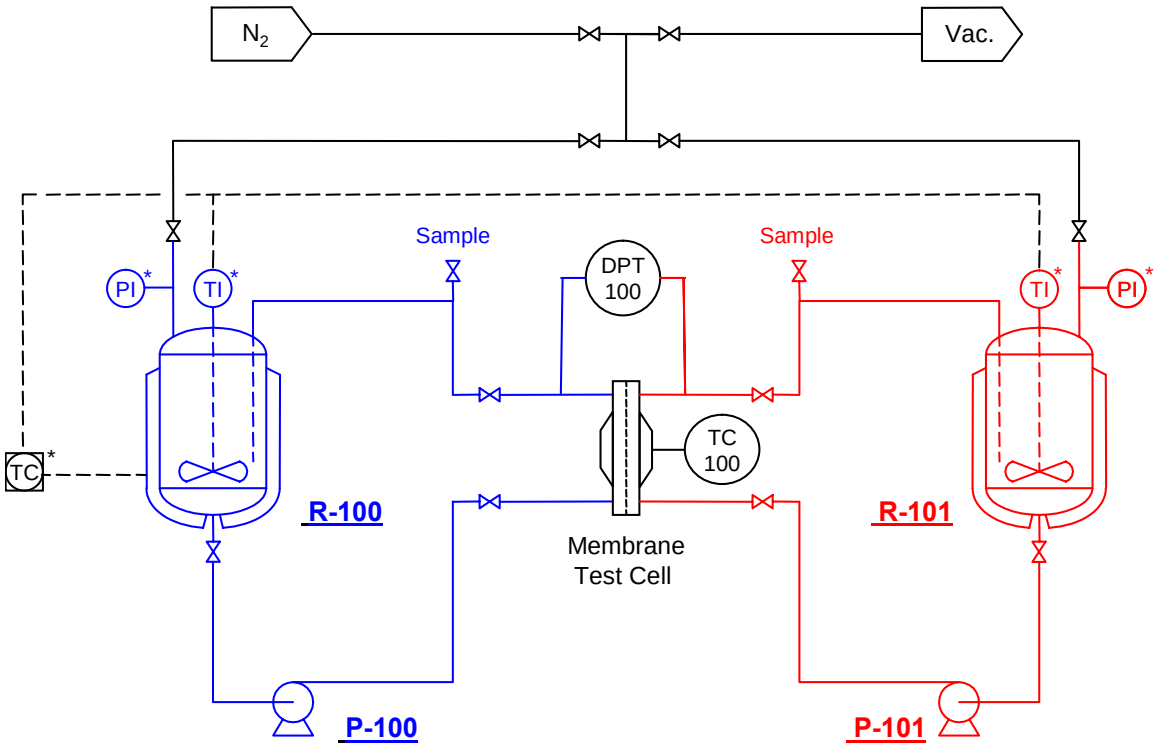

Item No.	Description	Mat.	Capacity	Provider	Model
R-100 / 101	Reactor	316 SS	100 cm^3 / 3000 psi	Parr Instrument	4565
P-100 / 101	Pump	316 SS	0 – 300 cm^3/min	Micropump	185
DPT-100	Diff. Press. Transducer	316 SS	0 – 300" H_2O diff.	Omega	PX-771A
TC-100	Temp. Controller	-	-	Barnant	689
PI*	Press. Gauge		0 – 600 psi		
TC*	Temp. Controller				
TI*	Thermocouple		0 – 250 °C		

* Items shown with asterisk on drawing are part of Parr Reactor package

Figure A.2: Diagram of membrane test permeation system for dialysis, hydraulic permeation, and rejection experiments.

contact with the process material were 316 stainless steel or gasket materials rated for toluene service.

A.2 Hydraulic Permeation of Toluene

Hydraulic permeation is the permeation of a single liquid component feed through a membrane, driven by an applied pressure difference across the membrane. The theory behind determining the penetrant diffusivity and hydraulic permeability through the experiments performed in this work is reviewed. That will be followed by the experimental procedures that were employed and a sample calculation.

A.2.1 Equilibrium Thermodynamic Model

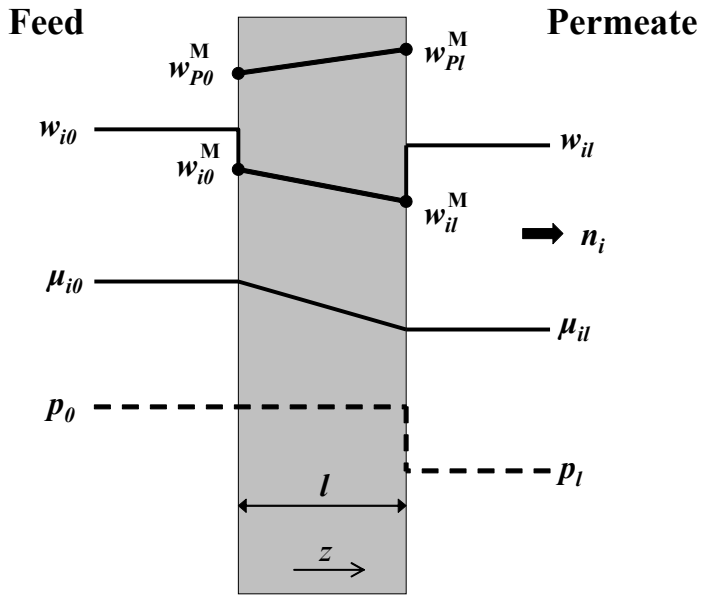

Figure A.3: Schematic representation of transport of component *i* in a membrane. Gradients and concentration differences are exaggerated for effect.

In pressure-induced liquid permeation, it is widely accepted that under diffusion-controlled transport in polymers the membrane is uniformly at the feed pressure, p_o, and diffusion occurs as a result of a concentration gradient in the membrane caused by the pressure difference, as depicted in Figure A.3. The theoretical reasons for this argument can be developed from equilibrium thermodynamics. Starting from the equality of chemical potentials at phase equilibrium and the definition of chemical potential, we see:

$$\mu_i^M = \mu_i^L \tag{A.1}$$

$$\mu_i - \mu_i^{ref} = RT \ln a_i + \overline{V}_i (p - p_{ref}) \tag{A.2}$$

$$\mu_i^{M(ref)} = \mu_i^{L(ref)} \tag{A.3}$$

which gives for the feed side equilibrium equation:

$$\mu_{i0}^{M(ref)} + RT \ln a_{i0}^M + \overline{V}_{i0}^M (p_0 - p_{ref}) = \mu_{i0}^{L(ref)} + RT \ln a_{i0}^L + \overline{V}_{i0}^L (p_0 - p_{ref}) \tag{A.4}$$

Because of the pressure differences involved in the phase equilibrium, the pressure dependence of the chemical potential is included. If it is assumed that the partial molar volumes of component *i* in the fluid and membrane phases are equal to the molar volume of pure *i* ($\overline{V}_i^M = \overline{V}_i^L = V_i$) then the activity of component *i* on the feed boundary of the membrane is simply equal to its activity in the feed fluid phase (Eq. A.5).

$$a_{io}^M = a_{io}^L \tag{A.5}$$

Evidence of a uniform pressure equal to the feed pressure, $p_{0,}$ across the membrane has been observed experimentally.[1,2] In the chemical potential expression for the permeate boundary of the membrane, the membrane phase has a pressure equal to p_0 while the liquid phase has a pressure equal to the downstream pressure, p_l. Using the same assumptions as the feed activity calculation yields Equations A.6 and A.7 as permeate equilibrium expressions.

$$RT \ln a_{il}^{M} + V_i (p_0 - p_{ref}) = RT \ln a_{il}^{L} + V_i (p_l - p_{ref}) \tag{A.6}$$

$$a_{il}^{M} = a_{il}^{L} \exp\left[\frac{-V_i (p_0 - p_l)}{RT}\right] \tag{A.7}$$

Equation A.7 illustrates that the source of the concentration driving force for diffusion arises from the pressure difference applied to the membrane. The lower activity (due to the lower pressure of the fluid phase) of the permeate boundary of the membrane results in a lower concentration of penetrant than the feed side. Several compelling experimental studies have supported this theory as well as demonstrated that the assumptions made are valid for a broad range of polymer-penetrant systems. Examples include the observation of an asymptotic approach to a limiting flux with increasing pressure[3] (this due to the fact that a_l cannot be less than zero), a decrease in the downstream penetrant concentration instead of an increase in the upstream concentration when examining the cross-section of a membrane after exposure to an applied pressure,[4] and the previously cited work indicating a uniform membrane pressure.

Now it is simply a matter of using a solution theory such as an ideal mixture or UNIFAC to calculate the activity in the liquid phase and equate it to the membrane activity. From sorption equilibrium experiments such as those in Chapter 4, an equilibrium relationship between permeant activity and sorption in the polymer is established from which the concentration of permeant in the membrane phase can be predicted. For polymers in the rubbery state, the Flory-Rehner[5] equation for crosslinked rubbers is a good means of describing the activity / sorption relationship (shown for single component and polymer):

$$\ln a_1 = \ln(1-\phi_M) + \phi_M + \chi_1(\phi_M)^2 + \nu\bar{V}_1\left[(\phi_M)^{1/3} - \phi_M/2\right] \qquad \text{(A.8)}$$

A.2.2 Determination of Diffusion Coefficient

Now that the equilibrium relationships and concentration driving force are defined, a transport description is needed. The diffusion theory for hydraulic permeation in swollen polymers developed by Paul[6] and Ebra-Lima[3] has been used to determine the diffusivity and hydraulic permeability of toluene in the various polymer materials studied. For swollen membranes, it is important to use the proper frame of reference. In the case of the membrane permeability experiments, this is the stationary membrane at steady-state flux conditions. Therefore, the transport model starts out with Fick's law for diffusion in a stationary system:[7]

$$n_1 = w_1(n_1 + n_M) - \rho D_{1M}\frac{dw_1}{dz} \qquad \text{(A.9)}$$

Equation A.9 is in the form of a binary system containing the permeating species, component 1, and membrane polymer, component M. Diffusion is considered to occur in

only the z dimension, the thickness of the membrane. The stationary frame of reference renders $n_M = 0$ and the expression for the flux of component 1 becomes:

$$n_1 = -\frac{\rho D_{1M}}{1 - w_1}\frac{dw_1}{dz} \tag{A.10}$$

and using an assumption of no volume change on mixing[3] yields Eq. A.11, giving flux in terms of volume fraction.

$$\frac{n_1}{\hat{\rho}_1} = \hat{n}_1 = -\frac{D_{1M}}{1 - \phi_1}\frac{d\phi_1}{dz} \tag{A.11}$$

$\hat{\rho}_1$ is the pure component 1 density which means that Eq. A.11 is expressed in volumetric flux , $\hat{n}_1$, introduced in Chapter 6. The volume fractions, ϕ_1, in Eq. A.11 of component 1 are those of the polymer phase. Integration of A.11 with the limits $\phi_1 = \phi_{10}(z = 0)$ and $\phi_1 = \phi_{1l}(z = l)$, where l is the membrane thickness yields:

$$\hat{n}_1 = \frac{D_{1M}}{l}\ln\left(\frac{1 - \phi_{1l}}{1 - \phi_{10}}\right) \tag{A.12}$$

To be entirely accurate, l is the thickness of the swollen membrane under the diffusion conditions. If the swelling is assumed to be isotropic, the thickness of the swollen membrane placed in the test cell is given by:

$$l_0 = \frac{l_d}{\phi_{M0}^{2/3}} \tag{A.13}$$

where l_0 is the freely swollen thickness of the membrane exposed to pure toluene, l_d is measured thickness of the membrane prior to swelling, and ϕ_{M0} the volume fraction of polymer in the freely swollen membrane determined from sorption experiments. A gradient in swelling occurs during diffusion as a result of the concentration gradient induced by the difference in feed and permeate pressures. The thickness of the mem-

brane cannot be measured under these conditions, but can be determined by constraining the area of membrane to be constant and obtaining the following material balance:

$$\phi_{M0} = \int_0^l \phi_M \, dz \tag{A.14}$$

which gives upon integration of the concentration profile given by Eq. A.11 and substituting $\phi_1 = 1 - \phi_M$:

$$\frac{l_0}{l} = \frac{\phi_{10} - \phi_{1l}}{(1-\phi_{10}) \ln\left(\frac{1-\phi_{1l}}{1-\phi_{10}}\right)} \tag{A.15}$$

Inserting Eqs. A.13 and A.15 into the flux equation A.12 to give the true membrane thickness yields:

$$\boxed{\hat{n}_1 = \frac{D_{1P}}{l_d (1-\phi_{10})^{2/3}} (\phi_{10} - \phi_{1l})} \tag{A.16}$$

which is a relatively simple relationship predicting that the flux is directly proportional to the difference in volume fraction at either surface of the membrane. Now for a flux experiment at a specific pressure drop the diffusivity can be determined using volume fractions calculated from the above equilibrium relationships. If the diffusion coefficient is constant, the flux and difference and volume fractions form a linear relationship.

A.2.3 Hydraulic Permeability

While Eq. A.16 is used to calculate the diffusivity, the complex thermodynamic relationship between the sorbed volume fraction and activity does not allow for a direct calculation of a permeability that relates flux to driving force (in this case pressure). However, a simplified approach can be used to obtain a hydraulic permeability, A_0, that is a proportionality factor between the flux and applied driving force. If we assume that the

membrane volume fraction varies linearly with activity (a good assumption for low sorbing compounds, it but should be tested for linearity in other systems), then from Eq. 2.5 and A.7 we have:

$$\hat{j}_i = \frac{A_0'}{l}\left[1 - \exp\left(\frac{-V_i(p_0 - p_l)}{RT}\right)\right] \tag{A.17}$$

where $\hat{j}_i$ is the experimentally measured volumetric flux and A_0' is the hydraulic permeability in units of cm^2/s. Because of the small values of the exponential term in this work resulting from moderate pressures and molar volumes, the simplification that 1-exp(x) $\rightarrow x$ as $x \rightarrow 0$ can give a simplified hydraulic permeability A_0 in units of cm^2/s-atm. Equation A.18 results from these simplifications:

$$\hat{j}_i = \frac{A_0(p_0 - p_l)}{l} \tag{A.18}$$

$$A_0 = A_0' \frac{V_i(p_0 - p_l)}{RT} \tag{A.19}$$

The hydraulic permeability in equation A.18 is an empirical value often reported in literature for reverse osmosis and nanofiltration. It is a convenient way of predicting flux of a component through a material at various pressure drops. Because it has not taken into account the stationary frame of reference of Eq. A.9, $A_0' \neq D_{iM}\phi_{io}$. For a prediction of A_0 from solubility and diffusivity values, Paul[8] has developed a method utilizing thermodynamic diffusion coefficients.

A.2.4 Experimental

To run hydraulic permeation experiments, only one of the reactors in Figure A.2 is used to supply toluene to the membrane test cell. One of the permeate outlets of the

test cell is connected to a capillary flow meter (0.00 – 0.20 cm^3), with the other outlet valved off. A nitrogen pressure head is supplied to the reactor for the driving force and is adjusted with a pressure regulator, the pressure drop, $\Delta p = (p_0 - p_l)$, for the experiment is read as the nitrogen supply pressure.

Polymer films were preswelled before the start of the experiment in liquid toluene. It was to important have the film fully immersed in toluene on both the feed and permeate sides to prevent failure from swelling-related dimensional changes upon exposure to toluene. Before the start of the experiment, air bubbles on the downstream side of the cell were removed by flowing a small amount of toluene through the inverted cell before placing it in the system. To ensure that membrane was fully immersed in toluene during the course of a permeation test, the cell remained inverted during the run (cell was fed from the bottom). Once the membrane test cell was attached to the reactor, the feed liquid was circulated briefly to ensure full liquid contact on the feed side as well.

Upon application of nitrogen pressure, the system was allowed to reach steady-state permeation rates. Because the films were preswelled, the approach to steady-state was observed as a "burst" effect rather than the time lag that is seen in gas permeation studies.[9] On average, steady-state flow was observed in less than one hour, but at least two hours were allowed to pass before the flow rate was recorded for a specific pressure, with another measurement performed two hours later to confirm the reading. With the known area of the films (taken to be the area inside the O-ring), fluxes could then be calculated from the flow rates.

A.2.5 Sample Calculation

Fluxes of toluene through dense films have been measured at various pressures. The toluene diffusion coefficients can be calculated from this driving force versus flux data using Eq. A.16. Looking at the variables of the equation, an average dry film thickness, l_d, can be measured with a micrometer before film preswelling. From the sorption versus activity relationships determined in Chapter 4, values for the volume fractions of toluene at the film feed and permeate are calculated for activities determined from Eqs. A.5 and A.7, respectively, and assuming no volume change on mixing.[3] If the diffusion coefficient of toluene in the film remains constant under the various conditions tested, the flux should have a linear relationship with the driving force $(\phi_{10} - \phi_{1l})$ according to A.16. Testing this relationship by plotting measured flux versus driving force (Figure A.4) and we do indeed have a good linear fit to the data. An average toluene diffusivity can be calculated for the pressure range studied.

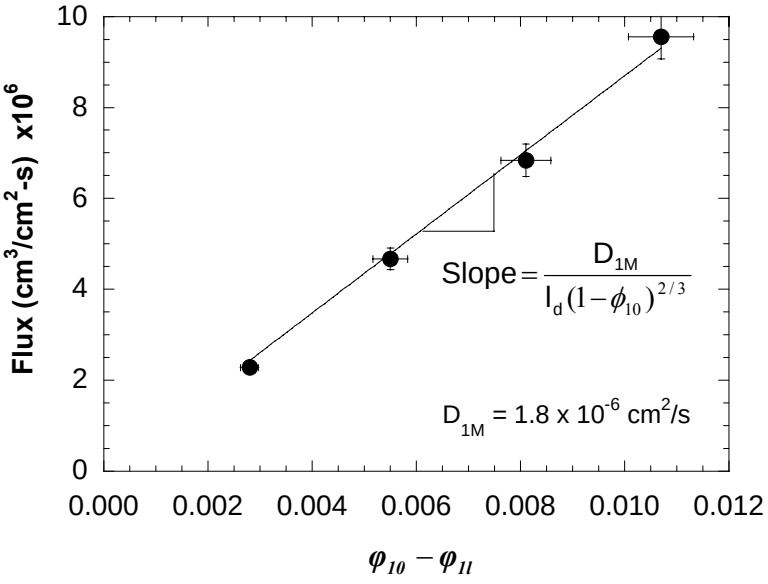

Figure A.4: Sample calculation of toluene diffusivity in annealed Matrimid film in a hydraulic permeation experiment. The volume fraction driving force arises from the application of a pressure drop across the film. An average toluene diffusivity for the experiments is calculated from the slope of this line. Determination of volume fraction differences is shown in Table A.1.

Table A.1: Example of calculated volume fraction differences for the hydraulic permeation of toluene in annealed Matrimid at various pressures.

	Feed		**Permeate**		
Δp (atm)	a_{10}	φ_{10}	a_{1l}	φ_{1l}	$\varphi_{1o} - \varphi_{1l}$
1.7	1	0.3842	0.993	0.3814	0.0028
3.4	1	0.3842	0.986	0.3787	0.0055
5.1	1	0.3842	0.979	0.3760	0.0081
6.8	1	0.3842	0.971	0.3735	0.0105

A similar procedure can be followed for the determination of the hydraulic permeability (Figure A.5). The hydraulic permeability is dependent only on the pressure driving force; the equilibrium sorption of toluene is inferred in its value. The hydraulic permeability is a good measure of the relative fluxes of various materials because it is simply a proportionality factor relating flux to driving force. The value determined in Figure A.5 is A_0' in units of cm^2/s, which is the form presented in Chapter 5. The benefit of using this term as opposed to A_0 of Eq. A.18 is that it eliminates the nonlinearity introduced by the simplification of the exponential term in Eq. A.17.[10]

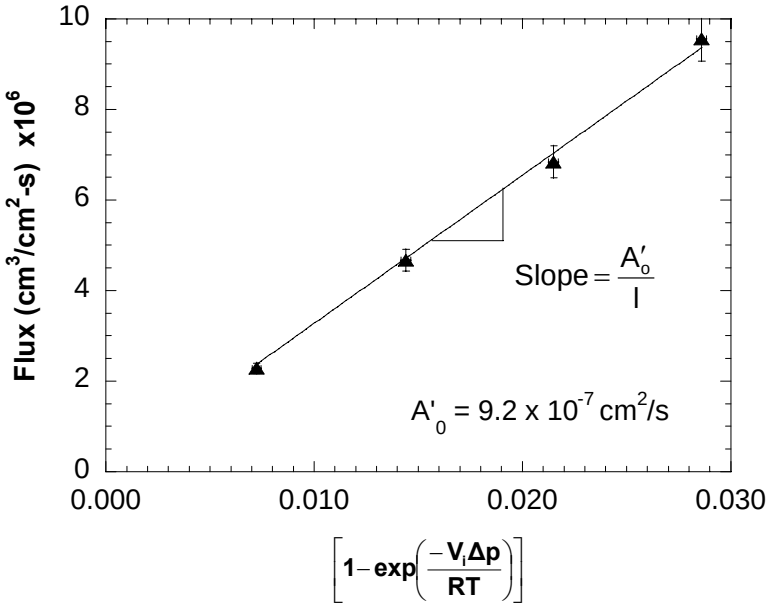

Figure A.5: Sample calculation for the hydraulic permeability, A_0', for an annealed Matrimid film. Fluxes have been measured at various pressure drops, Δp, across the film. The linear relationship between driving force (abscissa) and flux allows determination of an average hydraulic permeability for the experimental pressure range.

A.3 Dialysis Measurements

A.3.1 Theory

Data analysis and determination of transport parameters in dialysis in this work follows the conventional approach for this type of experiment.[11,12] Dialysis is the transport of a solute across a membrane separating liquid solutions of different concentration. The only driving force in dialysis is the concentration of the two solutions separated by the membrane. Due to the low concentrations of solutes studied in the dialysis experiments of this research, the stationary frame of reference and moving frame of reference reduce to the same equation for flux, which in terms of concentration gives Eq. 2.6:

$$J_i = D_i \frac{(K_{io} c_{io} - K_{il} c_{il})}{l} \tag{2.6}$$

If it is assumed that the solute partition coefficient, K_i, is constant for the concentration range, then a permeability, P_i, can be used to relate the flux of solute i to the concentrations of the two solutions:

$$J_i = \frac{P_i (c_{io} - c_{il})}{l} \tag{A.20}$$

In the execution of a dialysis experiment, the membrane is initially exposed a feed and permeate solution of known concentration. Permeability is determined through measurement of the solute concentration change as a function of time in one of the solutions (in the development presented, this is the permeate solute concentration). Therefore the concentrations of Eq. A.20 are instantaneous and it is a pseudo steady-state description of the flux at time t. If the volumes of the permeate and feed side are assumed to remain constant, the flux of the permeating component can also be written as:

$$J_i = \frac{\partial c_{il}}{\partial t}\frac{v_l}{A} \tag{A.21}$$

and the mass balance for the concentration of solute on the feed side is:

$$c_{i0} = c_{i0}^o - c_{il}\left(\frac{v_l}{v_0}\right) \tag{A.22}$$

with v as the liquid volume and the subscripts *0* and *l* denote quantities for the liquid feed and permeate, respectively. c_{i0}^o is the known feed concentration of the solute at time t = *0*. Substitution of Eqs. A.21 and A.22 into Eq. A.20 gives the time dependence of the permeate concentration of solute *i*, based on the species mass balance and the solution-diffusion model:

$$\frac{\partial c_{il}}{\partial t} = \frac{P_i A}{v_l l}\left[c_{i0}^o - c_{il}\left(\frac{v_p}{v_f}+1\right)\right] \tag{A.23}$$

and integration of this equation gives

$$c_{ip} = c_{ip}^o + \left(\frac{c_{if}^o}{v_p/v_f+1} - c_{ip}^o\right)\left\{1-\exp\left[\frac{-P_i A}{v_p l_0}\left(\frac{v_p}{v_f}+1\right)t\right]\right\} \tag{A.24}$$

Since it is the only unknown, the permeability can be determined by fitting the concentration versus time data to Eq. A.24. Often the initial permeate concentration is zero, which can lead to further simplification. To ensure that the constant volume assumption is valid, the permeability experiments have been run over small concentration differences in the feed and permeate phases, where the diffused amount of solute is less than 0.1% of the volume of the feed and permeate phases. The film thickness, l_0, used in the determination of the permeability was taken to be that of the freely swollen film in toluene determined by Eq. A.13. Further details of the experimental procedure are provided in the following section (A.3.3).

The flux coupling effects discussed in Chapter 6 have been omitted in this treatment of dialysis. Gross and Heintz[12] and Ghoreyshi et al.[13] have justified this omission through experimental analysis of dialysis of low concentration solutes and subsequent analysis using the Maxwell-Stefan transport equations.

A.3.2 Experimental

Dialysis experiments were run with both Parr reactors connected to the membrane test cell as shown in Figure A.2. Development of the flux equations in Section A.3.1 has ignored boundary layer effects. To ensure that this is a valid approach, pump flow rates were set so turbulence would be achieved within the test cell as determined by the Reynolds number. The approximate flow rate for either reactor loop was 100 cm^3/min, which is well above the minimum flow requirement for turbulence. Minimization of boundary layer resistance was confirmed through observation of fluxes independent of increasing flows. The differential pressure transmitter measured the trans-membrane pressure and allowed for minute flow adjustments of either reactor loop to prevent the introduction of pressure driving forces for flux. Reactor impellers were run at a speed of 400 rpm to ensure uniform concentration throughout each reactor loop. Isothermal conditions were maintained by temperature control for the reactors and membrane test cell within ±0.1 °C.

At the beginning of an experiment, solutions of either 1-dodecene or triphenylphosphine in toluene were prepared and their concentrations confirmed via gas chromatography (GC). This solution was designated as the "feed" and pure toluene served as the permeate. 100 cm^3 of each solution was charged into a separate reactor and heated to the

experimental temperature of 35 °C. The time at which the recirculation pumps were started and the membrane was exposed to each solution was taken to be $t = 0$. The rise in solute concentration of the permeate was measured by GC at various times. The sample volume for GC analysis was quite small (<1 μL) relative to the feed and permeate solutions and therefore not accounted for in their final values.

As in the hydraulic permeability experiments, all films tested were pre-soaked in toluene for at least four days to reduce the time to achieve steady-state, which is slowed by polymer relaxation when sorbing toluene (Chapter 4). Preswelling of the films also reduced the possibility of film failure due to volume changes of the polymer after exposure to the toluene solutions. However, extremely careful technique is required when handling the swollen films.

A.3.3 Sample Calculation

A sample calculation for the dialysis of 1-dodecene in solution with toluene through a 10% Oligomer 1 blend is shown in Figure A.6. By plotting the dodecene concentration measured via GC versus experiment time, a good fit to Eq. A.24 is obtained. The permeability of dodecene in the toluene-swollen polymer is determined from this fit.

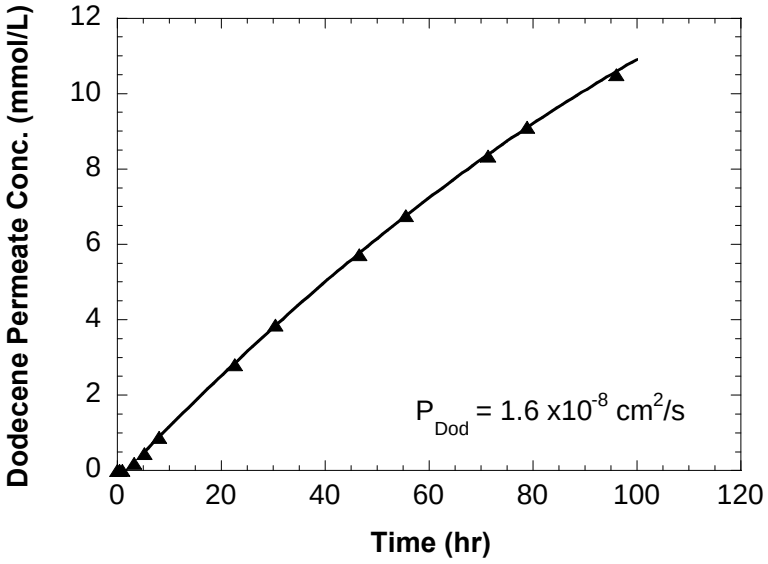

Figure A.6: Dodecene permeate concentration vs. time in dialysis experiment for a 10% Oligomer 1 Blend polymer film. The line shown is a fit of Eq. A.24 with dodecene permeability as the adjustable parameter.

A.4 References

1. Paul, D. R. In *Permeability of Plastic Films and Coatings to Gases, Vapors and Liquids*, H. B. Hopfenberg, Ed.; Plenum Press: New York, p 35 (1974).

2. Ham, J. S., M. C. Bolen and J. K. Hughes, "The use of high pressure to study polymer-solvent interaction," *J. Polym. Sci.*, **57**, 25 (1962).

3. Paul, D. R. and O. M. Ebra-Lima, "Pressure-induced diffusion of organic liquids through highly swollen polymer membranes," *J. Appl. Polym. Sci.*, **14**, 2201 (1970).

4. Paul, D. R. and O. M. Ebra-Lima, "The mechanism of liquid transport through swollen polymer membranes," *J. Appl. Polym. Sci.*, **15**, 2199 (1971).

5. Flory, P. J. and J. Rehner Jr., "Statistical mechanics of crosslinked polymer networks. Part 2. swelling," *J. Chem. Phys.*, **11**, 521 (1943).

6. Paul, D. R., "The solution-diffusion model for swollen membranes," *Sep. Purif. Method*, **5**, 33 (1976).

7. Bird, R. B., W. E. Stewart and E. N. Lightfoot, *Transport Phenomena*, John Wiley & Sons: New York (1960).

8. Paul, D. R., "Further comments on the relation between hydraulic permeation and diffusion," *J. Polym. Sci.: Polym. Phys. Ed.*, **12**, 1221 (1974).

9. Crank, J. and G. S. Park, *Diffusion in Polymers*, Academic Press: New York (1968).

10. Bhanushali, D., S. Kloos, C. Kurth and D. Bhattacharyya, "Performance of solvent-resistant membranes for non-aqueous systems: solvent permeation results and modeling," *J. Memb. Sci.*, **189**, 1 (2001).

11. Paul, D. R., M. Garcin and W. E. Garmon, "Solute diffusion through swollen polymer membranes," *J. Appl. Polym. Sci.*, **20**, 609 (1976).

12. Gross, A. and A. Heintz, "Diffusion coefficients of aromatics in nonporous PEBA membranes," *J. Memb. Sci.*, **168**, 233 (2000).

13. Ghoreyshi, S. A. A., F. A. Farhadpour and M. Soltanieh, "Multicomponent transport across nonporous polymeric membranes," *Desalination*, **144**, 93 (2002).

VITA

David Desrocher was born to Ron and Carol Desrocher on February 15, 1973 in Providence, RI. He attended Mount Saint Charles Academy in Woonsocket, RI and graduated in 1991. Dave earned his Bachelor of Science in Chemical Engineering from Lehigh University (Bethlehem, PA) in 1995. Following that, he worked for four years as a process engineer at two contract engineering firms: CP Design, Inc. (Trumbull, CT) and IDEA Engineering (Branford, CT). In their employ, Dave performed detailed engineering design for the construction of commercial facilities in the pharmaceutical, plastics, and specialty chemical industries. After a tremendous learning experience in industry, he returned to academia, enrolling in the School of Chemical Engineering at the Georgia Institute of Technology in August of 1999. There, he joined the membrane separations research group of Dr. Mary Rezac. He is joining the Intel Corp. in Hillsboro, OR as a Senior Process Engineer in August of 2004.